USE OF T CELL RECEPTOR-LIKE ANTIBODY FRAGMENTS FOR IMAGING AND IMMUNOTHERAPY

Keith Russell Miller

A dissertation submitted to the faculty of the University of North Carolina at Chapel Hill in partial fulfillment of the requirements for the degree of Doctorate of Philosophy in the Department of Biochemistry and Biophysics.

Chapel Hill
2013

Approved by:

Edward J. Collins, Ph.D.

Brian Kuhlman, Ph.D.

Matthew Redinbo, Ph.D.

Ashutosh Tripathy, Ph.D.

Russell Mumper, Ph.D.

Roland Tisch, Ph.D.

Abstract

KEITH RUSSELL MILLER: Use of T Cell Receptor-like Antibody Fragments for Imaging and Immunotherapy
(Under the direction of Edward J. Collins)

The cellular proteome, in both healthy and diseased cells, is presented on the cell membrane surface as peptides bound to the major histocompatibility complex (pMHC). During disease, the interaction of specific disease associated pMHC with T cell receptors (TCR) expressed on $CD8^+$ cytotoxic T cells allows the priming and activation of the immune system. Thus, the immune system can actively identify and kill diseased cells by recognition of the pMHC on the diseased cells' surface. Sometimes non-disease associated pMHC are misidentified on healthy cells, which are attacked leading to autoimmune disease. The association of the pMHC molecule with infection, cancer, and autoimmunity has made the pMHC a valuable target for immunotherapeutic development. In order to identify disease-associated pMHC molecules, high affinity antibodies endowed with TCR-like specificity have been developed as a novel means to target tumor and virus-infected cells and for studying autoimmune disease.

Our goal is to improve disease treatment by using TCR-like antibody fragments (Fabs) that mimic the specificity of a TCR to study cancer and autoimmune Type 1 Diabetes (T1D). Using our phage-displayed derived TCR-like Fabs, we show specific identification of both human tumors and beta cells in mice. Specifically, one Fab, fE75, binds to the human epidermal growth factor Receptor 2

peptide, E75, bound to the MHC called Human Leukocyte Antigen-A2 expressed on many human cancer cells. fE75 binding improved *in vivo* imaging of human tumors in a tumor mouse model. Translation of such technology into the clinic may revolutionize how cancer is monitored and treated. Another Fab, fIGRP, binds the islet-specific glucose-6-phosphatase catalytic subunit-related protein peptide (IGRP), restricted to the MHC, histocompatibility-2 K^d (H-2K^d). IGRP peptide-bound H-2K^d is expressed on beta cells in the nonobese diabetic mouse model. Using fIGRP, we show that the Fab specifically localizes to beta cells in mouse pancreas and can prevent activation of autoimmune T cells. Thus, TCR-like Fabs have the potential to protect against T1D onset and be developed for targeted therapies for beta cell recovery. The ability to generate TCR-like Fabs has vast potential for studying antigen presentation in cancer, viral infections, and autoimmunity and for targeted therapeutics.

Dedication

To my loving parents, Carl and Mary Miller, and to my amazing girlfriend, Samantha Greenlee, your patience, advice, continual love, and unwavering support have made this work possible.

Acknowledgements

It is difficult to place the significance of a person's contribution to another's life. Often, lives become busy with the tasks at hand and time is never quite available to reflect on the numerous positive impacts people have on one's life. In a day, there are 86,400 seconds and I intend to spend a few of these to express my gratitude and thanks.

First, I would like to thank my many collaborators that have assisted in making my research and this dissertation possible. These include Shoihe Koide at the University of Chicago, the Macromolecular Interactions Facility, and the Tisch, Jay, Cairns, and Bourett labs. Special thanks for their generosity in reagents and experiment design advice goes to Mark Johnson, Nick Spidale, Ashutosh Tripathy, Bob Immormino, Jonathan Fitzsimmons, Peter Thompson, and Rob Maile.

I truly appreciate the opportunities provided by the biological and biomedical sciences program (BBSP), the training initiative in biomedical and biological sciences (TIBBS), and the biophysics training program especially the ability to mentor and advise undergraduate research for several of the summer undergraduate research opportunities. Individuals that made this possible and provided this opportunity for me include Barry Lentz, Lisa Phillippie, Patrick Brandt, Brenda Brock, and Jeff Steinbach.

Moreover, I would like to thank the numerous friends I have made in the UNC-Chapel Hill scientific community that have made graduate school such a

pleasure and memory filled experience. In particular, I would like to thank Bob Immormino for his brain teasers, editing expertise, great listener, and being an encouraging running partner, Peter Thompson for his friendship and assisting in my transition to NC, Mike Henderson for his insistence that we play all the boardgames in my closet and organization of camping/social activities, and Jose Roques for his cooking prowess and advice during the trying times of graduate school.

I thank the undergraduates that I have had the privilege to mentor and advise. It allowed me to practice my teaching skills and to improve my own scientific knowledge. I have had the joy of working with Meredith, Taylor, Almin, Brittany, James, Youseff, Blake, Carlie, Joe, Rachel, Brandon, and Aver. Your hard work is greatly appreciated. Good luck with your future endeavors.

The experiences and education I received during my graduate education will serve me well in the future. I have much thanks and gratitude for the support, advice, encouragement, and mentoring I received from Ed in his laboratory over these past five years. His breadth of scientific knowledge, love of research, and ability to convey scientific concepts easily are all characteristics I will continue to emulate in my own teaching career.

Finally, I thank my loving, supporting, and ever-wise family members. Their support and encouragement have helped me overcome the stressful times of graduate school. I thank my wonderful parents for their skype conversations and making the nine-hour drive to NC throughout the years. We have been on numerous adventures and will continue them into the future. Much thanks is required for my life-changing girlfriend, Samantha. The past two years of graduate

school flew by as we went on numerous adventures from Fort Bragg, Iraq, botanical gardens, the ocean, and many more. She was a constant source of love outside of the lab.

Table of Contents

Table of Tables

Table of Figures

List of Abbreviations

Ab	Antibody
APC	Antigen-presenting cell
β_2M	Beta-2-microglobulin
CAR	Chimeric antibody T cell receptors
CD	Cluster of differentiation
CDR	Complementarity determining regions
CHO	Chinese hamster ovary
Ci	Curie
CT	Computed tomography
CTL	Cytotoxic T lymphocyte
^{64}Cu	Copper-64
DAPI	4'-6-Diamidino-2-phenylindole
DARPin	Designed ankyrin repeat proteins
DIC	Differential interface contrast
DNA	Deoxyribonucleic acid
DOTA-NCS	S-2-(4-Isothiocyanatobenzyl)-1,4,7,10-tetraazacyclo-dodecane-tetraacetic acid
E. coli	*Escherichia coli*
EDTA	Ethylenediaminetetraacetic acid
EGFR	Epidermal growth factor receptor
eIF4G	Eukaryotic translation initiation factor 4 gamma
ELISA	Enzyme-linked immunosorbent assay

ENV	Envelope
EPR	Enhanced retention and permeability
Fab	Antibody fragment
Fc	Fragment crystallizable region
GAD	Glutamic acid decarboxylase
GP100	Glycoprotein 100
HA	Hemaglutinin
HBV	Hepatitis B virus
HEL	Hen egg lysozyme
HER2/neu	Human epidermal growth factor receptor-2
HIV	Human immunodeficiency virus
HLA	Human leukocyte antigen
HRP	Horseradish peroxidase
HTLV-1	Human T cell lymphotropic virus type I
IGRP	Islet-specific glucose-6-phosphatase catalytic subunit related protein
IFN-γ	Interferon-gamma
K_D	Dissociation constant
LN	Lymph node
LNCAP	Left supraclavicular lymph node prostate adenocarcinoma
M	Molar
M1	Matrix protein 1
MAGE	Melanoma-associated antigen

Mart-1	Melanoma antigen recognized by T cells
MCF7	Michigan Cancer Foundation-7
MDA-MB-231	Mammary derived adenocarcinoma – mammary breast-231
MHC	Major histocompatibility complex
MFI	Mean fluorescence intensity
MOG	Myelin oligodendrocyte glycoprotein
MRI	Magnetic resonance imaging
MUC	Mucin
Nef	Negative regulatory factor
nM	Nanomolar
Ni-NTA	Nickel-nitrilotriacetic acid
$NiSO_4$	Nickel sulfate
NOD	Non-obese diabetic
NY-ESO	New York esophageal squamous cell carcinoma
OSEM	Ordered subsets-expectation maximization
PBS	Phosphate buffered saline
PCR	Polymerase chain reaction
PE38	Pseudomonas exotoxin
PE	R-phycoerythrin
PET	Positron emission tomography
PhoA	Alkaline phosphatase
PLN	Pancreatic lymph node

PMSF	Phenylmethanesulfonylfluoride
pMHC	Peptide bound major histocompatibility complex
PP65	polypeptide-65
PR1	Proteinase
ROI	Region of interest
RU	Response units
S	Seconds
SARS	severe acute respiratory syndrome
SCID	Severe combined immunodeficiency
SKOV3	Human ovarian adenocarcinoma
SOD1	Superoxide dismutase-1
SSX	Synovial sarcoma
SUV	Standardized uptake values
T1D	Type 1 diabetes
TAP	Transporter associated with antigen processing
TARP	TCR-γ Alternative Reading frame Protein
TAX	Trans-activator X
TCR	T cell receptor

Chapter 1

A review of T cell receptor-like antibodies

1.1 Introduction

Over 100 years ago, Paul Ehrlich, the German physician and scientist, first proposed the idea of antibodies as “magic bullets” that not only activate effective immune system responses, but also can be used to deliver drugs or toxins to disease sites. Now, antibodies are commonly used to treat a variety of diseases including cancer (1). One of the most successful examples is the use of monoclonal antibodies directed against the Human Epidermal Growth Factor Receptor-2 (HER2/neu) for the treatment of breast cancer (2). These antibodies can interfere with signals generated by the bound receptor and deliver conjugated drugs to the tumor cells. The use of antibodies for treatment relies on cell surface expression of antigens specific for the cancer or diseased cell. Examples include Cetuximab, targeting epidermal growth factor receptor in colorectal and head and neck cancer; Rituximab, targeting CD20 in Non-Hodgkin lymphoma; and Trastuzumab, binding epidermal growth factor receptor, ErbB2, in breast cancer (1,2). Even though there are hundreds of clinical trials using such monoclonal antibodies, the number of known antigens exclusively found on the surface of diseased cells is limited. Thus, there is a significant need for markers that distinguish infected or cancerous cells from endogenous healthy cells based on the extracellular and intracellular proteome (3).

The immune system differentiates infected or cancerous abnormal cells from endogenous normal healthy cells via the Major Histocompatibility Complex (MHC) class I molecules. These MHC molecules are expressed constitutively on the surface of all nucleated cells and function to present peptides from proteins synthesized within the cell. Eight to twelve amino acid long peptides derived from proteasome-degraded proteins are bound to the MHC in the endoplasmic reticulum and presented on the surface of the cell. Thus, the peptide-bound MHC (pMHC) provides a view of the intracellular protein content of the cell; if the cell becomes abnormal, the proteins that are translated are abnormal, the peptides produced by proteasomal degradation are abnormal, and the composition of peptide then presented by the MHC are abnormal. Similarly, the distribution of peptides presented by MHC on a heart cell is different from the population of peptides presented by a beta cell. This process results in a display of cell-specific antigens on the cell surface that could be detected. Instead of antibodies, the immune system has cytotoxic T lymphocytes (CTLs) that recognize viral, tumor, or abnormal peptides presented by the MHC. Upon binding of the disease-associated pMHC with the CTLs T cell receptor (TCR), the CTLs are activated to kill the cancerous or diseased cells and to recruit other immune cells to the site of disease. The ability of the pMHC presentation system to present an extracellular representation of the inner proteome of the cell provides a mechanism for the immune system to distinguish and target diseased cells with high sensitivity (4). Therefore, pMHC molecules are an exciting potential target for antibodies to detect diseased/abnormal cells for targeted therapeutics.

1.2 Identification of disease associated peptide/MHC class I molecules

Before antibodies against pMHC are generated, disease associated pMHC molecules must be identified. There are two main approaches, indirect and direct discovery, for identifying peptides associated with MHC molecules. Indirect discovery relies on genomic, proteomic, or immunologic data to predict the peptides that are bound to particular MHC molecules in a variety of diseases (5). Often, it is assumed that proteins that are over-expressed as a result of a disease state will be over-represented as pMHC molecules on the surface of diseased cells. Following identification of disease-associated genes and proteins, algorithms and/or computational modeling peptide binding assays are used to identify theoretically high binding affinity peptides for the MHC. These identified peptides are then synthesized and tested *in vitro* for MHC binding and/or activation of a CTL response (6). Direct discovery methods for identifying disease-associated pMHC molecules rely on peptides elution from pMHC complexes purified from diseased cell lysate. The primary sequence of the peptides is determined by mass spectrometry (7).

Both indirect and direct peptide binding MHC identification approaches have limitations. The indirect methods suffer from relying on computational algorithms and selection criteria based on assumptions that may be wrong. Moreover, even though it is logical that highly over-expressed proteins should be over-represented on pMHC molecules, this is not necessarily always the case. The peptide processing and presentation pathways have numerous moving parts resulting in greater difficulty in predicting how and whether highly expressed viral or tumor associated proteins will even be presented by MHC molecules. Because of these

limitations, indirect discovery methods may not uncover main disease associated pMHC or give false positive hits for irrelevant pMHC molecules. In direct discovery methods, the peptides eluted are often from cell lines, which can provide their own bias to peptide discovery. Moreover, this technique of direct purification of peptides relies on the solubility and ionization potential of the given peptides. It is assumed that peptides with high hydrophobicity and/or poor ionization are not detected by direct discovery. Thus, both indirect and direct discovery methods have their own technical issues, but these methods provide starting points for identifying disease-associated pMHC molecules upon careful validation (6).

1.3 Generation of TCR-like antibodies

The use of CTL TCR for targeting disease-associated pMHC has been attempted by numerous approaches, but has ultimately failed as a reliable research tool. Genetically engineered T cells expressing only one TCR have been used to indirectly assess pMHC molecules via cell lysis and cytokine assays and CTL proliferation assays with varied success. The maintenance of such cell lines is costly and labor intensive with the added difficulty of quality control. Therefore, interest in using soluble TCRs as reagents grew, but recombinant TCRs had issues including: low affinities (high micromolar) and limited stability (8-14). Both of these issues were addressed by multimerization of the TCRs and protein engineering for improved affinity and stability (15, 16).

Antibodies and antibody fragments specific for pMHC molecules provide numerous advantages over TCRs as soluble and specific reagents. First and foremost, they have higher affinities than TCRs and provide greater stability. TCR-

like antibodies can be used under a variety of different assay conditions including: immunoprecipitations and immunohistochemistry. Unfortunately, TCR-like antibodies have been difficult to make due to unknown reasons, but several have been produced by either classical hybridoma fusion technology after immunization or by phage display (3, 6). A list of isolated and tested TCR-like antibodies/antibody fragments is given in Table 1.

In the immunization and classical hybridoma technology approach for isolating TCR-like antibodies, B cells from antigen-immunized animals are fused with myeloma cells to create an antibody-producing hybridoma. Most attempts at using this technology have failed (17-19). Although there are a few groups that have been successful (20, 21). The success of these few instances is hypothesized to be due to the efficiency in inducing a specific B cell response during the immunization. This relies heavily on the pMHC immunogen formulation, which should be stable, homogeneous, and induce antibody responses to both peptide and the MHC combined instead of either alone (6). Initially, cells expressing the pMHC of interest were used as immunogens resulting in approximately one to three out of approximately 1000 growth-positive clones able to produce TCR-like antibodies specific for the target pMHC (22, 23). The use of recombinant purified pMHC class I molecules as immunogens showed successful production of monoclonal antibodies with affinities that were ten-fold higher than TCRs (24). The efficiency of this technique at 0.5% and the only moderate affinity of the antibodies compared to TCRs left this technique as requiring further optimization before it could reliably be used as a source of TCR-like antibodies (6).

Table 1: List of TCR-like Molecules and Their Associated Specificities

MHC	Peptide	Disease Association	Type	Isolation Method	K_D (nM)	Ref.
HLA-A2	gp100-154 KTWGQYWQV	Melanoma	Fab	Phage display	15-30	16
HLA-A2	gp100-209 ITDQVPFSV	Melanoma	Fab	Phage display	15-30	16
HLA-A2	gp100-280 YLEPGPVTA	Melanoma	Fab	Phage display	15-30	16
HLA-A2	Tyrosinase-369 YM*D*GTMSQV	Melanoma	Ab	Phage display	~50	17
HLA-A2	Mart-1 LAGIGILTV	Melanoma	Ab	Phage display	~50	17
HLA-A2	MAGE-A1 EADPTGHSY	Melanoma and solid tumors	Fab	Phage display	60	18, 19
HLA-A2	MAGE3-271 FLWGPRALV	Melanoma and solid tumors	Ab	Hybridoma	2.37	20
HLA-A2	p68 RNA helicase-128 YLLPAIVHI	Breast Cancer	Ab	Hybridoma	0.42	21, 22
HLA-A2	NY-ESO-1-157	Normal Testis and other tumors	Fab	Phage display	60	23
HLA-A2	TARP-29 FLRNFSLML	Breast and prostate cancer	Fab	Phage display	120	24
HLA-A2	human chorionic gonadotropin β GVLPALPQV	Ovarian, colon and breast cancer	Ab	Hybridoma	1.5	25
HLA-A2	HER2/neu-369 KIFGSLAFL	Ovarian, colon and breast cancer	Fab	Native phage dispay	59	26
HLA-A2	human chorionic gonadotropin β TMTRVLQGV	Ovarian, breast, and other cancers	Ab	Hybridoma	n/a	27
HLA-A2	PR1 VLQELNVTV	Leukemia	Ab	Hybridoma	9.9	28
HLA-A2	TAX-11 LLFGYPVYV	HTLV-1	Fab	Phage display	25-30	29

MHC	Peptide	Disease Association	Type	Isolation Method	K_D (nM)	Ref.
HLA-A2	MUC-1-D6-13 LLLTVLTVV	Glandular cancer	Fab	Phage display	15-25	29
HLA-A2	Telomerase-540 ILAKFLHWL	Most human cancers	Fab	Phage display	~5	30
HLA-A2	Telomerase-865 RLVDDFLLV	Most human cancers	Fab	Phage display	10-15	30
HLA-A2	SSX2-103 RLQGISPKI	Normal Testis and melanoma	Fab	Phage display	270	31
HLA-A2	M1-58 GILGFVFTL	Influenza	Fab	Phage display	n/a	32
HLA-A2	Nef-105 KRQDILDLWVY	HIV-1	Ab	Phage display	4	33
HLA-A2	ENV-183 FLLTRILTI	EBV	Ab	Hybridoma	n/a	34
HLA-A2	eIF4G-720 VLMTEDIKL	HIV-1	Ab	Hybridoma	n/a	35
HLA-A2	Nef138-10/A24 RYPLTFGWCF	HIV-1	Ab	Phage display	2700	36
HLA-A2	pp65-495 NLVPMVATV	CMV	Ab	Phage display	300	37
I-A^k	HEL46 NTDGSTDYGIL QINSR	n/a	Ab	Hybridoma	n/a	38, 39
I-A^k	HEL116 KGTDVQAWIRG CRL	n/a	Ab	Hybridoma	n/a	40
HLA-DR2	MOG-35-55 MEVGWYRPPF SRVVHLYRNGK	Multiple Sclerosis	Ab	Phage display	30-60	41
H-$2K^b$	Ovalbumin SIINFEKL	n/a	Ab	Hybridoma	256	41
H-$2K^k$	HA255 FESTGNLI	Influenza	Ab	Phage display	56	42, 43

The major advancement for isolation of TCR-like antibodies was the development of antibody phage-display approaches as an alternative to classical hybridoma technologies. This technology utilizes phage particle libraries expressing antibodies as fusion proteins on their surface. One unique antibody fragment or single-chain variable fragment is displayed on each phage particle and is encoded by the phage genes. Repeated rounds of selection using magnetic beads displaying the pMHC molecules followed by bacterial amplification are used to isolate phage expressing antibody-derived molecules specific for pMHC (25-28). Using this methodology, high affinity TCR-like antibody-derived molecules have been produced. These molecules generally have low affinity, but can be genetically-engineered for higher affinity for their target pMHC molecule. Random and rational affinity maturation strategies have been reported to increase binding affinities of phage-display isolated TCR-like antibody-derived molecules into the nanomolar range (~50-300 nM) (29, 30). Therefore, large phage-display libraries are now the method of choice and the most common approach for isolating TCR-like antibody-derived molecules.

1.4 TCR-like antibody applications

TCR-like antibodies have great potential to be valuable tools for understanding immunological processes and for the development of novel therapeutics. Their ease of use, specificity, and sensitivity makes them very versatile for research assays. Applications of such reagents include: monitoring and quantifying antigen presentation on diseased cells and comparing it to endogenous healthy cells, understanding the importance of pMHC molecules for

immune responses, targeted delivery of toxins to sites of disease or infection, and activation of effective immune responses against tumors (3, 6).

TCR-like antibodies are novel reagents that may expand the tool set immunologists use to monitor and quantify antigen presentation during disease. The small set of available antibodies have been used to determine the presence of particular pMHC on cancer cells (27, 31-34). Moreover, methods for quantifying levels of specific pMHC on cell surfaces by flow cytometry are being developed (35). Using these and similar methods, TCR-like antibodies have quantified that there are several hundreds of specific pMHC complexes on non-peptide pulsed cancer cells (32). This number is in agreement with estimates on the level of pMHC density required for CTL activation and lysis (36, 37). In other studies, an expression hierarchy of T cell epitopes from melanoma antigens was analyzed. Analysis of pMHC expression levels of human gp100, Melan-A/Mart-1, and tyrosinase antigen showed that there was high level of tyrosinase derived pMHC molecules on the surface of melanoma compared to the other antigens. It was determined that the quantity of the melanoma pMHC antigens did not correlate with the gene expression profiles. Moreover, melanoma cells given a drug that stabilizes tyrosinase showed a decrease in the tyrosinase antigen derived pMHC levels. Thus, it was hypothesized that protein stability was the dominating factor resulting in the differences between the antigens in their antigen presentation (34). In addition, TCR-like antibodies have been shown to aid in developing cancer vaccines. In one example, TCR-like antibodies specific for peptides derived from the NY-ESO-1 protein were used to

differentiate between the CTL reactivity to immunological eliciting NY-ESO-1 vaccination peptides compared to cryptic, nonimmune responsive peptides (33).

The specificity of some TCR-like antibodies for cancer pMHC molecules makes them promising agents to deliver toxins to the cancer cells or as antitumor agents in themselves. TCR-like antibodies fused to *Pseudomonas* exotoxin (38-40) and saporin (41) are effective at killing cancer cells *in vitro* and *in vivo*. These TCR-like antibodies fused to toxins specifically identified and killed a variety of cancer cells including: prostate (40), breast (41), and melanoma (38, 39). In addition, TCR-like antibodies can induce effective immune responses against tumors without use of toxins. Full TCR-like antibodies with Fc domains can elicit complement-dependent cytotoxicity (CDC) and activate antibody-dependent cellular cytotoxicity (ADCC) of cancer cells. Activation of any of these immune responses leads to inhibition of tumor growth in mouse models injected with the TCR-like antibodies (21, 42-45).

Alternatively, it has become possible to engineer T cells to attack cancer by transfection of T cells with viruses encoding chimeric antibody T cell receptors (CARs) consisting of a tumor specific antibody fused to an intracellular signaling domain able to activate T cells. Often, these CARs consist of an extracellular single chain variable fragment of a monoclonal antibody fused to a co-stimulatory signaling domain such as CD28 and an intracellular CD3 zeta chain (46). By using TCR-like antibodies, the specificity of T cells can be engineered against certain disease-associated pMHC molecules. In one example, T cells were designed to display chimeric receptors of the TCR-like Fabs fused to the FcεRI γ-chain signaling molecule. Increased sensitivity, faster cytotoxic responses, and enhanced tumor cell

killing capacity were observed for these engrafted T cells (29). All together, these results demonstrate that TCR-like antibodies specific for tumor antigens can be isolated and effectively deliver drugs, kill tumors directly and may be used to engineer autologous T cells for immunotherapy.

TCR-like antibodies have been used to understand antigen presentation during viral infection and to specifically target virally infected cells for therapy. TCR-like antibodies have been isolated against viral pMHC presented on cells infected with human immunodeficiency virus (HIV) (47, 48), influenza (49, 50), cytomegalovirus (51), human T cell lymphotropic virus type I (HTLV-1) (52), and Hepatitis B virus (HBV) (20, 53). One TCR-like antibody, specific for the HTLV-1-derived Tax_{11-19} peptide bound to HLA-A2, detected pMHC complexes as low as 100 complexes per cell (52). This is near the threshold number of pMHC molecules required for cytokine secretion by T cells (54, 55). Thus, TCR-like antibodies can be isolated that have similar if not greater sensitivity for pMHC than T cells. The dynamics of antigen presentation during viral infection have been studied using TCR-like antibodies. In one study, a TCR-like antibody was used to show that the majority of viral antigen pp65 protein bound to HLA-A2 molecules during early infection were localized to the Golgi with only a small portion expressed on the cell surface (51). This information provides further understanding of the complex events leading to viral antigen presentation. The TCR-like antibody allowed for the direct visualization, distribution, and localization of the cytomegalovirus-derived peptide associated MHC during viral infection. Finally, TCR-like antibodies targeting viral pMHC molecules have been used to kill infected cells. Lentiviruses engineered to

display TCR-like antibodies and Fas ligand specifically killed HIV-1 Nef protein expressing cells. In this study, the TCR-like antibody endowed the lentivirus with the specificity and the Fas ligand expression provided the lentivirus with the ability to kill based on the interaction between the Fas ligand and the Fas receptor on the targeted cells inducing apoptosis of the virally infected cells (47). Also, similar to the cancer therapies, TCR-like antibodies fused to toxins can kill influenza infected target cells in a pMHC specific manner. In one example, a TCR-like antibody specific for the MHC class I H-2K^k bound to the virus-derived hemagglutinin peptide HA was fused with the *Pseudomonas* exotoxin, PE38. This TCR-like antibody fused toxin specifically killed influenza virus-infec

ted cells presenting the HA peptide bound H-2K^k molecule on their surface (49). As a whole, TCR-like antibodies provide necessary tools to understand antigen presentation during infection and are versatile targeting probes for therapeutics.

1.5 Conclusion

Disease either induced by genetic defects or by infection is often guided by intricate molecular mechanisms. Molecules that function like TCR with pMHC specificity are a promising new technology that can probe fundamental elements of these processes. Further work in the generation of TCR-like antibody-derived molecules is required to make the process more streamlined and easier to generate proteins with high affinity and specificity for pMHC. The few TCR-like antibody-derived molecules that have been isolated do show promising results. Several studies have shown that TCR-like antibodies can aid in understanding and revealing

important aspects of antigen processing and pMHC presentation mechanisms in cancer and virally infected cells. Furthermore, these antibodies provide a new realm of targets for delivery of therapeutics to the sites of disease. Our work discussed in this dissertation focuses on generating and utilizing TCR-like antibody fragments for *in vivo* xeno-transplanted tumor imaging for cancer treatment and imaging/immunotherapy of beta cells in type 1 diabetes. We show that TCR-like antibody fragments with high affinity and specificity for their disease-specific pMHC molecule can be isolated and used as imaging agents and potential immunotherapeutics. Therefore, TCR-like molecules may just be a “magic bullet” to assist in understanding MHC-based immunity and improving our use of immunotherapy in the future.

1.6 References

1. Rahbarizadeh, F., D. Ahmadvand, and Z. Sharifzadeh. 2011. Nanobody; an old concept and new vehicle for immunotargeting. *Immunol. Invest.* 40: 299–338.

2. Leyland-Jones, B. 2002. Trastuzumab: hopes and realities. *Lancet Oncol* 3: 137–144.

3. Dahan, R., and Y. Reiter. 2012. T-cell-receptor-like antibodies - generation, function and applications. *Expert Rev Mol Med* 14: e6.

4. Abbas, A. K., and A. H. H. Lichtman. 2010. *Basic Immunology Updated Edition*. Saunders.

5. Stevanovic, S. 2005. Antigen processing is predictable: From genes to T cell epitopes. *Transplant Immunol.* 14: 171–174.

6. Weidanz, J. A., O. Hawkins, B. Verma, and W. H. Hildebrand. 2011. TCR-like molecules target peptide/MHC Class I complexes on the surface of infected and cancerous cells. *Int. Rev. Immunol.* 30: 328–340.

7. Hawkins, O. E., R. S. VanGundy, A. M. Eckerd, W. Bardet, R. Buchli, J. A. Weidanz, and W. H. Hildebrand. 2008. Identification of breast cancer peptide epitopes presented by HLA-A*0201. *J. Proteome Res.* 7: 1445–1457.

8. Alberti, S. 1996. A high affinity T cell receptor? *Immunol. Cell Biol.* 74: 292–297.

9. Clements, C. S., M. A. Dunstone, W. A. Macdonald, J. McCluskey, and J. Rossjohn. 2006. Specificity on a knife-edge: the alphabeta T cell receptor. *Curr. Opin. Struct. Biol.* 16: 787–795.

10. Collins, E. J., and D. S. Riddle. 2008. TCR-MHC docking orientation: natural selection, or thymic selection? *Immunol. Res.* 41: 267–294.

11. Edwards, L. J., and B. D. Evavold. 2011. T cell recognition of weak ligands: roles of signaling, receptor number, and affinity. *Immunol. Res.* 50: 39–48.

12. Plaksin, D., K. Polakova, P. McPhie, and D. H. Margulies. 1997. A three-domain T cell receptor is biologically active and specifically stains cell surface MHC/peptide complexes. *J. Immunol.* 158: 2218–2227.

13. Wilson, D. B., D. H. Wilson, K. Schroder, C. Pinilla, S. Blondelle, R. A. Houghten, and K. C. Garcia. 2004. Specificity and degeneracy of T cells. *Mol. Immunol.* 40: 1047–1055.

14. Wulfing, C., and A. Plückthun. 1994. Correctly folded T-cell receptor fragments in the periplasm of Escherichia coli. Influence of folding catalysts. *J. Mol. Biol.* 242: 655–669.

15. Altman, J. D., P. A. Moss, P. J. Goulder, D. H. Barouch, M. G. McHeyzer-Williams, J. I. Bell, A. J. McMichael, and M. M. Davis. 1996. Phenotypic analysis of antigen-specific T lymphocytes. *Science* 274: 94–96.

16. Holler, P. D., P. O. Holman, E. V. Shusta, S. O'Herrin, K. D. Wittrup, and D. M. Kranz. 2000. In vitro evolution of a T cell receptor with high affinity for peptide/MHC. *Proc. Natl. Acad. Sci. U.S.A.* 97: 5387–5392.

17. Rubin, B., B. Malissen, P. N. Jørgensen, and J. Zeuthen. 1989. Recognition of insulin on MHC-class-II-expressing L929 cells by antibody and T cells. *Res. Immunol.* 140: 67–74.

18. Sergeeva, A., G. Alatrash, H. He, K. Ruisaard, S. Lu, J. Wygant, B. W. McIntyre, Q. Ma, D. Li, L. St John, K. Clise-Dwyer, and J. J. Molldrem. 2011. An anti-PR1/HLA-A2 T-cell receptor-like antibody mediates complement-dependent cytotoxicity against acute myeloid leukemia progenitor cells. *Blood* 117: 4262–4272.

19. Tamminen, W. L., D. Wraith, and B. H. Barber. 1987. Searching for MHC-restricted anti-viral antibodies: antibodies recognizing the nucleoprotein of influenza virus dominate the serological response of C57BL/6 mice to syngeneic influenza-infected cells. *Eur. J. Immunol.* 17: 999–1006.

20. Sastry, K. S. R., C. T. Too, K. Kaur, A. J. Gehring, L. Low, A. Javiad, T. Pollicino, L. Li, P. T. F. Kennedy, U. Lopatin, P. A. Macary, and A. Bertoletti. 2011. Targeting hepatitis B virus-infected cells with a T-cell receptor-like antibody. *J. Virol.* 85: 1935–1942.

21. Wittman, V. P., D. Woodburn, T. Nguyen, F. A. Neethling, S. Wright, and J. A. Weidanz. 2006. Antibody targeting to a class I MHC-peptide epitope promotes tumor cell death. *J. Immunol.* 177: 4187–4195.

22. Dadaglio, G., C. A. Nelson, M. B. Deck, S. J. Petzold, and E. R. Unanue. 1997. Characterization and quantitation of peptide-MHC complexes produced from hen egg lysozyme using a monoclonal antibody. *Immunity* 6: 727–738.

23. Porgador, A., J. W. Yewdell, Y. Deng, J. R. Bennink, and R. N. Germain. 1997. Localization, quantitation, and in situ detection of specific peptide-MHC class I complexes using a monoclonal antibody. *Immunity* 6: 715–726.

24. Polakova, K., D. Plaksin, D. H. Chung, I. M. Belyakov, J. A. Berzofsky, and D. H. Margulies. 2000. Antibodies directed against the MHC-I molecule H-2Dd complexed with an antigenic peptide: similarities to a T cell receptor with the same specificity. *J. Immunol.* 165: 5703–5712.

25. Andersen, P. S., A. Stryhn, B. E. Hansen, L. Fugger, J. Engberg, and S. Buus. 1996. A recombinant antibody with the antigen-specific, major histocompatibility complex-restricted specificity of T cells. *Proc. Natl. Acad. Sci. U.S.A.* 93: 1820–1824.

26. Chames, P., S. E. Hufton, P. G. Coulie, B. Uchanska-Ziegler, and H. R. Hoogenboom. 2000. Direct selection of a human antibody fragment directed against the tumor T-cell epitope HLA-A1-MAGE-A1 from a nonimmunized phage-Fab library. *Proc. Natl. Acad. Sci. U.S.A.* 97: 7969–7974.

27. Lev, A., G. Denkberg, C. J. Cohen, M. Tzukerman, K. L. Skorecki, P. Chames, H. R. Hoogenboom, and Y. Reiter. 2002. Isolation and characterization of human recombinant antibodies endowed with the antigen-specific, major histocompatibility complex-restricted specificity of T cells directed toward the widely expressed tumor T-cell epitopes of the telomerase catalytic subunit. *Cancer Res.* 62: 3184–3194.

28. Stryhn, A., P. S. Andersen, L. O. Pedersen, A. Svejgaard, A. Holm, C. J. Thorpe, L. Fugger, S. Buus, and J. Engberg. 1996. Shared fine specificity between T-cell receptors and an antibody recognizing a peptide/major histocompatibility class I complex. *Proc. Natl. Acad. Sci. U.S.A.* 93: 10338–10342.

29. Chames, P., R. A. Willemsen, G. Rojas, D. Dieckmann, L. Rem, G. Schuler, R. L. Bolhuis, and H. R. Hoogenboom. 2002. TCR-like human antibodies expressed on human CTLs mediate antibody affinity-dependent cytolytic activity. *J. Immunol.* 169: 1110–1118.

30. Stewart-Jones, G., A. Wadle, A. Hombach, E. Shenderov, G. Held, E. Fischer, S. Kleber, N. Nuber, F. Stenner-Liewen, S. Bauer, A. McMichael, A. Knuth, H. Abken, A. A. Hombach, V. Cerundolo, E. Y. Jones, and C. Renner. 2009. Rational development of high-affinity T-cell receptor-like antibodies. *Proc. Natl. Acad. Sci. U.S.A.* 106: 5784–5788.

31. Verma, B., O. E. Hawkins, F. A. Neethling, S. L. Caseltine, S. R. Largo, W. H. Hildebrand, and J. A. Weidanz. 2010. Direct discovery and validation of a peptide/MHC epitope expressed in primary human breast cancer cells using a TCRm monoclonal antibody with profound antitumor properties. *Cancer Immunol. Immunother.* 59: 563–573.

32. Cohen, C. J., N. Hoffmann, M. Farago, H. R. Hoogenboom, L. Eisenbach, and Y. Reiter. 2002. Direct detection and quantitation of a distinct T-cell epitope derived from tumor-specific epithelial cell-associated mucin using human recombinant antibodies endowed with the antigen-specific, major histocompatibility complex-restricted specificity of T cells. *Cancer Res.* 62: 5835–5844.

33. Held, G., M. Matsuo, M. Epel, S. Gnjatic, G. Ritter, S. Y. Lee, T. Y. Tai, C. J. Cohen, L. J. Old, M. Pfreundschuh, Y. Reiter, H. R. Hoogenboom, and C. Renner. 2004. Dissecting cytotoxic T cell responses towards the NY-ESO-1 protein by peptide/MHC-specific antibody fragments. *Eur. J. Immunol.* 34: 2919–2929.

34. Michaeli, Y., G. Denkberg, K. Sinik, L. Lantzy, C. Chih-Sheng, C. Beauverd, T. Ziv, P. Romero, and Y. Reiter. 2009. Expression hierarchy of T cell epitopes from melanoma differentiation antigens: unexpected high level presentation of tyrosinase-HLA-A2 Complexes revealed by peptide-specific, MHC-restricted, TCR-like antibodies. *J. Immunol.* 182: 6328–6341.

35. Dolan, B. P. 2013. Quantitating MHC class I ligand production and presentation using TCR-like antibodies. *Methods Mol. Biol.* 960: 169–177.

36. Christinck, E. R., M. A. Luscher, B. H. Barber, and D. B. Williams. 1991. Peptide binding to class I MHC on living cells and quantitation of complexes required for CTL lysis. *Nature* 352: 67–70.

37. Sykulev, Y., M. Joo, I. Vturina, T. J. Tsomides, and H. N. Eisen. 1996. Evidence that a single peptide-MHC complex on a target cell can elicit a cytolytic T cell response. *Immunity* 4: 565–571.

38. Klechevsky, E., M. Gallegos, G. Denkberg, K. Palucka, J. Banchereau, C. Cohen, and Y. Reiter. 2008. Antitumor activity of immunotoxins with T-cell receptor-like specificity against human melanoma xenografts. *Cancer Res.* 68: 6360–6367.

39. Denkberg, G., A. Lev, L. Eisenbach, I. Benhar, and Y. Reiter. 2003. Selective targeting of melanoma and APCs using a recombinant antibody with TCR-like specificity directed toward a melanoma differentiation antigen. *J. Immunol.* 171: 2197–2207.

40. Epel, M., I. Carmi, S. Soueid-Baumgarten, S. K. Oh, T. Bera, I. Pastan, J. Berzofsky, and Y. Reiter. 2008. Targeting TARP, a novel breast and prostate tumor-associated antigen, with T cell receptor-like human recombinant antibodies. *Eur. J. Immunol.* 38: 1706–1720.

41. Kuroda, K., H. Liu, S. Kim, M. Guo, V. Navarro, and N. H. Bander. 2010. Saporin toxin-conjugated monoclonal antibody targeting prostate-specific membrane antigen has potent anticancer activity. *Prostate* 70: 1286–1294.

42. Verma, B., R. Jain, S. Caseltine, A. Rennels, R. Bhattacharya, M. M. Markiewski, A. Rawat, F. Neethling, U. Bickel, and J. A. Weidanz. 2011. TCR mimic monoclonal antibodies induce apoptosis of tumor cells via immune effector-independent mechanisms. *J. Immunol.* 186: 3265–3276.

43. Verma, B., F. A. Neethling, S. Caseltine, G. Fabrizio, S. Largo, J. A. Duty, P. Tabaczewski, and J. A. Weidanz. 2010. TCR mimic monoclonal antibody targets a specific peptide/HLA class I complex and significantly impedes tumor growth in vivo using breast cancer models. *J. Immunol.* 184: 2156–2165.

44. Weidanz, J. A., T. Nguyen, T. Woodburn, F. A. Neethling, M. Chiriva-Internati, W. H. Hildebrand, and J. Lustgarten. 2006. Levels of specific peptide-HLA class I complex predicts tumor cell susceptibility to CTL killing. *J. Immunol.* 177: 5088–5097.

45. Hawkins, O., B. Verma, S. Lightfoot, R. Jain, A. Rawat, S. McNair, S. Caseltine, A. Mojsilovic, P. Gupta, F. Neethling, O. Almanza, W. Dooley, W. Hildebrand, and J. Weidanz. 2011. An HLA-presented fragment of macrophage migration inhibitory factor is a therapeutic target for invasive breast cancer. *J. Immunol.* 186: 6607–6616.

46. Park, T. S., S. A. Rosenberg, and R. A. Morgan. 2011. Treating cancer with genetically engineered T cells. *Trends Biotechnol.* 29: 550–557.

47. Herschhorn, A., W. A. Marasco, and A. Hizi. 2010. Antibodies and lentiviruses that specifically recognize a T cell epitope derived from HIV-1 Nef protein and presented by HLA-C. *J. Immunol.* 185: 7623–7632.

48. Nunoya, J.-I., T. Nakashima, A. Kawana-Tachikawa, K. Kiyotani, Y. Ito, K. Sugimura, and A. Iwamoto. 2009. Short communication: generation of recombinant monoclonal antibodies against an immunodominant HLA-A*2402-restricted HIV type 1 CTL epitope. *AIDS Res. Hum. Retroviruses* 25: 897–904.

49. Reiter, Y., A. Di Carlo, L. Fugger, J. Engberg, and I. Pastan. 1997. Peptide-specific killing of antigen-presenting cells by a recombinant antibody-toxin fusion protein targeted to major histocompatibility complex/peptide class I complexes with T cell receptor-like specificity. *Proc. Natl. Acad. Sci. U.S.A.* 94: 4631–4636.

50. Wylie, D. E., L. A. Sherman, and N. R. Klinman. 1982. Participation of the major histocompatibility complex in antibody recognition of viral antigens expressed on infected cells. *J. Exp. Med.* 155: 403–414.

51. Makler, O., K. Oved, N. Netzer, D. Wolf, and Y. Reiter. 2010. Direct visualization of the dynamics of antigen presentation in human cells infected with cytomegalovirus revealed by antibodies mimicking TCR specificity. *Eur. J. Immunol.* 40: 1552–1565.

52. Cohen, C. J., O. Sarig, Y. Yamano, U. Tomaru, S. Jacobson, and Y. Reiter. 2003. Direct phenotypic analysis of human MHC class I antigen presentation: visualization, quantitation, and in situ detection of human viral epitopes using peptide-specific, MHC-restricted human recombinant antibodies. *J. Immunol.* 170: 4349–4361.

53. Low, J. L., A. Naidoo, G. Yeo, A. J. Gehring, Z. Z. Ho, Y. H. Yau, S. G. Shochat, D. M. Kranz, A. Bertoletti, and G. M. Grotenbreg. 2012. Binding of TCR multimers and a TCR-like antibody with distinct fine-specificities is dependent on the surface density of HLA complexes. *PLoS ONE* 7: e51397.

54. Demotz, S., H. M. Grey, and A. Sette. 1990. The minimal number of class II MHC-antigen complexes needed for T cell activation. *Science* 249: 1028–1030.
55. Harding, C. V., and E. R. Unanue. 1990. Quantitation of antigen-presenting cell MHC class II/peptide complexes necessary for T-cell stimulation. *Nature* 346: 574–576.

Chapter 2

T cell receptor-like recognition of tumor *in vivo* by synthetic antibody fragment[1]

2.1 Introduction

One of the most important lessons learned about cancer in the past 100 years is the understanding that each cancer is as unique as the patient. Effective treatment of the patient is linked to knowing which proteins, such as hormone receptors or HER2/neu, are actively expressed in the tumor. Probes that allow us to ascertain the molecular details of each patient's tumors will greatly enhance treatment. Biopsies can be used to determine molecular details, but biopsy is invasive, not always possible and does not allow for the fact that the tumor may change characteristics over time or location [1]. It would be preferable to be able to perform a noninvasive technique first followed by treatment [2]. Our long-term goal is to develop agents that can specifically target tumor cells for detection and delivery of toxins or chemotherapeutics.

Any noninvasive approach to determining molecular details of the tumor must use a probe that binds to the tumor cells with high affinity and high specificity. Monoclonal antibodies with affinity for cell-surface receptors on tumors have had

[1]This chapter has been published as: Miller, K. R., A. Koide, B. Leung, J. Fitzsimmons, B. Yoder, H. Yuan, M. Jay, S. S. Sidhu, S. Koide, and E. J. Collins. 2012. T cell receptor-like recognition of tumor in vivo by synthetic antibody fragment. *PLoS ONE* 7: e43746.

great success in the clinic, but this approach appears to be limited because of the expression of that same cell surface receptor on normal cells that cause side effects during treatment. One of the best examples of successful use of monoclonal antibodies to tumor-associated antigens is Herceptin. Herceptin targets the human epidermal growth factor receptor 2 (HER2/neu). HER2/neu is over-expressed in 15-30% of solid tumors including breast, ovarian, colorectal, esophageal, squamous head and neck and stomach [3]. Over-expression of HER2/neu correlates with poor prognosis for therapy of breast cancer [4-8] and has been linked to increased metastases [9]. Monoclonal antibodies directed towards HER2/neu such as Herceptin have shown great efficacy in the clinic, but patients do develop resistance over time [10] and some patients do not respond at all [11]. Therefore, other approaches to target HER2/neu over-expressing tumor cells would be of great value.

Our approach to targeting HER2/neu positive tumor cells is to use the same mechanism that the immune system uses to target and kill tumors, that is to target peptides derived from the HER2/neu protein when bound and presented by the Major Histocompatibility Complex (MHC). The interaction of the T cell receptor (TCR) with peptide/MHC complex is the fundamental event that triggers the adaptive immune response [12]. T cells identify tumor cells by recognizing peptides derived from tumor-associated molecules. The TCR would theoretically be an excellent probe to use for tumors, except that the TCR is frequently not amenable to manipulation and recombinant expression and its affinity for particular pMHC is relatively poor (the dissociation constant in the high μM range) [13-19]. Monoclonal antibodies would be a much better approach, because they are robust molecules

and their production is well established. Antibodies that target specific pMHC on the surface of tumor cells have been produced but for some unknown reason, producing them conventionally is very difficult. When available, these TCR-like antibody fragments appear to bind similarly to TCR binding pMHC [20,21]. Antibodies (or antibody fragments) previously isolated from phage-display libraries exhibited relatively low affinity for the pMHC complexes [22-24].

In this study, we isolated a T-cell receptor like Fab that specifically targets the HER2/neu peptide, E75 (KIFGSLAFL), bound to the human MHC, Human Leukocyte Antigen, HLA-A2 from a synthetic antibody library using phage display. The Fab binds with nanomolar binding affinity and high specificity for the E75/HLA-A2 pMHC molecule. The Fab was then modified to attach radioactive ^{64}Cu and used for *in vivo* PET/CT imaging experiments on tumor-bearing mice that express HLA-A2 transgenically. The Fab showed increased retention in the HER2/neu pMHC positive tumors compared to HER2/neu pMHC negative tumors. These TCR-like antibodies can be used to study antigens presented on diseased and antigen-presenting cells and for delivering therapies in tumor and T-cell based diseases.

2.2 Materials and methods

Ethics statement. This study was completed in strict accordance with the Association for Assessment and Accreditation of Laboratory Animal Care at the University of North Carolina (UNC) Animal Facility and the mice were handled according to the UNC Office of Animal Care and Use. All experimentation was in accordance with the protocol (08-235.0) approved by the UNC Institutional Animal Care and Use Committee.

Cells and culture conditions. MDA-MB-231, MCF7, and LNCAP tumor cells, CHO cells, T2 lymphoblast cells were purchased from ATCC. SKOV3 and SKOV3 cells transfected with HLA-A2 were a generous gift from Dr. Jonathan Serody (Department of Microbiology, UNC – Chapel Hill, NC) [25]. Unless otherwise mentioned all media supplies were purchased from Mediatec, Inc. (Manassas, VA). Each of the cell lines were grown in RMPI 1640 supplemented with 10% heat-inactivated FBS (Atlanta Biologicals, Inc.; Lawrenceville, GA), 10 mM sodium pyruvate, and penicillin/streptomyocin in humidified CO_2 (5%) incubator at 37 °C. SKOV3 transfected HLA-A2 cells and CHO transfected HLA-A2 cells were grown in the same conditions as above with the addition of 2.5 mg/ml G418.

Antibodies and synthetic peptides. Anti-c-erb B-2 Ab-2 (9G6.10) was purchased from NeoMarkers (Fremont, Ca). Alexa Fluor 647 labeled Goat anti-mouse IgG1, PE labeled mouse IgG2b, and Alexa Fluor 647 labeled Streptavidin were purchased from Invitrogen, Inc. PE labeled mouse anti-Human HLA-A2 clone BB7.2 was purchased from BD Biosciences. The peptides: E75 (from HER2/neu; KIFGSLAFL, residues 369-377); ML (from calreticulin; MLLSVPLLL, residues 1-9); YM (from human papillomavirus 16 (HPV-16) E7 oncoprotein; YMLDLQPETT, residues 11-20); RL (from HER2/neu; RLLQETELV, residues 689-697); HY (from HER2/neu; HLYQGCQVV, residues 48-56); KT (from gp100 glycoprotein; KTWGQYWQV, residues 154-162); IL (from HIV-1 RT ILKEPVHGV; residues 476-484); and HA (from influenza hemagglutinin; IYSTVASSL, residues 518-526) were synthesized by the UNC Peptide Synthesis Facility (Chapel Hill, NC).

Generation of peptide bound HLA-A2 complexes. The human MHC, HLA-A2.1, human beta-2-microglobulin (β_2M), mouse beta-2-microglobulin, and murine H-2 K^d were produced as inclusion bodies in *E. coli* BL21 (DE3) (Invitrogen, Inc.). Protein was folded *in vitro* as described previously [26]. Briefly, peptide, β_2M, and HLA-A2 heavy chain in a 10:1:1 molar ratio were injected into a folding buffer consisting of 100 mM Tris pH 8.0, 400 mM arginine, 2 mM EDTA, 5 mM glutathione (reduced), 0.5 mM glutathione (oxidized), and protease inhibitors PMSF, pepstatin and leupeptin. The total final protein concentration was never greater than 50 µg/ml. After incubation for 24-36 hours at 10 °C the folded pMHC was concentrated in an Amicon ultrafiltration cell (Millipore, Billerica, MA) and purified using gel filtration chromatography (Phenomenex, Inc.; Torrance, CA). The purified pMHC molecules were concentrated to greater than 3 mg/ml and stored at -80°C until use. Typical yield for each 1 L refold is about 5 mg of pMHC, which is approximately a 14% yield. The pMHC was site specifically biotinylated with the biotin ligase BirA (Avidity, LLC; Aurora, Colorado) according to the manufacturer's instructions. A non-denaturing SDS PAGE gel shift assay (no reducing agent, no heat treatment) was used to confirm that the pMHCs were biotinylated.

Construction of Fab library. We first constructed a template plasmid for constructing libraries, pFab007. This plasmid contains a modified version of the Fab-4D5 gene [27] fused to gene III of the M13 phage (corresponding to the carboxyl-terminal 208 residues of pIII). This fusion protein contains the cysteine residue of the heavy chain hinge region so as to enable bivalent display of the Fab [28]. Most residues in the CDR-L3, H1, and H2 loops were replaced with serine. A TAA stop

codon and a unique BamHI site were introduced to CDR-H3. The gene was assembled from a series of synthetic oligonucleotides using PCR. The synthesized gene and the phoA promotor segment were cloned into a phage-display vector, pAS38 [29] in such a way that the heavy chain of the Fab is fused to the carboxyl-terminal 208 residue segment of M13 phage pIII. The expression of both the light chain and the heavy chain-p3 fusion were placed under the control of the phoA promotor.

The library was constructed as follows. Oligonucleotides that encode biased amino acid mixture (indicated as "X"s in Figure 1B) for CDR-L3 and H3 were synthesized using a custom-made trimer phosphoramidite mixture (Glen Research, Sterling, VA) on an Expedite synthesizer (ABI) following instructions from Glen Research. After deprotection, the oligonucleotides were purified using acrylamide gel electrophoresis. Oligonucleotides for CDR-H1 and H2 that did not require the use of trimer phosphoramidetes were purchased from Integrated DNA Technologies. These oligonucleotides were used to introduce mutations of CDR-L3, CDR-H1, CDR-H2 and CDR-H3 using the Kunkel mutagenesis method [30]. After the initial transformation of the SS320 cells [30], the DNA for the library was purified and digested with BamHI and then used to transform the SS320 cells and produce phage particles, as described [27]. In this manner clones harboring non-mutated CDR-H3 were eliminated. This Fab library, "Library E," contained approximately 10^{10} independent clones.

Selection of phage-displayed antibody fragments. The library sorting was performed as previously described [27] with minor modifications. From the second

round on, enriched phages were first incubated with streptavidin-coated magnetic beads, and phages that bound to the beads were removed. The "precleared" phages were then incubated with biotinylated pMHCs in solution and then captured with the streptavidin-coated magnetic beads. The pMHC concentrations used were 100, 50, 10 and 10 nM for the first, second, third and fourth rounds, respectively. Phages captured on the beads were eluted in 100 µl of 0.1M Gly-HCl (pH 2.1) buffer and immediately neutralized with 35 µl of 1M Tris-Cl buffer (pH 8). Recovered clones were analyzed using phage ELISA and DNA sequencing as described previously [27].

Expression and purification of soluble recombinant Fabs. The phage-display vectors for the isolated clones were converted into Fab expression vectors by inserting a gene segment encoding an 8x histidine tag and a termination codon at the 3' end of the heavy chain gene. The carboxyl terminus of the light chain encoded a substrate tag for the biotin ligase BirA (AviTag, Avidity, LLC.). Fab proteins were expressed in the 55244 *E. coli* strain (ATCC) and purified using protein A affinity chromatography followed by cation exchange chromatography as described previously [27]. Approximately 2-5 mg of purified Fab were routinely obtained from 1 L bacterial culture. SDS-PAGE analysis showed that Fabs were in >90% purity.

Surface plasmon resonance experiments. Approximately three hundred response units (RUs) of each antibody fragment were bound to respective flow channels in a Biacore Ni-NTA sensor chip (GE Healthcare) using the 8x histidine tag on the antibody fragments. Soluble class I MHC (analyte) at concentrations ranging

from 200 nM to 1 nM in two fold dilutions was injected onto the surface at a flow rate of 20 µl/min in a 60-s pulse. The NTA surface was regenerated using 0.2 M EDTA to remove all bound protein and then recharged with 0.04 M $NiSO_4$. The procedure was repeated until at least three curves were obtained for each concentration of analyte. Curves obtained at each concentration were double referenced by first, subtracting the signal from the reference surface that contained no Fab from the signal for the reaction surface followed by subtraction of the average signal obtained from a set of buffer injections [31]. Data were processed using Scrubber (BioLogic Software, Campbell, Australia). The suitability of the fit was measured based on the appearance of residuals and χ^2 values. For each Fab-pMHC binding curve, the predicted curves visually overlaid well with the experimental curves. The residuals also were small and random and χ^2 was below 1.

Production of Fab tetramers. Purified Fabs were biotinylated using a site-specific biotin-ligase BirA (Avidity, LLC; Aurora, Colorado) according to the manufacturer's instructions. As described above for the biotinylation of pMHC, successful biotinylation of the Fabs was confirmed by gel shift analysis. Biotinylated Fabs were incubated with streptavidin-alexa 647 (Invitrogen, Inc.) at a 4 to 1 molar ratio for ten minutes at room temperature to make the Fab tetramers.

Flow cytometric analysis of peptide-loaded HLA-A2 on cell surface. T2 cells are deficient in the TAP1 and TAP2 proteins that are responsible for transporting antigenic peptides from the cytoplasm to the endoplasmic reticulum, but are able to be loaded with exogenous peptides for loading of HLA-A2 molecules on their cell surface. T2 cells (1×10^6/ml) were incubated in RPMI medium and incubated with

one of the peptides E75, ML, IL, YM, RL, HL, KT, or IL (50 mM) overnight. After the incubation, the cells were washed to remove the excess peptide and incubated with either BB7.2 Ab (0.5 mg/ml) to detect the level of HLA-A2 molecules present on the surface or the complex of biotinylated fE75 or fML1 with streptavidin-alexa 647 (Invitrogen, Inc.) for 30 min. at 4°C. Incubating the T2 cells with peptides leads to an observable increase in BB7.2 staining compared with untreated cells. In all experiments, the IgG2b isotype control was included for determining nonspecific binding. Flow cytometry data were analyzed using Summit software (Beckman Coulter, Inc.).

Tumor cell staining. All adherent tumor cell lines were detached from the tissue culture flask using 1 x trypsin/EDTA (Sigma-Aldrich, LLC). Cells were washed and then incubated with anti-HER2/neu antibody (Anti-c-erb B-2 Ab-2, 9G6.10) for 30 min. at 4°C followed by incubation with Alexa Fluor 647 labeled Goat anti-mouse IgG1 and PE labeled HLA-A2 clone BB7.2 to analyze the phenotype of each tumor cell line. Separately, each tumor cell line was prepared as before, but stained with Fab-Alexa Fluor 647-streptavidin tetramer for 30 min. at 4°C. After the final staining incubation, cells were washed and analyzed by flow cytometry (Cyan, Beckman Coulter, Inc.). Pearson's correlation coefficient and multiple linear regression analysis were completed for the mean and median fluorescence intensity observed for each cell line's HLA-A2, Her2/neu, and Fab staining. No difference was observed whether mean or median fluorescence was used for the analysis.

DOTA conjugation and ^{64}Cu radiolabeling. All solvents were prepared from 18MΩ water and eluted from a column of chelex 100 (Serological Research Institute)

to remove metals from all buffers. Free metals were removed from purified Fabs by dialysis twice with 1L of 0.2 M $NaHCO_3$ at pH 8.2. Fabs were conjugated to S-2-(4-Isothiocyanatobenzyl-)1,4,7,10-tetraazacyclo-dodecane-tetraacetic acid (DOTA-NCS) purchased from Macrocyclics (Dalax, TX) by using the isothiocyanate linkage method as described previously [32]. The molar ratio of the DOTA conjugate to Fab used was 5:1. The reaction proceeded at pH 8.2 in 0.2 M $NaHCO_3$ over 18 hours at room temperature. Unconjugated DOTA was removed from the reaction by a PD-10 desalting column (GE Healthcare). The average number of chelates per Fab was determined as described previously [33]. The positron emitting isotope ^{64}Cu (copper chloride in 0.1 mol/L HCl; radionuclide purity, >99%) was provided by Mallinckrodt Institute of Radiology (Washington University School of Medicine, St. Louis, WA). The DOTA-conjugated Fab (20 μM) was incubated with approximately 1.5 mCi of $^{64}CuCl_2$ in 1.0 mM citric acid (pH 5.5). The solution was incubated for 1 hr at 40 °C. The reaction was monitored by TLC (silica) and developed with 0.1 M ammonium acetate (25%)/0.001 M citric acid (25%) / methanol (50%). Free ^{64}Cu was complexed as ^{64}Cu citrate with an Rf>0.5 and ^{64}Cu DOTA-Fab had an Rf<0.5. The radiochemical yield was determined to be > 97.0%.

Cell binding assay of radiolabeled fE75 Fab. The SKOV3 cells transfected with HLA-A2 were harvested as previously described for tumor cell staining. The cells were incubated with the purified ^{64}Cu DOTA-Fab at increasing concentrations for 30 min. at 4°C. As a demonstration of specificity, the SKOV3 transfected HLA-A2 cell line was incubated with ^{64}Cu DOTA-Fab at increasing concentrations and 300 nM soluble E75/HLA-A2 pMHC. Following the incubation, the cells were washed twice

and then the bound radiolabeled fE75 counts per minute (cpm) was measured with a 2470 WIZARD^2 automatic gamma counter (PerkinElmer Inc.).

Micro Positron Emission Tomography/Computed Tomography (microPET-CT) imaging in tumor-bearing mice. The preliminary experiments used NOD.SCID (SCID) mice with single tumors injected subcutaneously into the flank of the mouse. SCID and HLA-A2 transgenic NOD.SCID mice were a gift from Dr. Jeffrey Frelinger (Department of Immunobiology, University of Arizona) [34]. All SCID mice were injected subcutaneously on either the right or left flank with either negative control tumors 1 x 10^6 SKOV3 (4 mice) or positive tumors SKOV3 transfected HLA-A2 cells (3 mice). Following these experiments, we used HLA-A2 transgenic SCID mice and because of limitations in the number of available mice, injected both tumors on opposite flanks of each mouse. The HLA-A2 transgenic SCID mice were injected with 1 x 10^6 MDA-MB-231 cells and SKOV3 cells on opposite flanks (3 mice). Mice were monitored every other day by palpation and the size of tumor growth was measured. Once the tumor growth could be observed by palpation, mice were injected with the Fab and imaged using a microPET-CT (eXplore Vista PET-CT, GE HealthCare, Inc.). Mice were injected with approximately 20 μg of ^{64}Cu-DOTA-Fab (specific activity: 50-60 μCi/μg) in PBS via the tail vein. For all scans, mice were anesthetized using 2% isoflurane, positioned in a prone position along the long axis of the microPET scanner and imaged. Dynamic PET acquisitions were taken over the first hour for selected mice. Static acquisitions were taken for 10 min. at one-hour post injection for all mice. All mice were additionally imaged by micro computed tomography (microCT) prior to the microPET scan in the same

bedposition for anatomical reference. Following the imaging, tumors were excised, cryopreserved with liquid nitrogen, and cryosectioned for radiographic analysis. PET images were reconstructed using an ordered subsets-expectation maximization (OSEM) algorithm with scatter, random, and attenuation corrections, and the PET pixel size was 0.3875 x 0.3875 x 0.775 mm [35]. Standardized uptake values (SUVs) were calculated pixel-wise by normalizing for injected dose and animal mass. The PET images were coregistered with the microCT images using the scanner software for identification of anatomical structures. Reconstructed microPET and microCT images were viewed and regions of interest (ROIs) drawn and SUVs quantified using AMIDE [36]. Tumor ROIs were drawn manually to avoid adjacent organs and tumor metastases because the metastases typically had very poorly defined borders. Average SUV was measured for each specified ROI. The student's t test was used to compare the SUVs from single tumor bearing SCID mice. The paired student's t test was used to compare the SUVs from the tumors of the double tumor-bearing, HLA-A2-transgenic SCID mice.

2.3 Results

Generation of synthetic antibody-fragments specific to pMHC complexes. Our goal is to develop tools to target specific tumor cells *in vivo* for diagnostic testing and treatment. We hypothesized that peptides bound to MHC would be good targets for such tools. The HER2/neu peptide E75 (KIFGSLAFL) was selected for analysis based on its clinical relevance to HER2/neu over-expression [37-39] and the success of E75 peptide vaccines and targeting using E75 in peptide-pulsed dendritic cell immunization therapies [40,41]. It has been notoriously difficult to

create monoclonal antibodies (mAb) to specific peptide/MHC complexes, presumably because of the sequence conservation between MHC molecules injected and present in the immunized mouse [42].

As an alternative to conventional mAb production, we sought to isolate antibody-fragments (Fabs) specific for peptide-bound MHC molecules using phage-display technology. We utilized a "synthetic" antibody library built on a highly stable 4D5 Fab scaffold (Figure 1A) [43] in which the amino acid diversity in the Complementarity Determining Regions (CDR) was designed using simple but highly tailored amino acid mixtures [27]. Because such synthetic antibody libraries are not subjected to clonal selection against self-antigens, unlike common recombinant antibodies derived from natural immune systems, we felt that synthetic antibody libraries, coupled with phage-display selection, offered a particularly effective approach to generating antibodies to pMHCs. Based on our previous work [27], we constructed a new antibody library in which four of the six CDRs were diversified, as described in Figure 1B. This library is similar to "Library D" of Fellouse et al. [27], but its amino acid diversity in CDR-L3 was expanded and also the composition of the expanded amino acid diversity, designated as X in Figure 1, was modified based on the analysis of antibody clones isolated from Library D [27].

We used the HER2/neu derived peptide, E75 (KIFGSLAFL), or calreticulin derived peptide, ML (MLSVPLLL), bound to the human MHC molecule HLA-A2 as the targets for sorting the synthetic antibody library. After four rounds of selection, an ELISA was used to test for specificity of the amplified phage Figure 1C. We identified three distinct classes of antibodies: (i) selective to E75/HLA-A2, (ii)

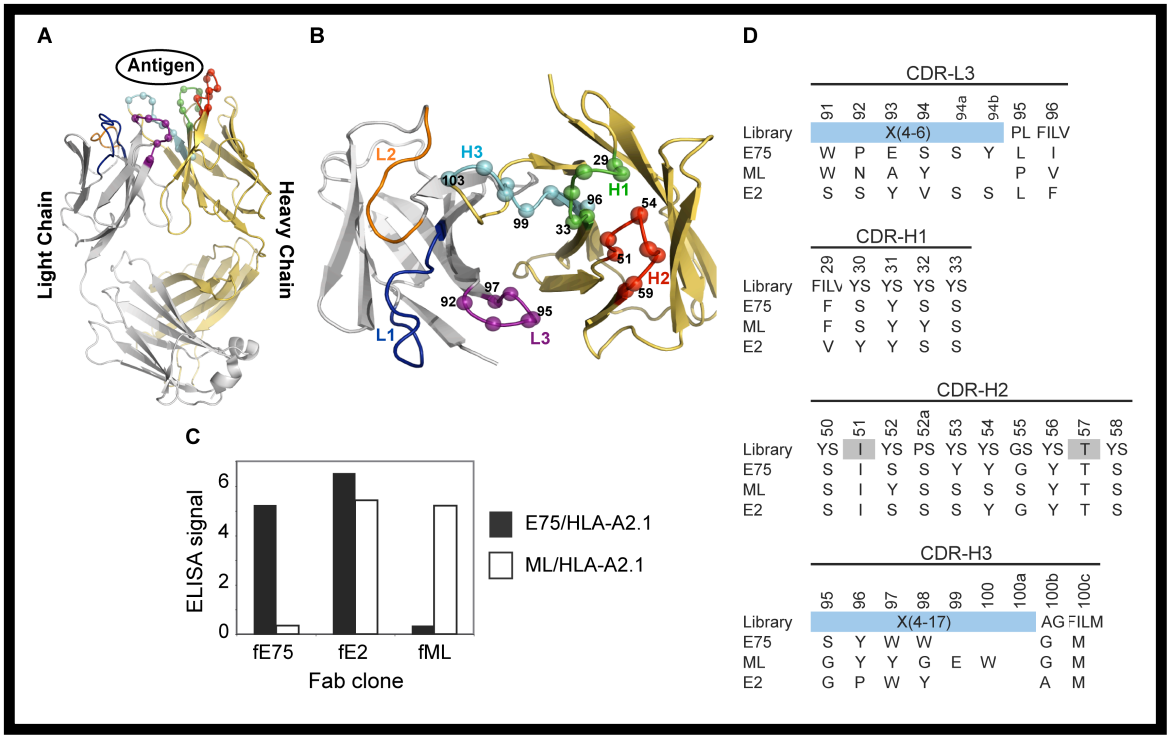

Figure 1: Phage-Display isolation of Fabs specific for pMHC molecules. Fabs specific for either E75/HLA-A2 or ML/HLA-A2 molecules were selected by phage-display technology. Each Fab construct was built from the highly stable 4D5 Fab scaffold containing both a heavy and light chain each with a single variable and constant domain (modeled from PDB ID: 1FVD) (A). The diversity of the Complementary Determining Regions (CDR) for the heavy chain; H1, H2, and H3, and the light chain; L3, was restricted in favor of tyrosine, serine, and other small amino acids. The Cα atoms of the synthetically modified H1, H2, H3, and L3 regions are shown as spheres (B). After three rounds of selection, an ELISA was used to test the specificity of the amplified clones (C). Three clones with three different specificities were identified. The Fab clones fE75 and fML bound E75/HLA-A2 and ML/HLA-A2 respectively with no detectable binding to the opposite pMHC molecule. The Fab clone fE2 showed binding to both E75/HLA-A2 and ML-HLA-A2. Following each Fab clone's specificity determination, the amino acid sequence of each clone was determined (D).

selective to ML/HLA-A2, and (iii) cross-reactive to the two pMHCs. Two clones, fE75 and fML, selective to E75/HLA-A2 and ML/HLA-A2 respectively, were chosen for further study based on the phage ELISA, which identified each phage clone to have high affinity and specificity for their respective pMHC. As expected, the two clones have distinct CDR sequences (Figure 1D).

To assess the binding affinity, kinetics and specificity of the two Fabs, they were produced as soluble proteins, with a His-tag at the C-terminus of the heavy chain and a biotinylation tag at the C-terminus of the light chain and characterized using Surface Plasmon Resonance. The results shown in Figure 2 demonstrate that the model appropriately describes the binding responses of each Fab for its cognate pMHC molecule, with curve fitting residuals at or below 1 RU. The K_D value for fE75 binding E75/HLA-A2 was determined to be 59 +/- 4 nM based on three separate experiments (Figure 2A). The K_D for fML binding ML/HLA-A2 was 79 +/- 4 nM based on three separate experiments (Figure 2D). No binding was observed for fE75 and fML binding the non-cognate pMHC (Figure 2B, 2C), or to other non-cognate pMHC molecules that differed in peptide alone or unrelated peptide bound to unrelated MHC (data not shown).

Fabs bind to cell surface pMHC. In order to test whether these Fabs can be used to find specific pMHC on the cell surface, Fab-displaying streptavidin tetramers were made and used to bind to peptide pulsed T2 cells. The T2 cell line is deficient in pMHC cell surface expression due to the absence of the transporter associated with antigen processing (TAP1 and TAP2). The MHC HLA-A2 on the surface of T2 cells is more “peptide-receptive” than on normal cells and therefore; specific

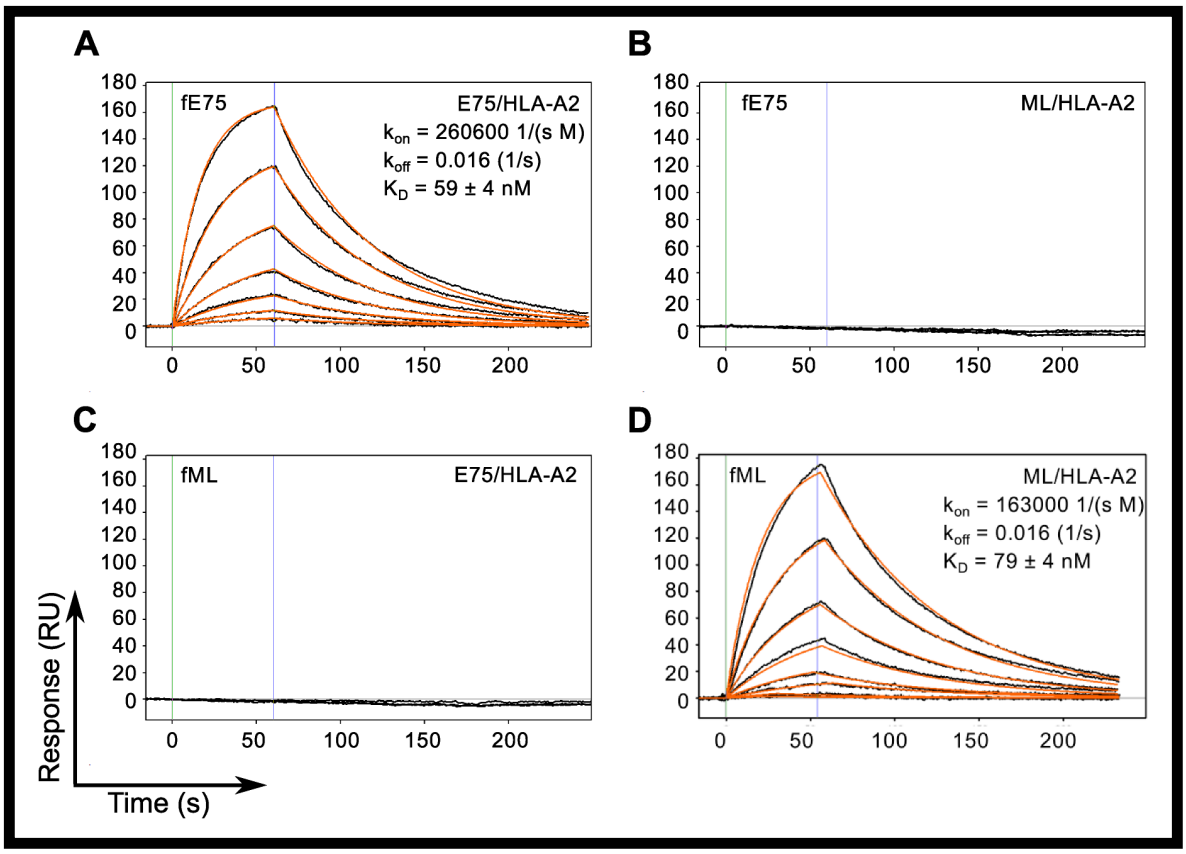

Figure 2. TCR-like Fabs Bind Cognate pMHC with Nanomolar Affinity. SPR binding response curves of fE75 binding E75/HLA-A2 (A) and ML/HLA-A2 (B) and fML binding E75/HLA-A2 (C) and ML/HLA-A2 (D) are shown. Each Fab was immobilized onto individual flow channels in an NTA-Ni chip. Kinetic data for each Fab binding each pMHC molecule were globally fit to a bimolecular reaction. Green and blue lines designate the start and end respectively of each pMHC injection. Binding curves and curve fits are drawn in black and orange respectively. Each binding curve represents a different concentration of pMHC beginning at 200 nM and decreasing to 1.5 nM in 2 fold dilutions. No binding was observed for either Fab binding non-cognate pMHC molecules up to 400 nM.

peptides may be loaded onto HLA-A2 by incubating these cells with exogenous peptides [44]. T2 cells were incubated with ML, E75 or control peptides. The biotinylated Fabs were respectively conjugated to fluorescently-labeled streptavidin to form “Fab tetramers”. The fE75 tetramer bound to T2 cells incubated with E75 (Figure 3A), but not to untreated cells. Similarly, the fML tetramer bound to T2 cells incubated with ML (Figure 3B), but not to untreated cells. Additionally, neither Fab bound to T2 cells incubated with any of the control peptides (Figure 3C). Therefore, in agreement with the SPR experiments, these Fabs bound specifically to their cognate pMHC expressed on the cell surface.

The Fabs detect endogenously processed and presented pMHC complexes. Addition of exogenous peptide to T2 cells generates a much higher density of the particular peptide/MHC molecule on the cell surface compared with endogenous levels found on normal TAP expressing cell types [45,46]. Thus, we evaluated the ability of fE75 and fML to recognize physiological levels of peptide presented by the HLA-A2 molecule using flow cytometric analysis of several human tumor cell lines: MDA-MB-231 breast tumor cells (HLA-A2^{pos} and HER2/neu^{pos}); SKOV3 HLA-A2 transfected ovarian tumor cells (HLA-A2^{pos} and HER2/neu^{pos}); MCF7 breast tumor cells (HLA-A2^{pos} and HER2/neu^{pos}); LNCaP prostate tumor cells (HLA-A2^{pos} and HER2/neu^{pos}); and negative control SKOV3 ovarian tumor cells (HLA-A2^{neg} and HER2/neu^{pos}). All the cell lines express HER2/neu at varying levels. Thus, as anticipated, the HLA-A2 positive human cell lines showed variable fE75 binding compared to the negative control tumor cell line SKOV3 (HLA-A2^{neg}) as shown in Figure 3D. All of the HLA-A2 positive cell lines had similar binding of the fML Fab

(Figure 3E), but comparable to fE75, neither Fab bound to the HLA-A2 negative control cell line SKOV3 (Figure 3F). In addition, a further control was added with a CHO cell line transfected with HLA-A2. This cell line was HLA-A2 positive but HER2/neu negative. No binding of either fE75 or fML1 was observed for this cell line (data not shown).

Next, we sought to understand the cause for the differences in fE75 binding to the tumor cell lines in order to improve our ability to use the TCR-like Fabs as diagnostic and treatment tools. The cell surface level of peptide/HLA-A2 complexes is dependent on multiple parameters including: protein antigen availability, peptide generation by the proteasome, antigen processing, and MHC expression [47]. The data allow us to determine which protein plays a more important role in the level of any particular pMHC complex at the cell surface: MHC (HLA-A2) or antigen (HER2/neu). We measured HER2/neu and HLA-A2 expression by flow cytometry. There were significant differences in both HLA-A2 expression and HER2/neu levels between the cell lines (Figure 4A-F). The MDA-MB-231 cell line had the highest level of HLA-A2 expression, but also the lowest HER2/neu levels. Both MCF7 and LNCaP cell lines had intermediate levels of HER2/neu, but lower expression of HLA-A2. The SKOV3 HLA-A2 cell line had the highest level of HER2/neu and the second highest MFI of HLA-A2.

Simple two-dimensional linear regression analysis models showed weak correlation of fE75 MFI with HLA-A2 (r^2=0.40) and weak, but stronger correlation with HER2/neu expression (r^2=0.62) (Figure 4 G-H). Both of the regression analyses were dominated by the contribution made by MDA-MB-231. If that cell line

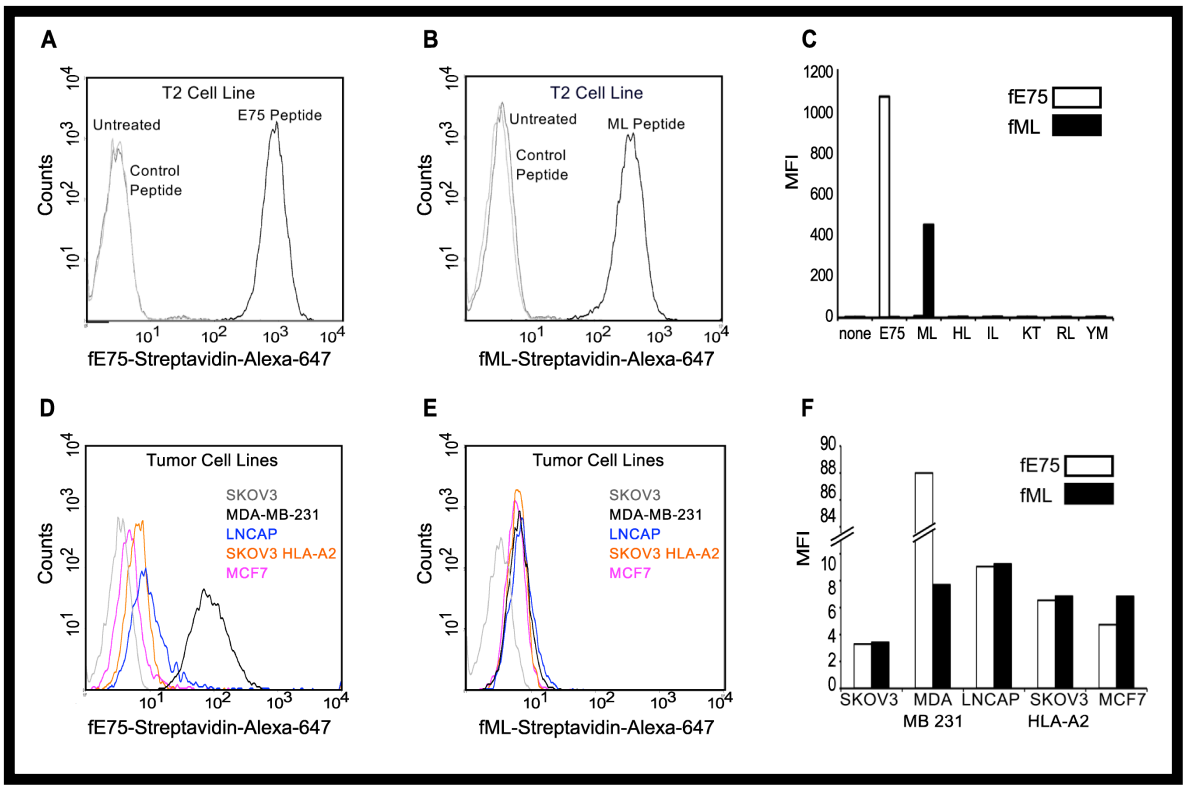

Figure 3. Fabs bind specifically to endogenously processed and presented levels of pMHC molecules. Flow cytometric analysis revealed that the Fab tetramer, composed of biotinylated fE75 (A) or fML (B) and streptavidin-Alexa-647, bound to T2 cells incubated with the cognate peptide, but not to control peptides or untreated T2 cells in three separate experiments. In C, a graph of the MFI for several other control peptides against the cognate peptide for each Fab was shown. The staining of HER2/neu positive tumor cell lines by the fE75 and fML tetramers was shown in D and E respectively. The graph of the MFI for one representative experiment from four total was shown in F.

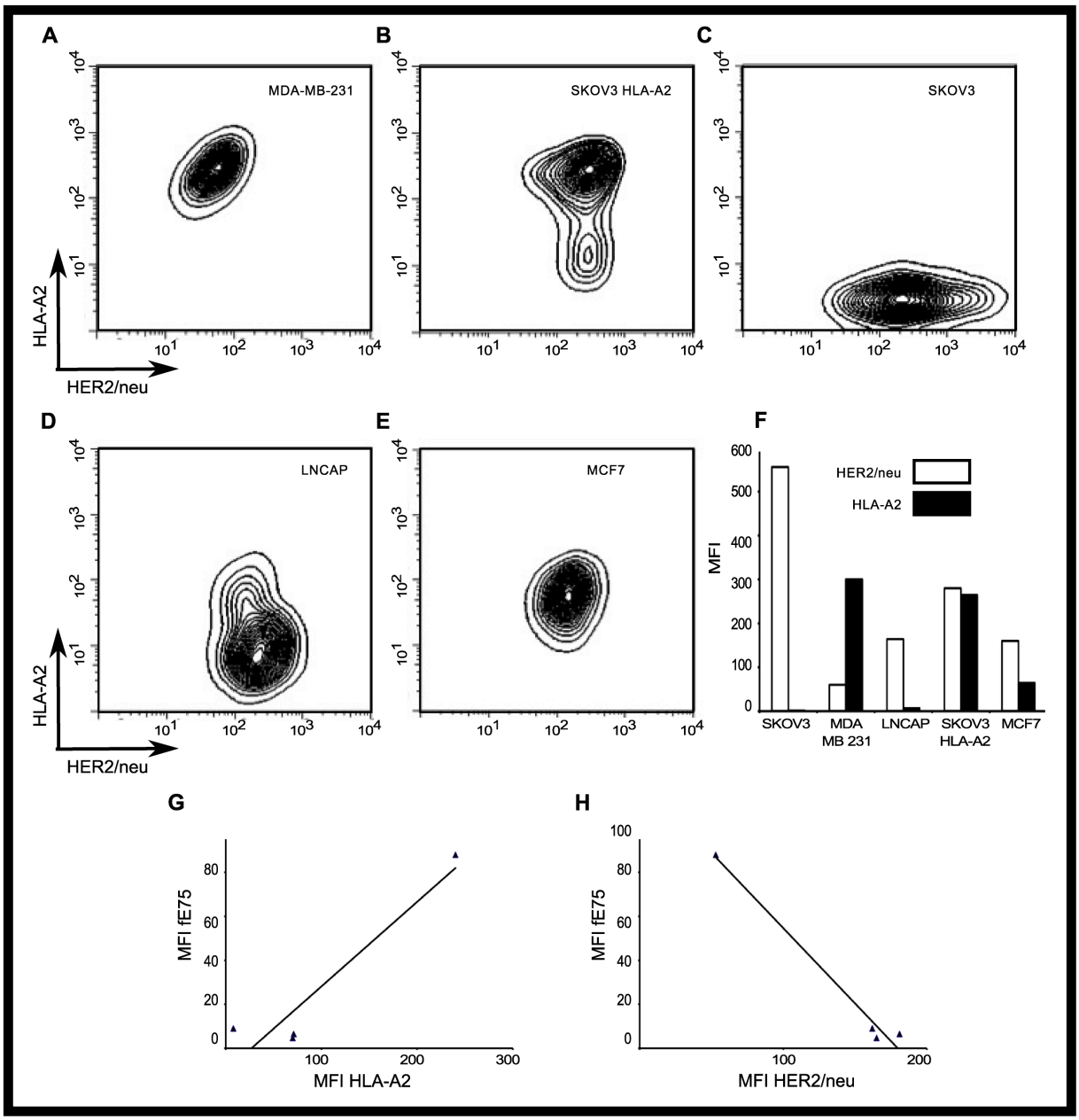

Figure 4. HLA-A2 and HER2/neu expression is high variable on each tumor cell line. The surface expression of HLA-A2 and HER2/neu for each human tumor cell line was measured by flow cytometry. The representative plots of HLA-A2 versus HER2/neu for each tumor cell line were shown in A-E. In F, a graph of the MFI of one representative experiment from four total was shown. G and H were plots of the MFI of fE75 versus the MFI of HLA-A2 or MFI of HER2/neu respectively. Simple two-dimensional linear regression analysis models do not model the system well. The black lines showed weak correlation of fE75 MFI with HLA-A2 (r^2=0.40) or HER2/neu expression (r^2=0.62).

were removed from the analysis, no correlation exists for fE75 MFI and HLA-A2 (r^2=0.09) nor HER2/neu (r^2=0.00). Since that is not meaningful biologically and we know that fE75 binding did vary for each cell line, we know that either there was another unknown important factor or that both HLA-A2 and HER2/neu influenced fE75 binding. The coordinated involvement of both HLA-A2 and HER2/neu on fE75 levels was modeled using multi-parameter linear regression analysis [48]. This model gave an excellent fit for the correlation of fE75 binding using both HLA-A2 and HER2/neu expression levels (r^2=0.97). Removing the MDA-MB-231 cell line from this analysis showed that there was still a significant correlation (r^2=0.89), suggesting that even though MDA-MB-231 appears to dominate the regression, the correlation between fE75 binding and both HLA-A2 and HER2/neu is valid even without the MDA-MB-231 cell line. These data show that both MHC expression levels and the antigen expression affect pMHC expression on tumor cell lines. Both MHC and source of the peptide antigen must be considered in order to accurately predict pMHC expression levels.

The TCR-like Fab recognizes E75/HLA-A2 positive tumors in a xenotransplanted-tumor mouse model. To address whether the TCR-like Fabs can be used *in vivo*, we used positron emission tomography-computed tomography (PET-CT), which provides excellent sensitivity to radiolabels, allowing quantification of the uptake of the imaging agent at the tumor [49]. The Fab, fE75, was made into a PET imaging agent by attaching a chelator, S-2-(4-Isothiocyanatobenzyl)-1,4,7,10-tetraazacyclo-dodecane-tetraacetic acid (DOTA-NCS). The DOTA chelator provides flexibility as it can chelate both ^{64}Cu for PET and ^{111}In for single-photon emission

computed tomography (SPECT). We routinely obtained an average of 0.7 moles of DOTA per mole of fE75. The yield of ^{64}Cu- fE75-DOTA conjugate was obtained in greater than 95% purity as determined by thin layer chromatography. To confirm that addition of this chelator and the radioactive metal did not alter the binding affinity of fE75 for E75/HLA-A2, in *vitro* cell binding studies were performed. The ovarian tumor cell line SKOV3 transfected with HLA-A2 was incubated with a range of concentrations of radiolabeled Fab. A Scatchard analysis was used to calculate a binding affinity of 111 nM (95% CI: 63-159), which was in good agreement with the SPR data (59 +/- 4 nM). The ^{64}Cu- DOTA-fE75- conjugate maintained its specificity for E75/HLA-A2, as soluble recombinant E75/HLA-A2 complexes were able to block binding of the radio-labeled fE75 to SKOV3/HLA-A2 cells (Figure S1).

The first test of uptake of the labeled fE75 used severe combined immunodeficiency (SCID) mice. These mice do not express either human HER2/neu or HLA-A2. The question asked is whether once the Fab is injected into the tail vein, will it be able to accumulate in the tumor. The ^{64}Cu- DOTA-fE75 conjugate was injected via the tail vein of SCID mice bearing either xenotransplanted SKOV3 or SKOV3 HLA-A2 tumors. MicroPET (color) and microCT (black and white) images of the mice were collected and overlayed (Figure 5A and5B). The xenografted human tumors on either the left or right flanks were clearly identifiable in all microPET/CT images. The relatively small size of the Fab (~55 kDa) was below the renal clearance threshold of approximately 64 kDa meaning that it should be rapidly eliminated by renal clearance [50-55]. Literature indicated that the large signal from the liver might be attributed to Cu/Zn superoxide

dismutase (SOD1), chelation of the ^{64}Cu [56,57]. Tumors have been shown to trap injected materials non-specifically [58], but, there was very little uptake of ^{64}Cu-DOTA-fE75 in the HLA-A2 negative SKOV3 control tumor (Figure 5A,C; labeled ct) suggesting that this is not a significant problem in our model. In contrast, there was easily observable uptake of the fE75 imaging agent in the HLA-A2 positive tumor (Figure 5B,D; labeled pt). Even after one hour, increased up-take at the HLA-A2 positive tumor sites was observed, but not at the negative control tumor. Accumulation of ^{64}Cu-DOTA-fE75 was observed at the edges of the tumor that suggested at first that the Fab did not penetrate the tumor well. However, visual inspection of the sectioned tumor showed necrosis in the center of the tumor and radiography of the tumors (Figure S2) showed that the Fab was bound appropriately on the outside where live tissue remains. PET/CT images of additional human tumor bearing SCID mice were shown in Figure S3. These data showed that the Fab does accumulate at the site of the correct tumor.

Dynamic scans over the course of sixty minutes (Figure 5E and 5F), show that there is an initial rapid accumulation of ^{64}Cu- DOTA-fE75 followed by a steady-state in all the tissues (liver, kidney, humoral muscle, and control tumor) except for the HLA-A2 positive tumor. The HLA-A2 positive tumors showed initial rapid accumulation followed by a steady rise in the ^{64}Cu- fE75-DOTA signal suggesting that specific binding occurs. The ratio of the slope of the Standard Uptake Values (SUVs) from 300 to 3600 sec. for the HLA-A2 positive tumors compared to the HLA-A2 negative control tumors was 6.6. This was expected if ^{64}Cu-DOTA-fE75 were to accumulate due to binding to its cognate pMHC, E75/HLA-A2, at the HLA-A2

positive tumors. Furthermore, an unpaired t test analysis of the SUVs of the ^{64}Cu-DOTA-fE75 signal sixty minutes post injection gave a statistically significant difference between the HLA-A2 positive tumors and the HLA-A2 negative tumors ($p < 0.004$, $n=4$). Together these experiments demonstrate that the fE75 Fab can accumulate in tumors that present E75/HLA-A2 on their cell surface *in vivo*.

While the experiments above show that ^{64}Cu-DOTA-fE75 can target a pMHC *in vivo*, they do not mimic an important consideration for human use. In humans, most cells in the body express HLA-A2 bound numerous different peptides found in each cell type [59,60]. If the ^{64}Cu-DOTA-fE75 imaging agent has a small degree of non-specific binding to HLA-A2 with other peptides, we would not see accumulation at the tumor because the Fab would be greatly diluted by the nonspecific binding before arriving at the tumor. Thus, we used an HLA-A2 transgenic mouse crossed to the SCID background, which allows for the tumors to grow and for all of the mouse cells to express HLA-A2. The HLA-A2 transgenic SCID mice were xenografted with the SKOV3 (control tumor, ct) and MDA-MB-231 (positive tumor, pt) (Figure 6A,B and Figure S3C). Dynamic scans were obtained over sixty minutes following tail-vein injection of ^{64}Cu-DOTA-fE75 (Figure 6C). The dynamic curves from the HLA-A2 transgenic SCID mice were similar to what was seen in the SCID mice that did not express HLA-A2 (Figure 5E-F). The ratio of the calculated slopes of the SUVs from 300-3600s for the HLA-A2 positive tumor compared to the HLA-A2 negative control tumor was 3.8, again indicating positive accumulation of ^{64}Cu-DOTA-fE75 at the HLA-A2 positive tumor. Furthermore, comparison of the SUVs sixty minutes post injection showed that the human tumors positive for HLA-A2 and

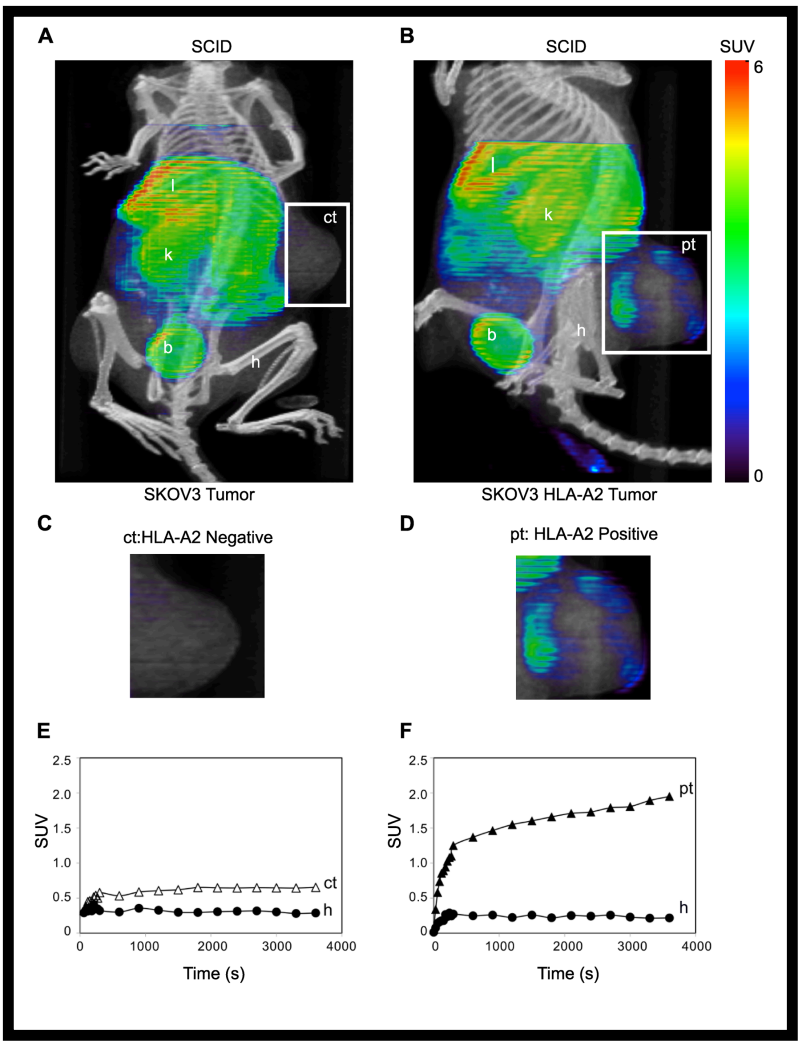

Figure 5. TCR-like Fab binds specifically to human tumor cells in SCID mice. Mice were injected intravenously with ^{64}Cu-DOTA-fE75, which binds to tumors expressing both HLA-A2 and HER2/neu *in vivo*. Coronal views of small-animal PET images with coregistered CT images of SCID mice bearing human tumor (SKOV3 or SKOV3 HLA-A2) xenografts (A and B) in flanks at 1 h post-injection. Intensities of PET slices were scaled to the same maximum. Cropped views of only the tumors designated by the white boxes for the mice presented in A and B were shown in C and D respectively. The standardized uptake values (SUV) for ^{64}Cu-DOTA-fE75 in the tumors and selected organs over time were shown below each respective mouse (E and F). B = bladder, h = humeral muscle, k = kidneys, l = liver, ct = control HLA-A2 negative tumor; SKOV3 cell line, pt = HLA-A2 positive tumor; SKOV3 HLA-A2.

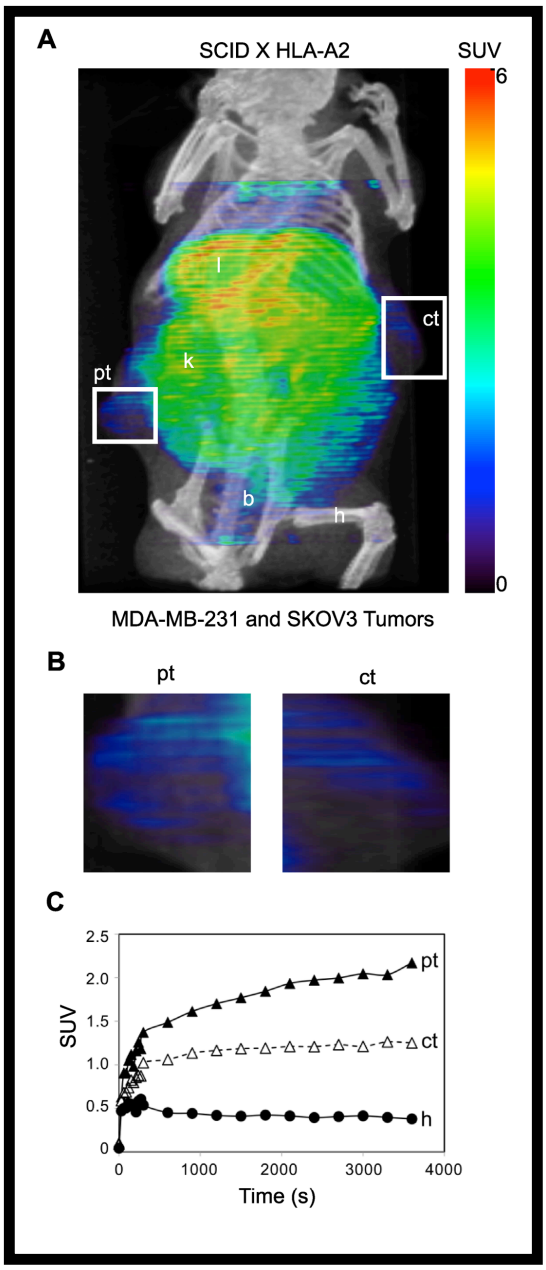

Figure 6. TCR-like Fab binds specifically to human tumor cells in HLA-A2 transgenic SCID mice. Similarly as describe for the SCID mice experiments (Figure 5), HLA-A2 transgenic SCID mice were injected intravenously with ^{64}Cu-DOTA-fE75. Coronal views of the small-animal PET image with coregistered CT images of a scid HLA-A2 transgenic mouse bearing human tumor (MDA-MB-231 and SKOV3) xenographs (A) in flanks at 1 h post-injection. Intensities of PET slices were scaled to the same maximum. Cropped views of only the tumors designated by the white boxes were shown in B respectively. The standardized uptake values (SUV) for ^{64}Cu-DOTA-fE75 in the tumors and selected organs over time were shown in C. B = bladder, h = humeral muscle, k = kidneys, l = liver, ct = control HLA-A2 negative tumor; SKOV3 cell line, pt = HLA-A2 positive tumor; MDA-MB-231 cell line.

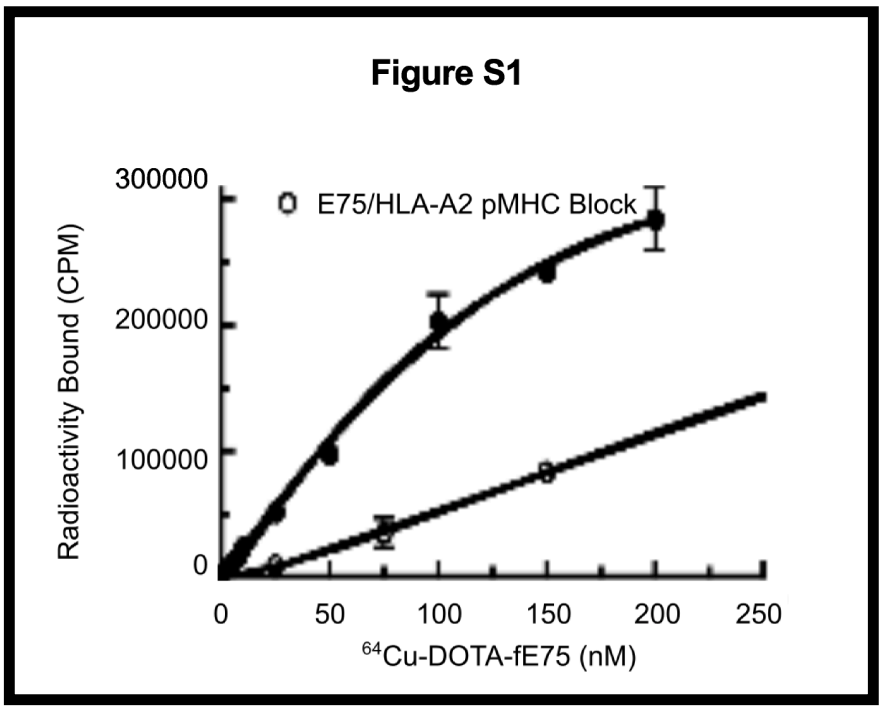

Figure S1. Saturation (•) binding curves of ^{64}Cu-DOTA-fE75 and SKOV3 HLA-A2 (E75/HLA-A2 pMHC positive) cells. Each data point represents the mean ± standard error of the mean of triplicate measurements. The K_D of ^{64}Cu-DOTA-fE75 was determined to be 111 nM (95% CIs: 63-159). ^{64}Cu-DOTA-fE75 binding (O) to SKOV3 HLA-A2 cells blocked by 300 nM soluble E75/HLA-A2 pMHC.

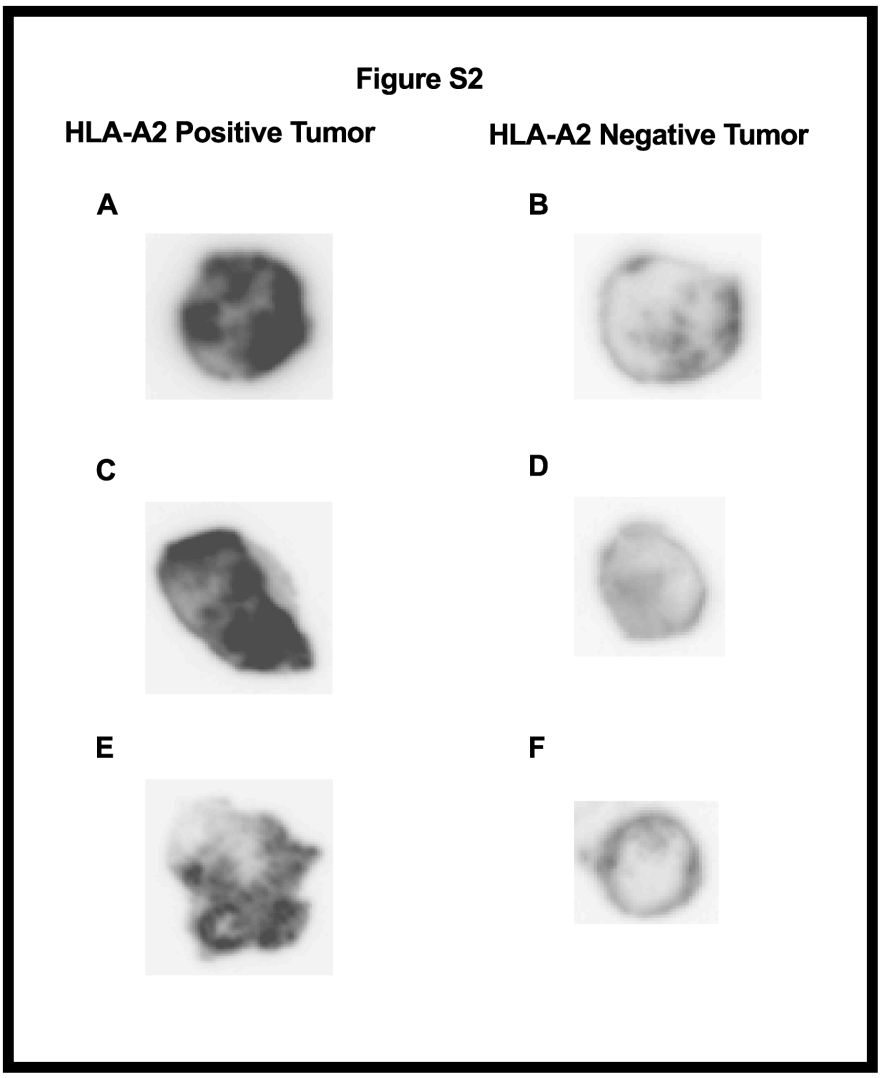

Figure S2. Radiography images of excised human tumors from ^{64}Cu-DOTA-fE75 injected SCID and HLA-A2 transgenic SCID mice. HLA-A2 positive and HLA-A2 negative tumors from SCID mice were shown in A and B. HLA-A2 positive and HLA-A2 negative tumors from HLA-A2 transgenic SCID mice were shown in C-F.

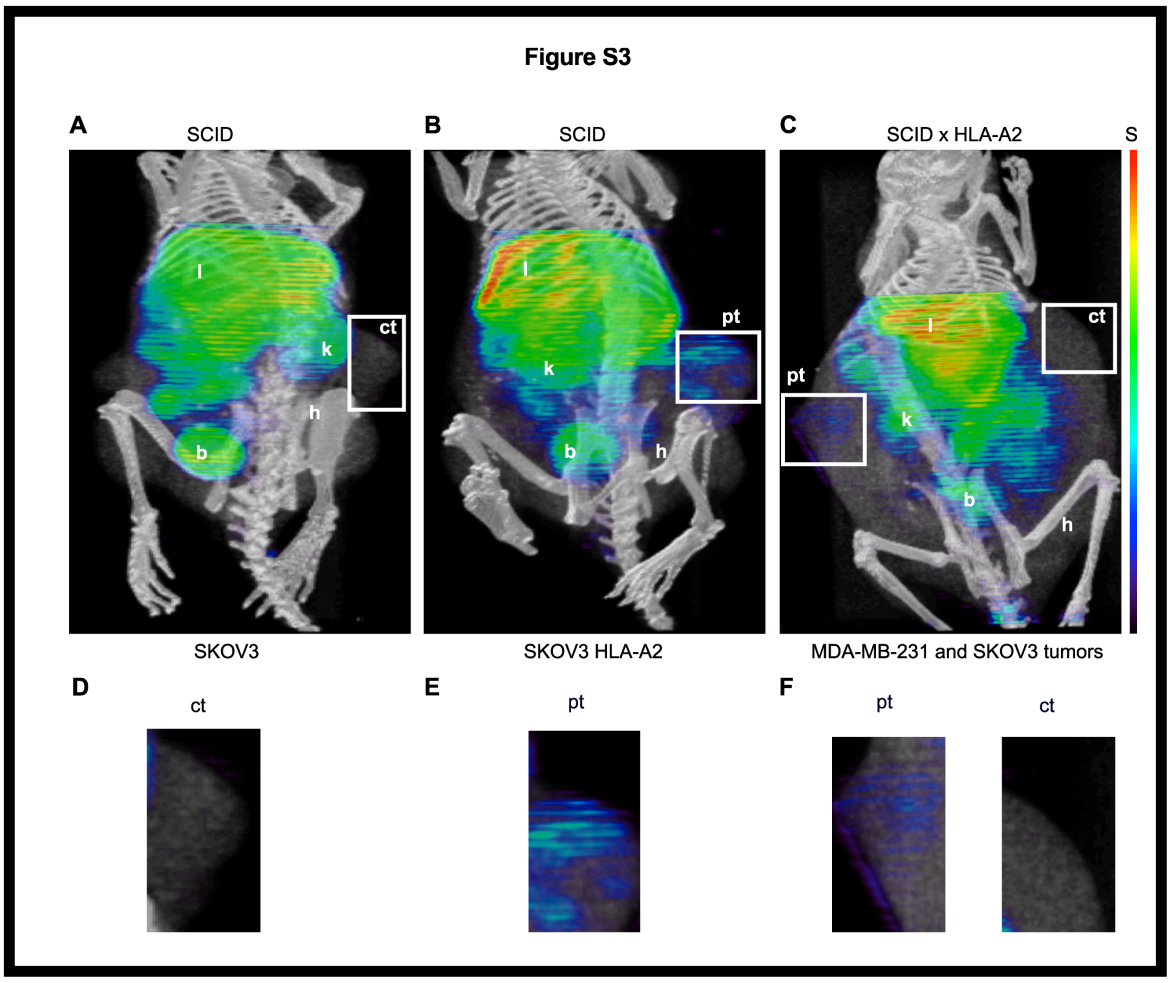

Figure S3. Additional PET/CT images of SCID and HLA-A2 transgenic SCID mice. Mice were injected intravenously with ^{64}Cu-DOTA-fE75, which binds to tumors expressing both HLA-A2 and HER2/neu *in vivo*. Coronal views of small-animal PET images with coregistered CT images of SCID mice bearing human tumor (SKOV3 or SKOV3 HLA-A2) xenografts (A and B) or HLA-A2 transgenic SCID mouse bearing two tumors (SKOV3 and MDA-MB-231) xenografts (C) in flanks at 1 h post-injection were shown. Intensities of PET slices were scaled to the same maximum. Cropped views of only the tumors designated by the white boxes for the mice presented in A, B, and C were shown in D, E and F respectively. B = bladder, h = humeral muscle, k = kidneys, l = liver, ct = control HLA-A2 negative tumor; SKOV3 cell line, pt = HLA-A2 positive tumor; SKOV3 HLA-A2 or MDA-MB-231.

HER2/neu had statistically significant uptake and retention of ^{64}Cu-DOTA-fE75 compared to the negative control tumor SKOV3 (paired t test, $p < 0.03$, $n=4$). This is a significant achievement in specificity because the ^{64}Cu- fE75-DOTA was exposed to millions of HLA-A2 molecules with various peptides and still accumulated at the HLA-A2 positive tumors.

2.4 Discussion

Our long-term goal is to construct a generalized approach to specifically target tumors *in vivo* for diagnostic and therapeutic use. We have used imaging as our first goal because we rationalize that if we can image specifically, we can target therapeutics specifically. We began with the observation that the immune system is fully competent to target tumors *in vivo* [61-70]. A major portion of this response is composed of cytotoxic T cells. T cells are able to recognize peptides derived from proteins in the cells, bound to MHC molecules (pMHC) using their clonotypic T cell receptor [71,72]. Unfortunately for the patient, the tumor infiltrating T cells do not always kill the tumors. As a substitute for tumor specific recombinant T cell receptors, monoclonal antibodies that recognize specific pMHC complexes have been generated [24,45,46,73-80], but usually have low affinities compared to those isolated from bacteriophage libraries [78,81-83]. Rational design of high affinity antibodies directed towards pMHC has yielded affinities in the nanomolar range [84], but that approach is laborious and must be done for each antibody individually.

The Fabs isolated from our synthetic antibody-fragment library have binding affinities in the mid-nM range, consistent with a previous work demonstrating the ability of these synthetic libraries to generate high-affinity antibodies without the

need for affinity maturation [27]. The level of affinity of our Fabs is approximately 1000 times better than that for TCRs binding pMHC, which is typically in the μM range [85]. This is also roughly a 100-fold improvement over TCR-like monoclonal antibodies produced from classical hybridoma technology [86]. These Fab have affinities similar to other peptide/HLA-A2-specific antibodies isolated from bacteriophage libraries [87,88].

Previous studies have suggested that the higher affinity of TCR-like Fab compared to T cell receptor is due to faster on-rates instead of slower off-rates [89]. Our data are partially consistent with this concept as our Fabs bind cognate pMHC with faster rates of association, but our Fabs also show significantly slower rates of dissociation. Therefore, increased affinity of TCR-like Fabs is not solely due to increased on-rates as has been suggested.

Using these Fabs, we have shown that predicting pMHC levels on the cell surface is dependent highly on both MHC and HER2/neu antigen expression. Different tumor cell lines showed varying levels of fE75 binding/staining because they have highly different levels of HLA-A2 and HER2/neu. In agreement with previous data [90], we observed no direct correlation between levels of E75/HLA-A2 detected by fE75 and HER2/neu detected by mAb suggesting that HER2/neu levels are not directly correlated with E75/HLA-A2 levels on the cell's surface. However, multiple components are involved in the levels of any particular pMHC and often these components may affect one another. Logically, it seems likely both HER2/neu and HLA-A2 levels would affect E75/HLA-A2 levels on the cell surface. Multi-parameter linear regression analysis yielded a strong correlation between fE75

binding and the both HLA-A2 and HER2/neu expression. We conclude that both variables, the source protein and MHC levels, are both highly important.

The fE75 Fab was demonstrated to bind selectively to HLA-A2 positive tumors *in vivo* in SCID mice. Thus, fE75, a TCR-like Fab, can be used *in vivo* and potentially used as a drug delivery vehicle. This is consistent with other reports that demonstrate that tumors xenografted in SCID mice were reduced or even eliminated as via complement fixation or induction of apoptosis [24,91]. Moreover, a TCR-like Fab fused to a truncated form of *Pseudomonas* exotoxin, PE38KDEL showed *in vivo* dose dependent xenografted tumor killing in SCID mice [87,92]. Immunotherapy and drug deliver by TCR-like Fabs is possible only if the specificity of the Fab is exceptional and does not bind to similar pMHC presented on healthy cell surfaces.

However, our tests went one important step farther than those performed previously. We showed that these TCR-like Fabs can function similarly to human T cells; they can be highly selective *in vivo* even in the context of human HLA-A2 expressed in HLA-A2. Even with the thousands of peptide/HLA-A2 complexes available on healthy cells of the HLA-A2 transgenic SCID mouse, the Fab still accumulated at the transplanted tumors. This is especially interesting considering that the sequence of the peptide E75 from HER2/neu is identical to that found in mouse epidermal growth factor receptor 2 [93] and that the HLA-A2 expression in the HLA-A2 transgenic mouse model is expressed at comparable levels to H-2D^{b} in thymus, bone marrow, and spleen [94]. The dynamic scans showed initial rapid accumulation of ^{64}Cu- DOTA-fE75 followed by a steady-state in all the tissues (liver, kidney, humoral muscle, and control tumor) except for the HLA-A2 positive tumor

similar to the SCID mouse experiments. It is not clear why we did not see accumulation of the Fab in sites other than the tumor and those predicted by the injection of this sized protein. Although the mouse antigen presenting machinery can process and present peptides recognized by human HLA-A2-restricted T cells [93], it is possible that there are differences that preclude presentation of the E75 peptide or that the expression level is so much lower in normal cells that there is a very small dilution of the signal compared to the tumor.

Theoretically, the best *in vivo* images of the ^{64}Cu-DOTA-Fab accumulation would occur after removal of the unincorporated label, but the half-life of fE75 binding to E75/HLA-A2 measured by SPR is on the order of minutes and due to the high vascularization of the tumors, the Fab is removed readily. We conclude that all of these Fab sized probes of roughly 55 kDa could be highly specific and bind very tightly, but they do not have a long enough half-life to be useful on their own unless they are endocytosed by the cell. The signal could be greatly increased by multimerization of the Fab [95,96]. However, this problem does not diminish the significance of the observation that the Fab targeting was successful even in the context of transgenic expression of HLA-A2 in all the cells of the mouse.

Antibodies specific for pMHC are useful tools for understanding antigen presentation *in vivo* and allowing targeted therapy for cancer. Not only can they be used to directly visualize T-cell epitopes [45,90,97], they can aid in method development for peptide-based immunotherapy, where visualization of a particular pMHC before and after treatment would be beneficial. This can include analysis of intracellular generation, trafficking, cell surface expression, and stability of pMHC

complexes on antigen presenting cells (APC). Antibody fragments with pMHC specificity can improve on the successes of adoptive T-cell therapy. Even though up to 50% of patients treated with *ex vivo* expanded tumor-infiltrating lymphocytes show clinical responses [70,98], it is not possible to produce significant quantities of tumor infiltrating T cells from all cancer patients due to the inability to either isolate or expand them *in vitro*. There is promise in the field of genetically modified T-lymphocytes, where TCR-like antibodies are transferred to T lymphocytes via retroviral infection for their expression on the T cell surface [99]. T cells expressing tumor-specific receptors, chimeric antigen receptors and modified TCRs specifically killed tumor cells and had antitumor effects *in vivo* [100-103].

In summary, we have demonstrated that pMHC specific Fabs can be quickly and efficiently isolated from our skewed bacteriophage library. These particular Fabs provide much greater stability and higher affinity than would T cell receptors making them particularly good imaging agents. One of the Fabs, fE75, shown to have high affinity and high specificity, was derivitized as an *in vivo* imaging agent and selectively localized to HLA-A2 positive tumors in SCID HLA-A2 transgenic mice. It is anticipated that phage display-derived TCR-like antibody fragments have a wide range of applications in research, diagnostic, and therapeutic applications.

2.5 References

1. Nishimura, R., T. Osako, Y. Okumura, R. Tashima, Y. Toyozumi, and N. Arima. 2011. Changes in the ER, PgR, HER2, p53 and Ki-67 biological markers between primary and recurrent breast cancer: discordance rates and prognosis. *World J Surg Onc* 9: 131–137.

2. Capala, J., and K. Bouchelouche. 2010. Molecular imaging of HER2-positive breast cancer: a step toward an individualized “image and treat” strategy. *Curr. Opin. Oncol.* 22: 559–566.

3. Ross, J. S., and J. A. Fletcher. 1998. The HER‐2/ neuOncogene in Breast Cancer: Prognostic Factor, Predictive Factor, and Target for Therapy. *Stem cells* 16: 413–428.

4. Gonzalez-Angulo, A. M., F. Morales-Vasquez, and G. N. Hortobagyi. 2007. *Advances in Experimental Medicine and Biology*, (N. Back, I. R. Cohen, A. Lajtha, J. D. Lambris, R. Paoletti, D. Yu, and M.-C. Hung, eds). Springer New York, New York, NY; :1–22.

5. Lohrisch, C., and M. Piccart. 2008. HER2/*neu* as a Predictive Factor in Breast Cancer. *Clin. Breast Cancer.* 2: 129–135.

6. Leyland-Jones, B. 2002. Trastuzumab: hopes and realities. *Lancet Oncol* 3: 137–144.

7. Witton, C. J., J. R. Reeves, J. J. Going, T. G. Cooke, and J. Bartlett. 2003. Expression of the HER1–4 family of receptor tyrosine kinases in breast cancer. *J. Pathol.* 200: 290–297.

8. Slamon, D., G. Clark, S. Wong, W. Levin, A. Ullrich, and W. McGuire. 1987. Human breast cancer: correlation of relapse and survival with amplification of the HER-2/neu oncogene. *Science* 235: 177–182.

9. Yu, D., and M.-C. Hung. 2000. Overexpression of ErbB2 in cancer and ErbB2-targeting strategies. *Oncogene* 19: 6115–6121.

10. Nahta, R., and F. J. Esteva. 2006. Herceptin: mechanisms of action and resistance. *Cancer Lett.* 232: 123–138.

11. Vogel, C. L., M. A. Cobleigh, D. Tripathy, J. C. Gutheil, L. N. Harris, L. Fehrenbacher, D. J. Slamon, M. Murphy, W. F. Novotny, M. Burchmore, S. Shak, S. J. Stewart, and M. Press. 2002. Efficacy and safety of trastuzumab as a single agent in first-line treatment of HER2-overexpressing metastatic breast cancer. *J. Clin. Oncol.* 20: 719–726.

12. Krogsgaard, M., and M. M. Davis. 2005. How T cells “see” antigen. *Nat. Immunol.* 6: 239–245.

13. Edwards, L. J., and B. D. Evavold. 2011. T cell recognition of weak ligands: roles of signaling, receptor number, and affinity. *Immunol Res.* 50: 39–48.

14. Clements, C. S., M. A. Dunstone, W. A. Macdonald, J. McCluskey, and J. Rossjohn. 2006. Specificity on a knife-edge: the alphabeta T cell receptor. *Curr. Opin. Struct. Biol.* 16: 787–795.

15. Wilson, D. B., D. H. Wilson, K. Schroder, C. Pinilla, S. Blondelle, R. A. Houghten, and K. C. Garcia. 2004. Specificity and degeneracy of T cells. *Mol. Immunol.* 40: 1047–1055.

16. Alberti, S. 1996. A high affinity T cell receptor? *Immunol. Cell Biol.* 74: 292–297.

17. Collins, E. J., and D. S. Riddle. 2008. TCR-MHC docking orientation: natural selection, or thymic selection? *Immunol. Res.* 41: 267–294.

18. Wulfing, C., and A. Plückthun. 1994. Correctly folded T-cell receptor fragments in the periplasm of Escherichia coli. Influence of folding catalysts. *J. Mol. Med.* 242: 655–669.

19. Plaksin, D., K. Polakova, P. McPhie, and D. H. Margulies. 1997. A three-domain T cell receptor is biologically active and specifically stains cell surface MHC/peptide complexes. *J. Immunol.* 158: 2218–2227.

20. Hülsmeyer, M., P. Chames, R. C. Hillig, R. L. Stanfield, G. Held, P. G. Coulie, C. Alings, G. Wille, W. Saenger, B. Uchanska-Ziegler, H. R. Hoogenboom, and A. Ziegler. 2005. A major histocompatibility complex-peptide-restricted antibody and t cell receptor molecules recognize their target by distinct binding modes: crystal structure of human leukocyte antigen (HLA)-A1-MAGE-A1 in complex with FAB-HYB3. *J. Biol. Chem.* 280: 2972–2980.

21. Mareeva, T., E. Martinez-Hackert, and Y. Sykulev. 2008. How a T cell receptor-like antibody recognizes major histocompatibility complex-bound peptide. *J. Biol. Chem.* 283: 29053–29059.

22. Denkberg, G., C. J. Cohen, A. Lev, P. Chames, H. R. Hoogenboom, and Y. Reiter. 2002. Direct visualization of distinct T cell epitopes derived from a melanoma tumor-associated antigen by using human recombinant antibodies with MHC-restricted T cell receptor-like specificity. *Proc.Natl. Acad. Sci. U.S.A.* 99: 9421–9426.

23. Anikeeva, N., T. Mareeva, W. Liu, and Y. Sykulev. 2009. Can oligomeric T-cell receptor be used as a tool to detect viral peptide epitopes on infected cells? *Clin. Immunol.* 130: 98–109.

24. Verma, B., F. A. Neethling, S. Caseltine, G. Fabrizio, S. Largo, J. A. Duty, P. Tabaczewski, and J. A. Weidanz. 2010. TCR mimic monoclonal antibody targets a specific peptide/HLA class I complex and significantly impedes tumor growth in vivo using breast cancer models. *J. Immunol.* 184: 2156–2165.

25. Mittendorf, E. A., C. E. Storrer, R. J. Foley, K. Harris, Y. Jama, C. D. Shriver, S. Ponniah, and G. E. Peoples. 2006. Evaluation of the HER2/neu-derived peptide GP2 for use in a peptide-based breast cancer vaccine trial. *Cancer* 106: 2309–2317.

26. Garboczi, D. N., D. T. Hung, and D. C. Wiley. 1992. HLA-A2-peptide complexes: refolding and crystallization of molecules expressed in Escherichia coli and complexed with single antigenic peptides. *Proc. Natl. Acad. Sci. U.S.A.* 89: 3429–3433.

27. Fellouse, F. A., K. Esaki, S. Birtalan, D. Raptis, V. J. Cancasci, A. Koide, P. Jhurani, M. Vasser, C. Wiesmann, A. A. Kossiakoff, S. Koide, and S. S. Sidhu. 2007. High-throughput generation of synthetic antibodies from highly functional minimalist phage-displayed libraries. *J. Mol. Biol.* 373: 924–940.

28. Lee, C. V., W.-C. Liang, M. S. Dennis, C. Eigenbrot, S. S. Sidhu, and G. Fuh. 2004. High-affinity human antibodies from phage-displayed synthetic Fab libraries with a single framework scaffold. *J. Mol. Biol.* 340: 1073–1093.

29. Koide, A., C. W. Bailey, X. Huang, and S. Koide. 1998. The fibronectin type III domain as a scaffold for novel binding proteins1. *J. Mol. Biol.* 284: 1141–1151.

30. Sidhu, S. S., H. B. Lowman, B. C. Cunningham, and J. A. Wells. 2000. [21] Phage display for selection of novel binding peptides. *Methods Enzymol.* 328: 333–IN5.

31. Homola, J. 2006. *Surface plasmon resonance based sensors*. Springer-Verlag, Berlin Heidelberg; :3–44.

32. Mohsin, H., J. Fitzsimmons, T. Shelton, T. J. Hoffman, C. S. Cutler, M. R. Lewis, P. S. Athey, G. Gulyas, G. E. Kiefer, R. K. Frank, J. Simon, S. Z. Lever, and S. S. Jurisson. 2007. Preparation and biological evaluation of 111In-, 177Lu- and 90Y-labeled DOTA analogues conjugated to B72.3. *Nucl. Med. Biol.* 34: 493–502.

33. Lewis, M. R., J. Y. Kao, A.-L. J. Anderson, J. E. Shively, and A. Raubitschek. 2001. An Improved Method for Conjugating Monoclonal Antibodies with N-Hydroxysulfosuccinimidyl DOTA. *Bioconjugate Chem.* 12: 320–324.

34. Whitfield-Larry, F., E. F. Young, G. Talmage, E. Fudge, A. Azam, S. Patel, J. Largay, W. Byrd, J. Buse, A. S. Calikoglu, L. D. Shultz, and J. A. Frelinger. 2011. HLA-A2-matched peripheral blood mononuclear cells from type 1 diabetic patients, but not nondiabetic donors, transfer insulitis to NOD-scid/γc(null)/HLA-A2 transgenic mice concurrent with the expansion of islet-specific CD8+ T cells. *Diabetes* 60: 1726–1733.

35. Hudson, H. M., and R. S. Larkin. 1994. Accelerated image reconstruction using ordered subsets of projection data. *IEEE Trans Med Imaging* 13: 601–609.

36. Loening, A. M., and S. S. Gambhir. 2003. AMIDE: a free software tool for multimodality medical image analysis. *Mol. Imaging.* 2: 131–137.

37. Fisk, B., T. L. Blevins, J. T. Wharton, and C. G. Ioannides. 1995. Identification of an immunodominant peptide of HER-2/neu protooncogene recognized by ovarian tumor-specific cytotoxic T lymphocyte lines. *J. Exp. Med.* 181: 2109–2117.

38. Knutson, K. L., K. Schiffman, M. A. Cheever, and M. L. Disis. 2002. Immunization of cancer patients with a HER-2/neu, HLA-A2 peptide, p369-377, results in short-lived peptide-specific immunity. *Clin. Cancer Res.* 8: 1014–1018.

39. Murray, J. L., M. E. Gillogly, D. Przepiorka, H. Brewer, N. K. Ibrahim, D. J. Booser, G. N. Hortobagyi, A. P. Kudelka, K. H. Grabstein, M. A. Cheever, and C. G. Ioannides. 2002. Toxicity, immunogenicity, and induction of E75-specific tumor-lytic CTLs by HER-2 peptide E75 (369-377) combined with granulocyte macrophage colony-stimulating factor in HLA-A2+ patients with metastatic breast and ovarian cancer. *Clin. Cancer Res.* 8: 3407–3418.

40. Brossart, P., S. Wirths, G. Stuhler, V. L. Reichardt, L. Kanz, and W. Brugger. 2000. Induction of cytotoxic T-lymphocyte responses in vivo after vaccinations with peptide-pulsed dendritic cells. *Blood* 96: 3102–3108.

41. Kono, K., A. Takahashi, H. Sugai, H. Fujii, A. R. Choudhury, R. Kiessling, and Y. Matsumoto. 2002. Dendritic cells pulsed with HER-2/neu-derived peptides can induce specific T-cell responses in patients with gastric cancer. *Clin. Cancer Res.* 8: 3394–3400.

42. Kaufman, J., J. Salomonsen, and M. Flajnik. 1994. Evolutionary conservation of MHC class I and class II molecules--different yet the same. *Sem. Immunol.* 6: 411–424.

43. Eigenbrot, C., M. Randal, L. Presta, P. Carter, and A. A. Kossiakoff. 1993. X-ray structures of the antigen-binding domains from three variants of humanized anti-p185HER2 antibody 4D5 and comparison with molecular modeling. *J. Mol. Biol.* 229: 969–995.

44. Luft, T., M. Rizkalla, T. Y. Tai, Q. Chen, R. I. MacFarlan, I. D. Davis, E. Maraskovsky, and J. Cebon. 2001. Exogenous peptides presented by transporter associated with antigen processing (TAP)-deficient and TAP-competent cells: intracellular loading and kinetics of presentation. *J. Immunol.* 167: 2529–2537.

45. Porgador, A., J. W. Yewdell, Y. Deng, J. R. Bennink, and R. N. Germain. 1997. Localization, quantitation, and in situ detection of specific peptide-MHC class I complexes using a monoclonal antibody. *Immunity* 6: 715–726.

46. Cohen, C. J., O. Sarig, Y. Yamano, U. Tomaru, S. Jacobson, and Y. Reiter. 2003. Direct phenotypic analysis of human MHC class I antigen presentation: visualization, quantitation, and in situ detection of human viral epitopes using peptide-specific, MHC-restricted human recombinant antibodies. *J. Immunol.* 170: 4349–4361.

47. Pamer, E., and P. Cresswell. 1998. Mechanisms of MHC class I--restricted antigen processing. *Annu. Rev. Immunol.* 16: 323–358.

48. Miles, J., and M. Shevlin. 2001. *Applying regression & correlation*. Sage Publications Ltd, London.

49. Chatziioannou, A. F. 2005. Instrumentation for molecular imaging in preclinical research: Micro-PET and Micro-SPECT. *Proc Am Thorac Soc* 2: 533–6, 510–11.

50. Wang, L., J. Shi, Y.-S. Kim, S. Zhai, B. Jia, H. Zhao, Z. Liu, F. Wang, X. Chen, and S. Liu. 2009. Improving tumor-targeting capability and pharmacokinetics of (99m)Tc-labeled cyclic RGD dimers with PEG(4) linkers. *Mol. Pharm.* 6: 231–245.

51. Orlova, A., J. Feldwisch, L. Abrahmsén, and V. Tolmachev. 2007. Update: affibody molecules for molecular imaging and therapy for cancer. *Cancer Biother. Radiopharm.* 22: 573–584.

52. Lo, B. K. C., and A. M Wu. 2003. *Antibody Engineering*. Humana Press, New Jersey; :209–226.

53. Colcher, D., G. Pavlinkova, G. Beresford, B. Booth, A. Choudhury, and S. Batra. 1998. Pharmacokinetics and biodistribution of genetically-engineered antibodies. *The quarterly journal.* 42: 225–241.

54. Fujimori, K., D. G. Covell, J. E. Fletcher, and J. N. Weinstein. 1989. Modeling analysis of the global and microscopic distribution of immunoglobulin G, F(ab')2, and Fab in tumors. *Cancer Res.* 49: 5656–5663.

55. Holton, O. D., C. D. Black, R. J. Parker, D. G. Covell, J. Barbet, S. M. Sieber, M. J. Talley, and J. N. Weinstein. 1987. Biodistribution of monoclonal IgG1, F(ab“)2, and Fab” in mice after intravenous injection. Comparison between anti-B cell (anti-Lyb8.2) and irrelevant (MOPC-21) antibodies. *J. Immunol.* 139: 3041–3049.

56. Lane, S. R., P. Nanda, T. L. Rold, G. L. Sieckman, S. D. Figueroa, T. J. Hoffman, S. S. Jurisson, and C. J. Smith. 2010. Optimization, biological evaluation and microPET imaging of copper-64-labeled bombesin agonists, [64Cu-NO2A-(X)-BBN(7-14)NH2], in a prostate tumor xenografted mouse model. *Nucl. Med. Biol.* 37: 751–761.

57. Boswell, C. A., X. Sun, W. Niu, G. R. Weisman, E. H. Wong, A. L. Rheingold, and C. J. Anderson. 2004. Comparative in vivo stability of copper-64-labeled cross-bridged and conventional tetraazamacrocyclic complexes. *J. Med. Chem.* 47: 1465–1474.

58. Heneweer, C., J. P. Holland, V. Divilov, S. Carlin, and J. S. Lewis. 2011. Magnitude of enhanced permeability and retention effect in tumors with different phenotypes: 89Zr-albumin as a model system. *J. Nucl. Med.* 52: 625–633.

59. Gonzalez-Galarza, F. F., S. Christmas, D. Middleton, and A. R. Jones. 2011. Allele frequency net: a database and online repository for immune gene frequencies in worldwide populations. *Nucleic Acids Res.* 39: D913–9.

60. Toseland, C. P., D. J. Clayton, H. McSparron, S. L. Hemsley, M. J. Blythe, K. Paine, I. A. Doytchinova, P. Guan, C. K. Hattotuwagama, and D. R. Flower. 2005. AntiJen: a quantitative immunology database integrating functional, thermodynamic, kinetic, biophysical, and cellular data. *Immunome Res* 1: 1–4.

61. Vose, B., and M. Moore. 1985. Human tumor-infiltrating lymphocytes: a marker of host response. *Semin. Hematol.* 22: 27–40.

62. Rosenberg, S. A. 1988. The development of new immunotherapies for the treatment of cancer using interleukin-2. A review. *Ann. Surg.* 208: 121–135.

63. Topalian, S. 1990. Tumor-infiltrating lymphocytes: evidence for specific immune reactions against growing cancers in mice and humans. *Important Adv. Oncol.* 19–41.

64. Melief, C. 1992. Tumor Eradication by Adoptive Transfer of Cytototic T Lymphocytes. *Adv. Cancer Res.* 58: 143–175.

65. Ioannides, C. G., and T. L. Whiteside. 1993. T cell recognition of human tumors: implications for molecular immunotherapy of cancer. *Clin. Immunol. Immunopathol.* 6: 91–106.

66. Whiteside, T. 1994. Tumor-infiltrating lymphocytes in human solid tumors. *Immunol. Ser.* 61: 137–148.

67. Faure, F., J. Even, and P. Kourilsky. 1998. Tumor-specific immune response: current in vitro analyses may not reflect the in vivo immune status. *Crit. Rev. Immunol.* 18: 77–86.

68. Phan, G. Q., E. Wang, and F. M. Marincola. 2001. T-cell-directed cancer vaccines: mechanisms of immune escape and immune tolerance. *Expert Opin Biol Ther* 1: 511–523.

69. Rosenberg, S. A., J. R. Yannelli, J. C. Yang, S. L. Topalian, D. J. Schwartzentruber, J. S. Weber, D. R. Parkinson, C. A. Seipp, J. H. Einhorn, and D. E. White. 1994. Treatment of patients with metastatic melanoma with autologous tumor-infiltrating lymphocytes and interleukin 2. *J. Natl. Cancer Inst.* 86: 1159–1166.

70. Dudley, M. E., J. C. Yang, R. Sherry, M. S. Hughes, R. Royal, U. Kammula, P. F. Robbins, J. Huang, D. E. Citrin, S. F. Leitman, J. Wunderlich, N. P. Restifo, A. Thomasian, S. G. Downey, F. O. Smith, J. Klapper, K. Morton, C. Laurencot, D. E. White, and S. A. Rosenberg. 2008. Adoptive cell therapy for patients with metastatic melanoma: evaluation of intensive myeloablative chemoradiation preparative regimens. *J. Clin. Oncol.* 26: 5233–5239.

71. Hedrick, S. M., D. I. Cohen, E. A. Nielsen, and M. M. Davis. 1984. Isolation of cDNA clones encoding T cell-specific membrane-associated proteins. *Nature* 308: 149–153.

72. Gotch, F., J. Rothbard, K. Howland, A. Townsend, and A. McMichael. 1987. Cytotoxic T lymphocytes recognize a fragment of influenza virus matrix protein in association with HLA-A2. *Nature* 326: 881–882.

73. Wylie, D. E., L. A. Sherman, and N. R. Klinman. 1982. Participation of the major histocompatibility complex in antibody recognition of viral antigens expressed on infected cells. *J. Exp. Med.* 155: 403–414.

74. Froscher, B. G., and N. R. Klinman. 1986. Immunization with SV40-transformed cells yields mainly MHC-restricted monoclonal antibodies. *J. Exp. Med.* 164: 196–210.

75. Tamminen, W. L., D. Wraith, and B. H. Barber. 1987. Searching for MHC-restricted anti-viral antibodies: antibodies recognizing the nucleoprotein of influenza virus dominate the serological response of C57BL/6 mice to syngeneic influenza-infected cells. *Eur. J. Immunol.* 17: 999–1006.

76. Abastado, J. P., S. Darche, H. Jouin, C. Delarbre, G. Gachelin, and P. Kourilsky. 1989. A monoclonal antibody recognizes a subset of the H-2Dd mouse major class I antigens. *Res. Immunol.* 140: 581–594.

77. Duc, H. T., P. Rucay, S. Righenzi, O. Halle-Pannenko, and P. Kourilsky. 1993. Monoclonal antibodies directed against T cell epitopes presented by class I MHC antigens. *Int. Immunol.* 5: 427–431.

78. Andersen, P. S., A. Stryhn, B. E. Hansen, L. Fugger, J. Engberg, and S. Buus. 1996. A recombinant antibody with the antigen-specific, major histocompatibility complex-restricted specificity of T cells. *Proc. Natl. Acad. Sci. U.S.A.* 93: 1820–1824.

79. Reiter, Y., A. Di Carlo, L. Fugger, J. Engberg, and I. Pastan. 1997. Peptide-specific killing of antigen-presenting cells by a recombinant antibody-toxin fusion protein targeted to major histocompatibility complex/peptide class I complexes with T cell receptor-like specificity. *Proc. Natl. Acad. Sci. U.S.A.* 94: 4631–4636.

80. Engberg, J., M. Krogsgaard, and L. Fugger. 1999. Recombinant antibodies with the antigen-specific, MHC restricted specificity of T cells: novel reagents for basic and clinical investigations and immunotherapy. *Immunotech.* 4: 273–278.

81. Hoogenboom, H. R., A. P. de Bruïne, S. E. Hufton, R. M. Hoet, J. W. Arends, and R. C. Roovers. 1998. Antibody phage display technology and its applications. *Immunotech.* 4: 1–20.

82. Dogan, I., K. Dorgham, H.-C. Chang, C. Parizot, F. Lemaître, L. Ferradini, E. L. Reinherz, P. Debré, and G. Gorochov. 2004. Phage-displayed libraries of peptide/major histocompatibility complexes. *Eur. J. Immunol.* 34: 598–607.

83. Somasundaram, R., K. Satyamoorthy, L. CAPUTO, H. YSSEL, and D. HERLYN. 2004. Detection of HLA class II-dependent T helper antigen using antigen phage display. *Clin. Exp. Immunol.* 135: 247–252.

84. Stewart-Jones, G., A. Wadle, A. Hombach, E. Shenderov, G. Held, E. Fischer, S. Kleber, N. Nuber, F. Stenner-Liewen, S. Bauer, A. McMichael, A. Knuth, H. Abken, A. A. Hombach, V. Cerundolo, E. Y. Jones, and C. Renner. 2009. Rational development of high-affinity T-cell receptor-like antibodies. *Proc. Natl. Acad. Sci. U.S.A.* 106: 5784–5788.

85. Stone, J. D., A. S. Chervin, and D. M. Kranz. 2009. T-cell receptor binding affinities and kinetics: impact on T-cell activity and specificity. *Immunol.* 126: 165–176.

86. Polakova, K., D. Plaksin, D. H. Chung, I. M. Belyakov, J. A. Berzofsky, and D. H. Margulies. 2000. Antibodies directed against the MHC-I molecule H-2Dd complexed with an antigenic peptide: similarities to a T cell receptor with the same specificity. *J. Immunol.* 165: 5703–5712.

87. Klechevsky, E., M. Gallegos, G. Denkberg, K. Palucka, J. Banchereau, C. Cohen, and Y. Reiter. 2008. Antitumor activity of immunotoxins with T-cell receptor-like specificity against human melanoma xenografts. *Cancer Res.* 68: 6360–6367.

88. Neumann, F., C. Sturm, M. Hülsmeyer, N. Dauth, P. Guillaume, I. F. Luescher, M. Pfreundschuh, and G. Held. 2009. Fab antibodies capable of blocking T cells by competitive binding have the identical specificity but a higher affinity to the MHC-peptide-complex than the T cell receptor. *Immunol. Lett.* 125: 86–92.

89. Mareeva, T., T. Lebedeva, N. Anikeeva, T. Manser, and Y. Sykulev. 2004. Antibody specific for the peptide.major histocompatibility complex. Is it T cell receptor-like? *J. Biol. Chem.* 279: 44243–44249.

90. Weidanz, J. A., T. Nguyen, T. Woodburn, F. A. Neethling, M. Chiriva-Internati, W. H. Hildebrand, and J. Lustgarten. 2006. Levels of specific peptide-HLA class I complex predicts tumor cell susceptibility to CTL killing. *J. Immunol.* 177: 5088–5097.

91. Hawkins, O., B. Verma, S. Lightfoot, R. Jain, A. Rawat, S. McNair, S. Caseltine, A. Mojsilovic, P. Gupta, F. Neethling, O. Almanza, W. Dooley, W. Hildebrand, and J. Weidanz. 2011. An HLA-presented fragment of macrophage migration inhibitory factor is a therapeutic target for invasive breast cancer. *J. Immunol.* 186: 6607–6616.

92. Falkenburg, J. H. F. 2011. PR1 on the edge of humoral immunotherapy. *Blood* 117: 4164–4165.

93. Shirai, M., T. Arichi, M. Nishioka, T. Nomura, K. Ikeda, K. Kawanishi, V. H. Engelhard, S. M. Feinstone, and J. A. Berzofsky. 1995. CTL responses of HLA-A2.1-transgenic mice specific for hepatitis C viral peptides predict epitopes for CTL of humans carrying HLA-A2.1. *J. Immunol.* 154: 2733–2742.

94. Le, A. X., E. J. Bernhard, M. J. Holterman, S. Strub, P. Parham, E. Lacy, and V. H. Engelhard. 1989. Cytotoxic T cell responses in HLA-A2.1 transgenic mice. Recognition of HLA alloantigens and utilization of HLA-A2.1 as a restriction element. *J. Immunol.* 142: 1366–1371.

95. Kelly, M. P., F. T. Lee, K. Tahtis, B. E. Power, F. E. Smyth, M. W. Brechbiel, P. J. Hudson, and A. M. Scott. 2008. Tumor targeting by a multivalent single-chain Fv (scFv) anti-Lewis Y antibody construct. *Cancer Biother. Radiopharm.* 23: 411–423.
96. Zhu, X., L. Wang, R. Liu, B. Flutter, S. Li, J. Ding, H. Tao, C. Liu, M. Sun, and B. Gao. 2010. COMBODY: one-domain antibody multimer with improved avidity. *Immunol. Cell Biol.* 88: 667–675.

97. Michaeli, Y., G. Denkberg, K. Sinik, L. Lantzy, C. Chih-Sheng, C. Beauverd, T. Ziv, P. Romero, and Y. Reiter. 2009. Expression hierarchy of T cell epitopes from melanoma differentiation antigens: unexpected high level presentation of tyrosinase-HLA-A2 Complexes revealed by peptide-specific, MHC-restricted, TCR-like antibodies. *J. Immunol.* 182: 6328–6341.

98. Besser, M. J., R. Shapira-Frommer, A. J. Treves, D. Zippel, O. Itzhaki, L. Hershkovitz, D. Levy, A. Kubi, E. Hovav, N. Chermoshniuk, B. Shalmon, I. Hardan, R. Catane, G. Markel, S. Apter, A. Ben-Nun, I. Kuchuk, A. Shimoni, A. Nagler, and J. Schachter. 2010. Clinical responses in a phase II study using adoptive transfer of short-term cultured tumor infiltration lymphocytes in metastatic melanoma patients. *Clin. Cancer Res.* 16: 2646–2655.

99. Willemsen, R., P. Chames, E. Schooten, J. W. Gratama, and R. Debets. 2008. Selection of human antibody fragments directed against tumor T‐cell epitopes for adoptive T‐cell therapy. *Cytometry A* 73: 1093–1099.

100. Morgan, R. A., M. E. Dudley, and S. A. Rosenberg. 2010. Adoptive Cell Therapy. *Cancer J.*16: 336–341.

101. Pinthus, J. H., T. Waks, V. Malina, K. Kaufman-Francis, A. Harmelin, I. Aizenberg, H. Kanety, J. Ramon, and Z. Eshhar. 2004. Adoptive immunotherapy of prostate cancer bone lesions using redirected effector lymphocytes. *J. Clin. Invest.* 114: 1774–1781.

102. Xue, S.-A., L. Gao, D. Hart, R. Gillmore, W. Qasim, A. Thrasher, J. Apperley, B. Engels, W. Uckert, E. Morris, and H. Stauss. 2005. Elimination of human leukemia cells in NOD/SCID mice by WT1-TCR gene-transduced human T cells. *Blood* 106: 3062–3067.

103. Kessels, H. W., M. C. Wolkers, M. D. van den Boom, M. A. van der Valk, and T. N. Schumacher. 2001. Immunotherapy through TCR gene transfer. *Nat. Immunol.* 2: 957–961.

Chapter 3

T Cell Receptor-like Antibody Fragment Binds to Insulin Secreting Beta Cells *in vivo*

3.1 Introduction

All autoimmune diseases share one common feature, the breaking of T cell tolerance. A common feature of autoreactive T cell stimulation is the interaction of the T Cell Receptor (TCR) with peptide-bound Class I Major Histocompatibility Complex (pMHC). Upon binding the pMHC, autoreactive T cells undergo a multitude of changes, resulting in proliferation, cytokine release and recruitment other immune cells inherent to disease progression. Collectively, this process either indirectly (class II MHC-mediated) or directly (class I MHC-mediated) leads to the death of the targeted endogenous cells, such as beta cells in the context of type I diabetes (T1D). Importantly, the interaction of specific antigenic peptides with disease-associated MHC is required for autoimmune disease. In addition, disease associated MHC allotypes may only differ in sequence by one or two amino acids in comparison to non-disease associated counterparts, while leading to drastic changes in the reactivity or selection of peptides that bind (1, 2). Despite this, the development of pMHC based therapeutics has been hindered due to the lack of knowledge concerning the range of pMHC presentation during autoimmunity and the overall contribution of different pMHC to autoimmune cell activation (3).

To directly monitor disease-associated pMHC on targeted cells during autoimmunity, an ideal reagent would allow the tracking of specific pMHC antigens, while having the same specificity as an autoreactive TCR. With this in mind, the use of recombinant TCRs have been tested, but have proven to be difficult to produce recombinantly and have relatively low affinity (high micromolar range) (4-9). In contrast, monoclonal antibodies are relatively easy to produce in bulk once the correct hybridoma is created and may have high affinity. However, generating these hybridomas has proven very difficult for most labs for unknown reasons.

TCR-like antibody-based molecules have improved understanding of antigen presentation in melanoma and hepatitis B viral infections (10-12), been used as immunotherapies against tumors (13), and targeted drug delivery for hepatitis B virus-infected cells (14). Phage libraries have been successfully used to select TCR-like molecules, mostly as antibody fragments (Fab) or single chain variable domain fragments (scFv), with nanomolar binding affinity for specific pMHC (15-17). However, monoclonal antibodies generate immune responses because of the Fc portion of the antibody via complement or Fc receptor mediated immune cell activation. This could be highly problematic, especially in the context of autoimmunity. Therefore, it would be better to use a TCR-like molecule without an Fc portion such as an antibody fragment (Fab) or dimer of Fab (Fab_2) for these cases. Previously, we demonstrated that such a TCR-like Fab, specific for human epidermal growth factor receptor (HER2/neu) derived peptide E75 associated with HLA-A2, could localize to human tumors *in vivo* in HLA-A2 transgenic *scid* mice (18). The high affinity and specificity of these TCR-like molecules suggests that similar

Fabs directed towards autoimmune T cell antigens may be excellent tools to study MHC antigen presentation in an autoimmune disease such as T1D.

T1D is a multi-factorial disease, with known environmental and genetic influences. While many immune cells are known to contribute to disease progression, the main mediators of beta cell destruction are autoreactive $CD4^+$ helper T cells and $CD8^+$ cytotoxic T cells (CTL). Autoreactive CTLs recognize unique pMHC presented by the beta cells localized in the islets of Langerhans. Upon binding of the pMHC, beta cell-specific CTLs become activated, resulting in the destruction of the endogenous beta cell mass (19-21). Death of the beta cells leads to reduced insulin production and an inability to regulate systemic blood glucose levels, resulting in the development of T1D once only 10-20% of the beta cell mass remains (19, 20). Importantly, CTL are required for T1D development, as mice that lack class I MHC due to a knockout of the beta-2-microglobulin gene do not develop diabetes (22, 23). As a result of this finding, searches were initiated to identify potential disease associated peptides presented on beta cells class I pMHC. Several candidate peptides were identified including: proinsulin (24, 25), insulin (24, 26), glutamic acid decarboxylase (27), and islet specific glucose-6-phosphatase catalytic subunit related protein (IGRP) (28), but the relative contribution of each peptide to overall disease progression is still a source of controversy.

To better understand the role that various pMHC complexes play in the initiation and progression of T1D, we developed several TCR-like Fabs that bind with high affinity to beta cell expressed pMHC. One of the TCR-like Fabs is specific for the murine MHC H-$2K^d$ carrying a disease-associated peptide derived from islet-

specific glucose-6-phosphatase catalytic subunit related protein, IGRP. The IGRP peptide was selected due to its relevance to the non-obese diabetic mouse model (NOD) of T1D. In these animals, IGRP/H-2K^d pMHC specific CTLs are part of the earliest islet infiltrates and the number of IGRP/H-2K^d pMHC specific CTLs in the peripheral blood correlates with T1D development (29-31). Furthermore, the sequence of murine IGRP has strong conservation across species including humans (32). In addition, we isolated another TCR-like antibody fragment specific for MHC H-2K^d carrying a peptide derived from influenza hemagglutinin, HA. The Fabs targeting the IGRP/ H-2K^d or HA/ H-2K^d are named fIGRP and fHA respectively. In addition to acting as a control for studies in the NOD mouse, the fHA Fab can be utilized for imaging studies in the NOD.InsHA model (33). In this mouse line, influenza hemagglutinin expression is driven by the insulin 1 promoter, resulting in HA/ H-2K^d linked expression on the surface of beta cells. Using these two Fabs, we have shown that TCR-like Fabs specifically localize to beta cells *in vivo* and that may allow for the noninvasive imaging of disease progression. In addition, we also have shown that administration of fIGRP and fHA respectively can block autoreactive T cell interactions with the beta cell specific pMHC *in vitro,* suggesting a potential role for these molecules as an immunotherapeutic, specifically in the context of combinatorial therapy.

3.2 Materials and methods

Ethics statement. Throughout the course of the study, all guidelines and standards of the Association for Assessment and Accreditation of Laboratory Animal Care at the University of North Carolina (UNC) Animal Facility were followed. The mice were

cared for according to the UNC Office of Animal Care and Use. The research was conducted under the protocol (10-236.0) with approval by the UNC Institutional Animal Care and Use Committee.

Antibodies, synthetic peptides, and reagents. The UNC Peptide Synthesis Facility (Chapel Hill, NC) synthesized the peptides: IGRP (from islet specific glucose-6-phosphatase catalytic subunit-related protein; VYLKTNVFL, residues 206-214) and HA (from influenza hemagglutinin; IYSTVASSL, residues 518-526). Rabbit monoclonal antibody C27C9 against mouse insulin was purchased from Cell Signaling. Alexa Fluor 488 conjugated goat anti-rabbit bound (A11034) and Alexa Fluor 647 conjugated streptavidin, Alexa Fluor 647 conjugated tyramide staining kit and 4'-6-diamidino-2-phenylindole (DAPI) were purchased from Invitrogen. Anti-fluorescein isothiocyanate (polyclonal, ab19224) was purchased from Abcam. PacBlue-conjugated CD4 antibody (clone RM4-5), PeCy7-conjugated CD8 antibody (clone 53-6.7), and FITC-conjugated CD3 (clone 145-2c11) were purchased from eBiosciences. APC conjugated rat anti-mouse IFN-γ antibody (clone XMG1.2) was purchased from BD Biosciences.

Generation of site-specifically biotinylated pMHC complexes. The mouse MHC, H-2K^d and mouse beta-2-microglobulin (β_2M) were produced as inclusion bodies in *E. coli* BL21 (DE3) (Invitrogen, Inc.). *In vitro* protein folding was completed as described previously (34). In summary, a 10:1:1 molar ratio of peptide, β_2M, and MHC heavy chain were injected into a folding buffer consisting of 100 mM Tris pH 8.0, 400 mM arginine, 2 mM EDTA, 5 mM glutathione (reduced), 0.5 mM glutathione (oxidized). Protease Inhibitors including PMSF, pepstatin and leupeptin were added

and the total final protein concentration was never greater than 50 µg/ml. The folded pMHC was concentrated in an Amicon ultrafiltration cell (Millipore, Billerica, MA) after incubation for 24-36 hours at 10 °C. Folded pMHC was purified by gel filtration chromatography (Phenomenex, Inc.; Torrance, CA). The purified pMHC molecules were concentrated to no greater than 3 mg/ml and stored at -80°C until use. Typical yield for each 1 L refold were approximately 14% at 5 mg of pMHC. The purified pMHC was site specifically biotinylated with biotin ligase BirA (Avidity, LLC; Aurora, Colorado) according to the manufacturer's instructions. Purified, putatively-biotinylated pMHC molecules were incubation with streptavidin and degree of biotinylation determined by gel-shift assay using non-denaturing SDS PAGE (no reducing agent, no heat treatment).

Fab library construction. The Fab library was constructed as discussed previously (18). Briefly, a template plasmid consisting of a modified version of the Fab-4D5 gene (35), where the heavy chain of the Fab is fused to the carboxyl-terminal 208 residue segment of M13 phage pIII, was used for construction of the libraries. Most residues in the H1, H2, and H3 loops were replaced with serine. In the CDR-H3, a TAA stop codon and a unique BAMHI site were introduced. A phoA promotor was used to control expression of both the light and heavy chain-pIII fusion proteins. A custom-made trimer phosphoramidite mixture (Glen Research, Sterling, VA) was used to synthesize oligonucleotides encoding biased amino acid mixtures for the CDR-L3 and H3 (indicated in Figure 1C as "X"s). The synthesis was completed on an Expedite synthesizer (ABI) according to Glen Research's instructions. The deprotected oligonucleotides were purified using acrylamide gel electrophoresis.

The CDR-H1 and H2 oligonucleotides were purchased from Integrated DNA technologies as they did not require trimer phosphoramidites. The Kunkel mutagenesis method (36) was used to introduce mutations in the CDR-L3, CDR-H1, CDR-H2 and CDR-H3 by the oligonucleotides. Following the first transformation of the SS320 cells (36), purification of the DNA for the library was completed. The purified DNA library was digested with BamHI and then used to transform the SS320 cells and produce phage particles, as described (35). This prevented clones expressing non-mutated CDR-H3. The Fab library consisted of approximately 10^{10} independent clones.

Selection of phage-displayed antibody fragments. Isolation of phage-displayed Fabs was performed as previously described (35) with minor modifications. After the first round of selection, the isolated phages were enriched and incubated with streptavidin-coated magnetic beads. Bound phages were removed creating a "precleared" phage pool by incubation with streptavidin-coated magnetic beads. Biotinylated pMHCs were incubated with these "precleared" phages followed by capture of phage bound pMHCs by additional streptavidin-coated magnetic beads. Concentrations of pMHC used were 100, 50, 10, and 10 nM for the four separate selection rounds respectively. Elution of the captured phages was done by using 100 µl of 0.1M Gly-HCl (pH 2.1) buffer, which was immediately neutralized with 35 µl of 1M Tris-Cl buffer (pH 8). The affinity of the recovered Fab expression phage were determined using phage ELISA and the sequence of the Fabs determined by DNA sequencing as described previously (35).

Production of soluble recombinant Fabs. Fab expression vectors containing an 8x histidine tag and a termination codon at the 3' end of the heavy chain gene were prepared using the phage-display vectors for the isolated phage clones. A biotin ligase BirA (AviTag, Avidity, LLC.) substrate tag was added to the carboxyl terminus of the light chain in the Fab expression vector. Fab proteins were expressed in chemically competent 55244 *E. coli* (ATCC). Protein A affinity chromatography followed by cation exchange chromatography were used to purify the Fab proteins as described previously (35). Typical yields were between 2-5 mg of purified Fab from 1 L bacterial culture. >90% purity was regularly obtained as measured by SDS-PAGE analysis.

Measurement of binding affinity of TCR-like Fab for pMHC by surface plasmon resonance. All SPR experiments were conducted using a Biacore Ni-NTA sensor chip (GE Healthcare). For each antibody fragment, approximately three hundred response units (RUs) were bound to their respective flow channels utilizing the 8x histidine tag on the Fabs. Soluble class I MHC (analyte) was injected onto the chip surface at a flow rate of 20 µl/min in a 300s pulse. The concentrations of injected pMHC ranged from 200 nM to 1 nM in two fold dilutions. Regeneration of the NTA surface was completed using 0.2 M EDTA, which removed Ni and all bound protein, followed by recharging the surface with 0.04 M $NiSO_4$. Each concentration of analyte was injected at least three times in random order to obtain three curves for analysis. The data were processed using Scrubber (BioLogic Software, Campbell, Australia). The SPR response curves at each concentration were double referenced as previously described (18, 37). A SPR response curve fit was used and its

suitability at predicting the raw SPR curve was measured based on the appearance of residuals and χ^2 values. The predicted curves for each Fab-pMHC binding curve visually overlaid well with the experimental curves and the residuals were small and random. χ^2 was below 1 for all reported curve fits.

Fab Tetramer Production. Site-specific biotin-ligase BirA (Avidity, LLC; Aurora, Colorado) was used to biotinylate the purified Fabs according to the manufacturer's instructions. Successful biotinylation of the Fabs was confirmed by gel shift analysis as described above for pMHC. Fab tetramers were made by incubating streptavidin-HRP (Invitrogen, Inc.) with the biotinylated Fabs in a 1 to 4 molar ratio for ten minutes at room temperature.

Immunofluorescence of murine pancreas sections *in vitro.* Pancreata from 12-week old NOD and C57BL/6 mice were excised, fixed in 1% paraformaldehyde for 10 minutes and embedded in optimal cutting temperature (OCT) media (Sakura Finetek, Torrance, CA). The embedded tissue was cryopreserved using an isopentane liquid nitrogen bath. Pancreas tissue blocks were cut into six micrometer sections using a Leica CM1950 cryostat (Leica Microsystems Inc., Buffalo Grove, IL), placed on slides, and stored at -80˚C until further use. For immunofluorescence staining of the pancreas sections, the slides were warmed to room temperature and washed in PBS. The alexa-Fluor-488 bound rabbit anti-mouse insulin antibody and the tetramer of flGRP Fab and streptavidin-HRP were added to the pancreas section for two hours. After washing in PBS, alexa fluor 647-tyramide was added to each section for 5 minutes and washed in PBS according to the manufacturer's instructions. Following this wash, 4'-6-Diamidino-2-phenylindole (DAPI) was added

to the pancreas section and then mounted using ProLong Gold antifade reagent (Invitrogen). The stained tissues were analyzed on an inverted Fluorescence/Differential Interface Contrast (DIC) microscope (Leica Microsystems Inc., Buffalo Grove, IL) with Hamamatsu OrcaER camera and MicroPublisher.

Fluorescein labeling of Fab. TCR-like antibody fragments were labeled with fluorescein isothiocyanate at a 1:10 molar ratio according manufacturer's instructions. Fluorescein labeled Fab was purified from free dye by desalting column chromatography. The degree of labeling was measured by absorbance and 2-3 fluorescein molecules per Fab were regularly obtained.

***In vivo* labeling of murine pancreas.** 200 µL of 5 µM fluoroscein-labeled Fab in PBS were injected into the tail vein of 8 to 10 week old NOD or NOD.InsHA mice. Three hours post injection, pancreata were removed and placed in a solution of 10% formalin at pH 6.5 for 10 minutes, followed by tissue transfer to a solution of 10% formalin at pH 11 for overnight incubation at 4℃. Following incubation, the pancreata tissue were embedded in OCT and cryopreserved using an isopentane liquid nitrogen bath. The embedded tissue blocks were cut into 6µm samples with a Leica CM1950 cryostat, placed on slides, and stored at ˉ80˚C until stained for additional markers.

For immunofluorescence staining, the slides were warmed to room temperature and washed twice in PBS. Rabbit monoclonal anti-insulin antibody and biotinylated anti-fluoroscein isothiocyanate (anti-FITC) were added to the pancreas sections for 2 hours. After extensive washing, secondary Alexa Fluor 488 labeled goat anti-rabbit antibody and streptavidin bound with horseradish peroxidase (HRP)

were applied to the pancreas section for 1.5 hours. Visualization of the Fab on the pancreas sections was accomplished with Alexa-Fluor 647 tyramide according to the manufacturer's instructions. Nuclei were stained with DAPI and sections were mounted for analysis. The stained tissues were analyzed on an inverted Fluorescence/Differential Interface Contrast (DIC) microscope (Leica Microsystems Inc., Buffalo Grove, IL) with Hamamatsu OrcaER camera and MicroPublisher.

Isolation of Transgenic T cells. Spleens from 10 week old transgenic 8.3 TCR expressing (38) or CL4 TCR expressing NOD mice (39) were excised and single-cell suspensions were prepared by grinding the tissue with frosted slides in RPMI 1640 complete medium (Mediatech, Inc., Manassas, VA). Red blood cells were lysed with red blood cell lysis buffer. 8.3 or CL4 transgenic $CD8^+$ were purified by negative selection using the $CD8^+\alpha$ isolation kit (Miltenyi Biotec) according to the manufacturer's instructions.

Competition T cell assay. Splenocytes in a single-cell suspension prepared from a 12 week old NOD male spleen were placed in serum free RPMI 1640 medium and incubated with either IGRP peptide or HA peptide (1-5 μM) for four hours. Following incubation, the splenocytes were irradiated and aliquoted 5×10^4 peptide-pulsed splenocytes per well. Increasing concentrations of fIGRP or fHA were added to individual wells containing the irradiated, peptide-pulsed splenocytes for 30 minutes. The Fab concentrations selected were based on the K_D of the given Fab. 8.3 or CL4 TCR-transgenic CD8 T cells were added at a 1 to 1 target (peptide pulsed splenocyte) to effector (T cell) ratio to IGRP peptide pulsed spleen cells or HA peptide pulsed spleen cells respectively. After 24 hr, supernatants were removed

and assayed for IFN-γ by ELISA according to the manufacturer's instructions. The remaining cells were stained for intracellular IFN-γ by flow cytometry. Briefly, cells were treated with brefeldin A for 5 hrs washed twice in PBS supplemented with 2% bovine serum albumin and EDTA, then stained with antibodies specific for the surface markers CD4, CD8, and CD3. Cells were then fixed, permeabilized and stained intracellularly with an antibody specific for IFN-γ overnight at 4℃. The next day, cells were washed in Perm/Wash buffer (BD Biosciences) and data was acquired using a Cyan Flow Cytometer (Cyan, Beckman Coulter, Inc.).

Glucose Tolerance Test. Intraperitoneal glucose tolerance tests were performed as previously described (40) with some modification. 11-week old NOD female mice were held without food for 18 hr, followed by a 200 µL tail vein injection of 5 µM fIGRP or PBS. Three hours post-injection, baseline blood glucose levels were measured followed by an intraperitoneal injection of glucose (2g/kg mouse weight). Blood glucose levels were acquired at set intervals over a two-hour timeframe.

3.3 Results

TCR-like Fabs have high affinity and specificity for cognate pMHC. In NOD mice, endogenous beta cells are known to present various autoantigens on MHC I molecules that contribute to the development of T1D (41). As a result, understanding the expression patterns of different autoantigens, both in magnitude and timing, may help to shed light on the role these antigens play in disease. Therefore, we generated sets of T cell receptor-like antibody fragments (TCR-like Fabs) to two different pMHC using bacteriophage-display technology (35) in order to track the expression of different pMHC specifically on beta cells. The first, named

fIGRP, recognizes a peptide derived from the islet-specific glucose-6-phosphatase catalytic subunit-related protein (IGRP) bound to the class I major histocompatibility complex, H-2K^d. Importantly, this complex is expressed on endogenous beta cells in the NOD mouse and is the target recognized by CD8$^+$ CTL derived from the 8.3 diabetes mouse model (38). In addition, we generated a second H-2K^d restricted TCR-like Fab, fHA, specific for an influenza hemagglutinin peptide. While acting as a control for studies in NOD mice, fHA also allows us to target beta cells in the NOD.InsHA mouse, where HA expression is driven by the insulin 1 promoter (33). Furthermore, similar to 8.3 cells in NOD mice, CD8$^+$ T cells derived from the CL4 mouse target HA and have been shown to induce T1D in transfer studies in NOD.InsHA recipients (39).

The TCR-like Fabs, fIGRP and fHA, were isolated by phage-display technology, which utilized a "synthetic" antibody library built on the stable 4D5 humanized Fab scaffold (Figure 1A) (42). The mutated hypervariable loops in the library lack fully randomized sequences, but do have reduced complexity favoring serine and tyrosine in the mutated loops (H1, H2, H3, L3) (35). Site-specific biotinylated pMHC, IGRP/ H-2K^d or HA/H-2K^d, were used as targets for sorting the Fab-expressing bacteriophage library. After four rounds of selection, an ELISA was used to determine the relative binding affinity and the specificity of the amplified Fab expressing phage (Figure 1B). Bacteriophages that did not bind with high affinity or did not bind specifically were excluded from further analysis. Both chosen Fab-expressing phage bound cognate pMHC, but not control pMHC. The distinct CDR sequences for fIGRP and fHA were shown in Figure 1C. The phage-display vectors

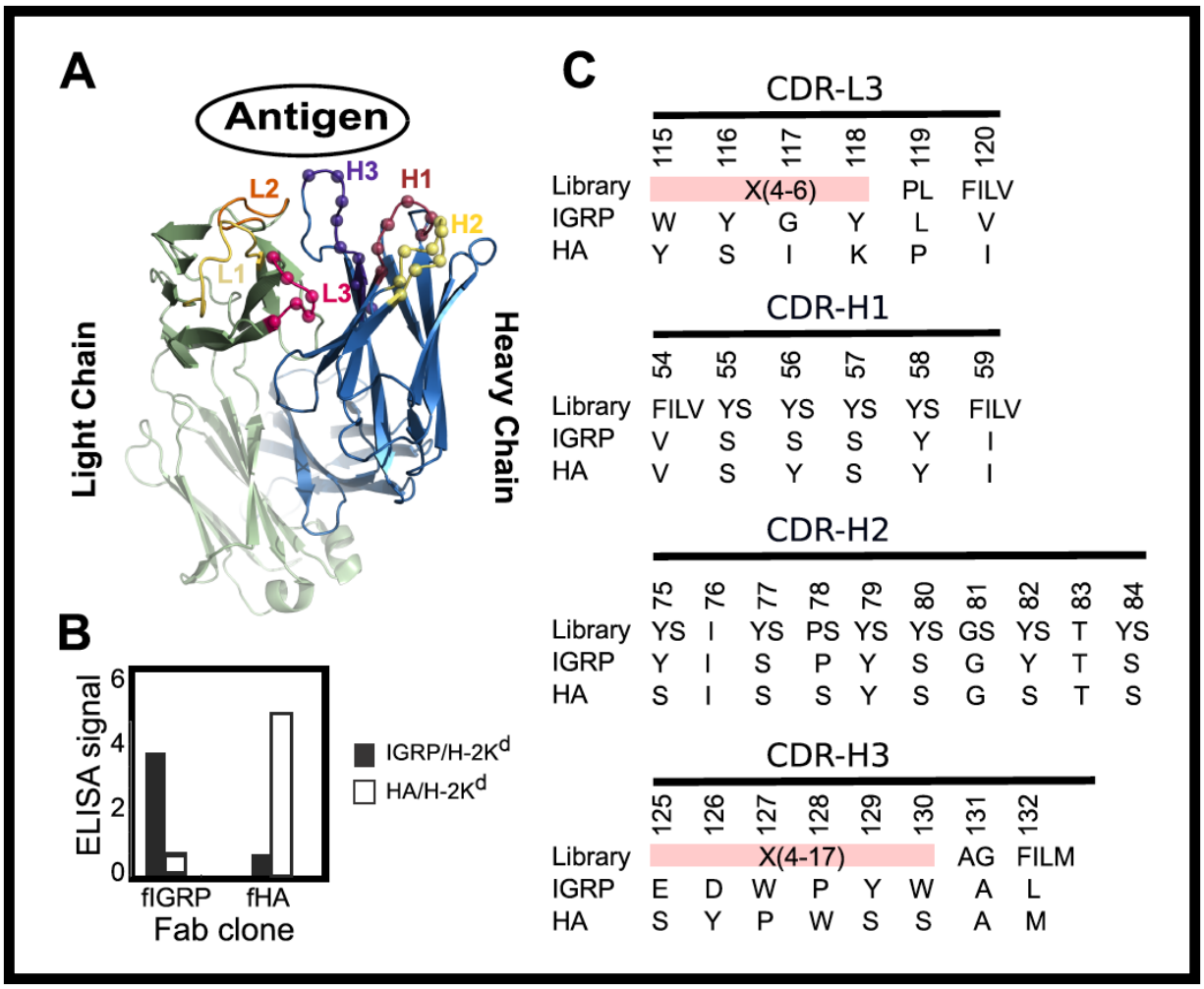

Figure 1: Isolation of TCR-like Fabs by Phage Display. Phage-display technology was used to isolate Fabs specific for either IGRP/H-2K^d or HA/H-2K^d. The stable 4D5 Fab scaffold consisting of a single heavy and a light chain each with a variable and constant domain was used to construct each Fab. The amino acid diversity of the Complementary Determining Regions (CDR) for the light chain L3, and the heavy chain; H1, H2, and H3 was restricted in favor of tyrosine, serine, and other small amino acids (modeled from PDB ID: 1FVD) (A). After three rounds of phage display selection, the specificity of the amplified clones was determined using an ELISA. The Fab clones fIGRP and fHA bound IGRP/H-2K^d and HA/H-2K^d respectively with no detectable binding to other pMHC molecules (B). The amino acid sequence of each clone was determined after the ELISA specificity determination (C).

for the isolated clones were then converted into Fab expression vectors for protein production in *E. coli* (35, 43).

Surface plasmon resonance was used to determine the binding affinity (K_D) of fIGRP and fHA binding to their cognate and noncognate pMHC. As shown in Figure 2, both Fabs bound cognate pMHC with nanomolar binding affinity. Specifically, fIGRP bound IGRP/H-2K^d with a K_D of 116 ± 8 nM (n=3) (Figure 2A), while fHA bound HA/H-2K^d with a mean K_D of 24 ± 5 nM (n=3) (Figure 2D). Levels of binding to non-cognate pMHC molecules was below background at concentrations up to 200 nM using different peptide (Figure 2B and 2C) or to unrelated pMHC (data not shown) for both Fabs. Therefore, these data indicate that phage display can be used to isolate TCR-like Fabs with high binding affinity and specificity to cognate pMHC.

TCR-like antibody fragments bind beta cells. To assess the ability of fIGRP to detect endogenously processed and presented IGRP/H-2K^d on beta cells in a NOD mouse, immunofluorescence of mouse pancreas cryosections was done (Figure 3). Insulin staining was used to identify islets of Langerhans in the pancreas (Figure 3A and 3D). Biotinylated fIGRP was multimerized by addition of streptavidin and used to stain the NOD and control C57BL/6 mouse pancreas sections. As expected, fIGRP staining was detected in only the NOD mouse pancreas sections (Figure 3B). Insulin and fIGRP colocalized across all of the islets in each pancreas section. Colocalization of insulin staining and fIGRP was observed on pancreas sections from the IGRP/H-2K^d expressing NOD islets (Figure 3C). In contrast, no detectable fIGRP immunofluorescence was observed in pancreas sections from the

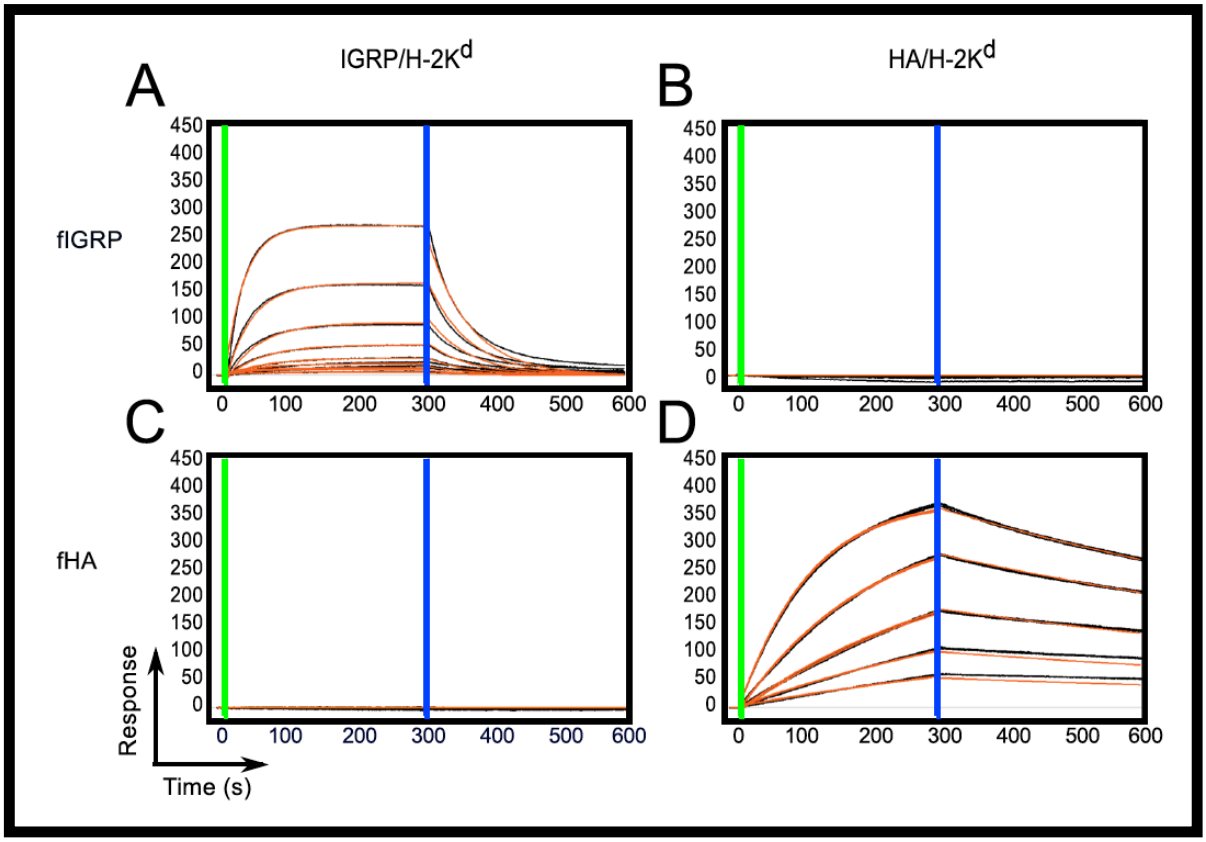

Figure 2: TCR-like Fabs Bind Cognate pMHC with Nanomolar Affinity. SPR binding response curves of pMHC, IGRP/H-2K^d, binding IGRP/H-2K^d specific Fab, fIGRP (A) and HA/H-2K^d specific Fab, fHA (C) and pMHC, HA/H-2K^d, binding fIGRP (B) and fHA (D) are shown. Each Fab was immobilized onto individual flow channels in an NTA-Ni chip. Kinetic data for each Fab binding each pMHC molecule were globally curve fit as a bimolecular reaction. Green and blue lines designate the start and end respectively of each pMHC injection. Binding curves and curve fits are drawn in black and orange respectively. Each binding curve represents a different concentration of pMHC beginning at 200 nM for fIGRP and 50 nM for fHA and decreasing in 2 fold dilutions. Specific binding was only observed between each Fab and its cognate pMHC i.e. fIGRP binding IGRP/H-2K^d and fHA binding HA/H-2K^d. The Fab, fIGRP, bound IGRP/H-2K^d with a K_D of 116 ± 8 nM (n=3). The Fab, fHA bound HA/H-2K^d with a mean K_D of 24 ± 5 nM (n=3). No binding above background was observed for either Fab binding non-cognate pMHC molecules up to 200 nM.

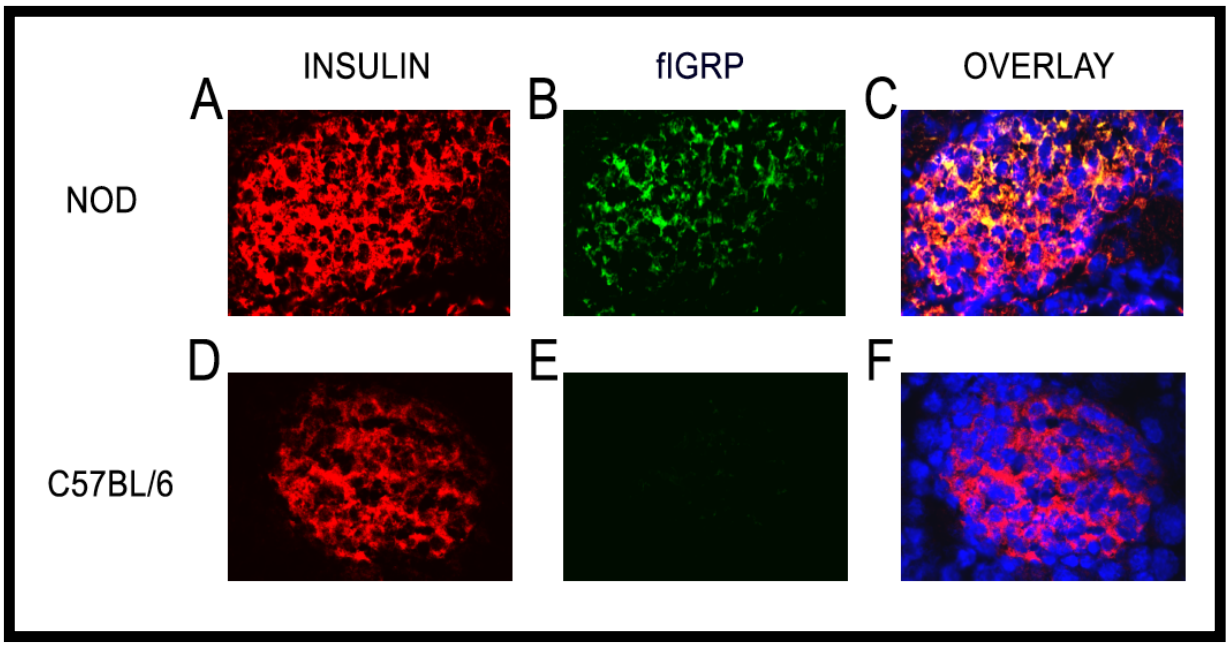

Figure 3: TCR-like Fab binds to insulin producing cells in pancreas cryosections. Immunofluorescence staining of representative pancreatic islets in 12-week old male NOD (A,B,C) and C57BL/6 (D,E,F) mice using TCR-like Fab, fIGRP, specific for IGRP/H-2K^{d}. Mouse pancreas were placed in OCT medium and cryofrozen using isopentane and liquid nitrogen. Tissue blocks were cut in 6 µm sections, fixed in 1% paraformaldehyde, and stained with primary antibodies rabbit anti-mouse insulin and tetramer consisting of biotinylated TCR-like Fab, fIGRP and streptavidin-HRP. Invitrogen Tyramide signal amplification kit was utilized for developing the fIGRP-streptavidin-HRP staining. Tissues were viewed with an inverted Leica fluorescence microscope with digital cameras at a 40x magnification. Insulin staining alone was shown in A and D, fIGRP staining alone was shown in B and E. The overlay of insulin, fIGRP, and Dapi was shown in C and F.

control C57BL/6 mouse, which expresses the H-2K^b, not the H-2K^d MHC haplotype (Figure 3E and 3F). Collectively, these studies show that fIGRP is highly specific for IGRP/H-2K^d expressed on endogenous NOD beta cells.

TCR-like antibody fragments accumulate on pancreatic beta cells in vivo. To investigate the ability of TCR-like Fabs to act as a diagnostic imaging tool, the accumulation of fIGRP and fHA on beta cells *in situ* was measured. 8-10 wk old NOD mice were injected in the tail-vein with either fIGRP or a control Fab, fE75, which uses the same Fab scaffold, but a different set of CDR loops (18). Three hours post Fab injection, the pancreata were harvested, cryopreserved, sectioned, and stained for insulin and the presence of TCR-like Fab. Insulin staining was used to identify islets of Langerhans in the pancreas (Figure 4A and 4D). Insulin is a secreted peptide hormone from the beta cells. Therefore, the staining for insulin is diffuse and surrounds the beta cells. Importantly, the only TCR-like Fab accumulation was in the NOD mice injected with fIGRP (Figure 4B). Furthermore, the overlay of insulin and the fIGRP staining indicated that fIGRP was binding specifically to insulin secreting beta cells (Figure 4C).

To assess if TCR-like Fab accumulation would occur with other islet-specific antigens, the accumulation of fHA on NOD.InsHA beta cells was measured. Again, insulin staining was used to identify the islet of Langerhans (Figure 4G and 4J). Similar to the fIGRP in NOD mice, the only detectable fHA binding was observed on the HA/H-2K^d expressing islets from NOD InsHA mice (Figure 4H), with no staining observed in control HA/H-2K^d negative NOD islets (Figure 4K). In addition, the colocalization of insulin and fHA again indicated specificity of the Fab for

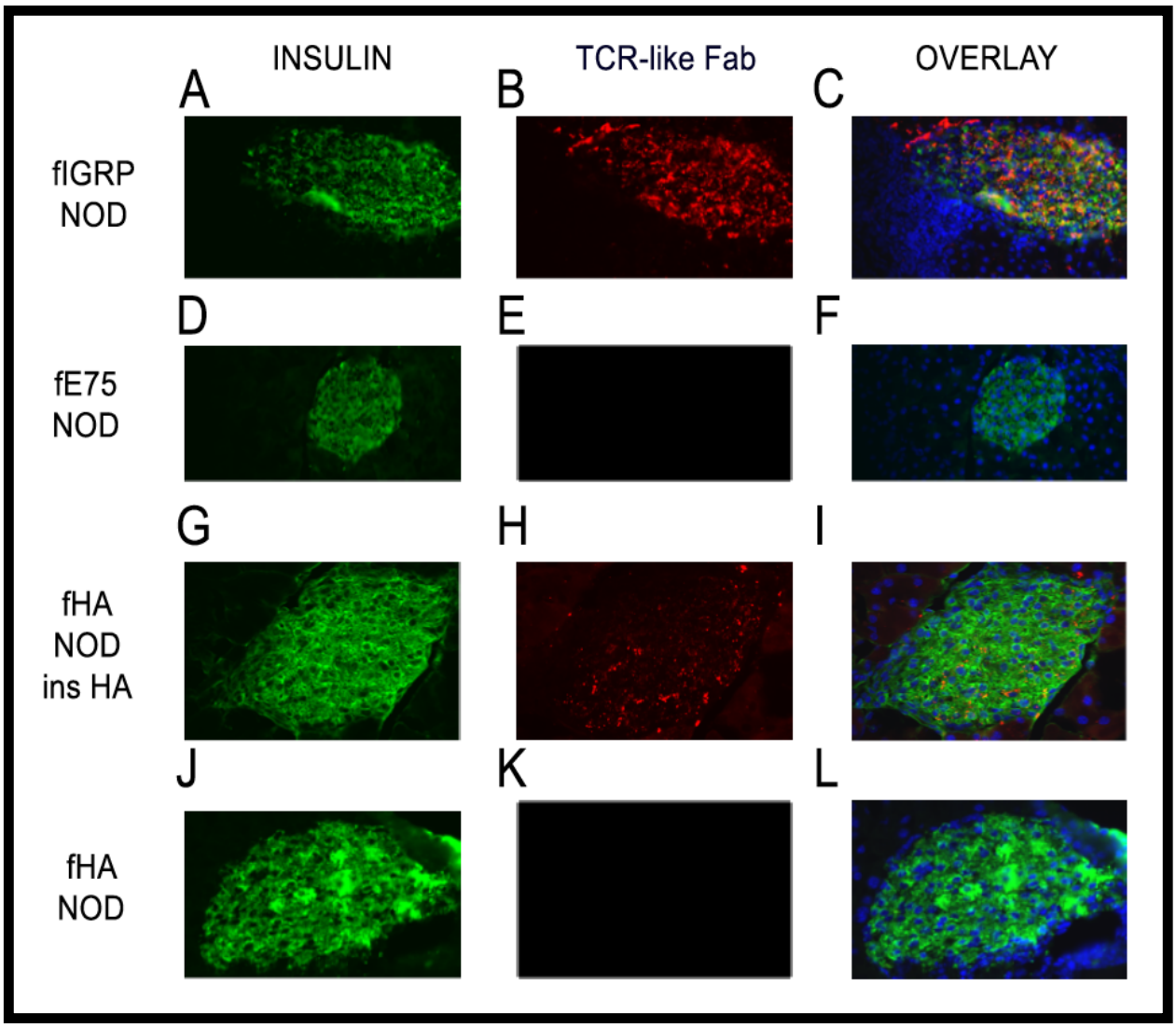

Figure 4: TCR-like Fabs accumulate on beta cells when injected *in vivo.* mmunofluorescence staining of representative pancreatic islets in 8-10-week old male NOD mice using TCR-like Fab, fIGRP, specific for IGRP/H-2K^{d} (A,B,C) or control TCR-like Fab, fE75, specific for E75/HLA-A2 (D,E,F) and representative pancreatic islets in 12-week old male NOD insHA (G,H,I) and control NOD (J,K,L) mice using TCR-like Fab, fHA, specific for HA/H-2K^{d}. Fabs were injected into the mice via tail-vein. Mouse pancreata were harvested 3 hr post injection, fixed, cryopreserved, and sectioned. Tissue sections were stained for insulin and TCR-like Fab. Tissues were viewed with an inverted Leica fluorescence microscope with digital cameras at a 40x magnification. Insulin staining alone was shown in A, D, G, and J; TCR-like Fab staining alone was shown in B, E, H, and K. The overlay of insulin, TCR-like Fab, and Dapi was shown in C, F, I, and L.

endogenous beta cells. Single stain controls are shown in Supplemental Figure 1. For both Fabs, clear staining was observed around islets structures and nowhere else. Furthermore, all islets analyzed on numerous tissue sections for both the fIGRP injected NOD and the fHA injected NOD ins HA mice showed positive staining and accumulation around the insulin producing beta cells. Further examples of other islets imaged are shown in Supplemental Figure 2. Notably, non-specific immunofluorescence from both fIGRP or fHA was below detection in regions that did not stain insulin positive. Together, these data demonstrate that different TCR-like Fabs, which bind to specific for beta cell pMHC, can traffic to and accumulate in detectable amounts in endogenous NOD islets.

TCR-like Fabs block autoreactive T cell interaction with beta cell specific pMHC in vitro. Autoreactive CTL recognition of beta cell pMHC is a key factor in development of T1D (19-23). As a result, disruption of the beta cell pMHC binding by the cytotoxic T cell could prevent disease onset by dampening CTL activation and subsequent beta cell destruction. One way in which CTL engagement of beta clel pMHC could be manipulated is through blocking studies utilizing the TCR-like Fabs, fIGRP and fHA. Therefore, to determine if pre-treatment with fIGRP or fHA could dampen the activation of antigen specific CTL *in vitro*, splenocytes were isolated from H-2K^{d} expressing NOD mice and were incubated with IGRP or HA peptides respectively, to mimic a beta cell pMHC. After pusling, these splenocytes were co-cultered with 8.3 or CL4 TCR-transgenic CD8^{+} T cells (specific for IGRP/H-2K^{d} or HA/H-2K^{d} pMHC respectively) and increasing concentrations of fIGRP or fHA TCR-like Fab. After twenty-four hours, interferon-gamma (IFN-γ) synthesis from activated

CTLs was measured in two ways: 1) by ELISA of supernatants (Figure 5) and 2) by intracellular IFN-γ staining by flow cytometry (Supplemental Figure 3). Detectable IFN-γ production inversely correlated with TCR-like Fab concentration in an antigen specific manner (i.e. fIGRP and IGRP peptide, fHA and HA peptide). By ELISA, the EC_{50} of fIGRP for the blockade of IFN-γ production by 8.3 T cells was 592 ± 50 nM (n=3) (Figure 5A). Alternatively, fHA had an EC_{50} of 314 ± 40 (n=3) for blockade of IFN-γ production by CL-4 T cells (Figure 5D). Importantly, no significant decrease in IFN-γ was observed when TCR-like Fabs were incubated with spleen cells expressing the noncognate pMHC (Figure 5B and 5C). Similar trends were observed by intracellular staining of IFN-γ by flow cytometry (Supplemental Figure 3). Collectively, these data show that the TCR-like Fabs can block IFN-γ production in an antigen specific manner *in vitro*.

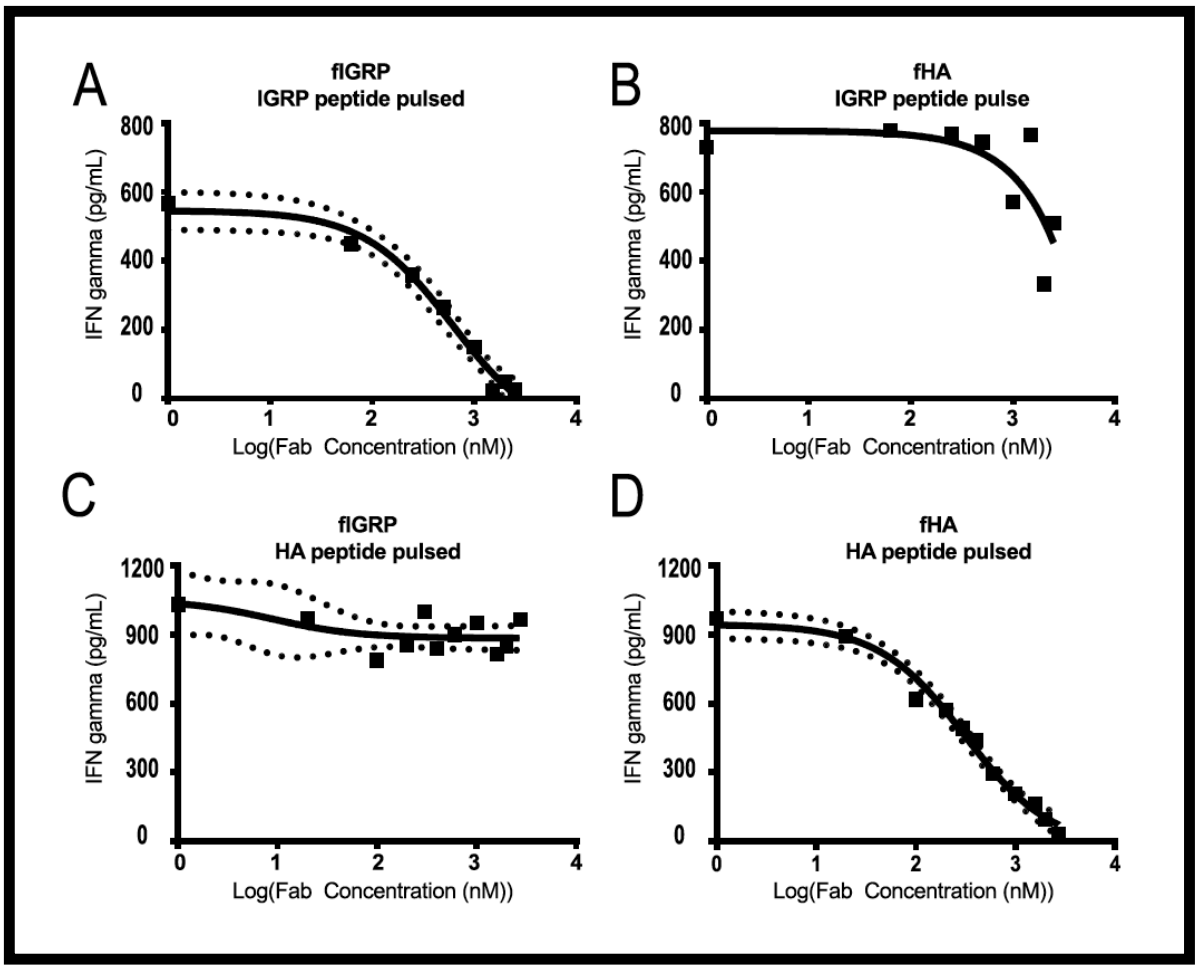

Figure 5: TCR-like Fabs block recognition by autoreactive T Cells. Spleen cells from NOD mice were incubated with either IGRP peptide (A, B) or HA peptide (C,D) for four hours. Increasing concentrations of flGRP or fHA were added to the peptide pulsed spleen cells for 30 minutes. Following incubation, 8.3 or CL4 TCR-transgenic CD8 T cells were added at a 1 to 1 target to effector ratio to IGRP peptide pulsed spleen cells or HA peptide pulsed spleen cells respectively. After 24 hr, supernatants were removed and assayed for IFN-gamma by ELISA. The Fab concentrations selected were based on the K_D of the given Fab. The black line is the curve fit for one-to-one competitive binding. 95% confidence intervals are shown as dotted lines. 95% confidence interval could not be determined in B because it did not converge.

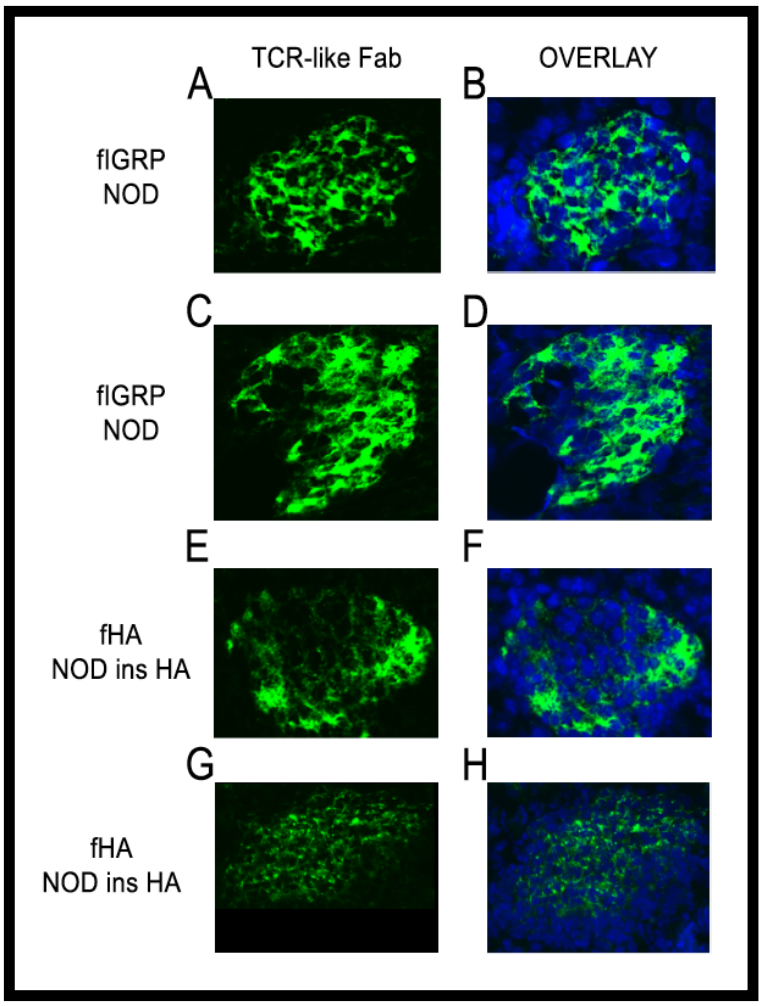

Supplemental Figure 1: TCR-like Fabs accumulate on beta cells when injected *in vivo* single staining controls. Immunofluorescence staining of representative pancreatic islets in 8-10-week old male NOD or NOD ins HA mice using TCR-like Fab, fIGRP, specific for IGRP/H-2K^{d} (A, B, C, and D) or TCR-like Fab, fHA, specific for HA/H-2Kd (E, F, G, and H). Fabs were injected into mice via tail-vein. Mouse pancreas were harvested 3 hr post injection and were prepared by placing in formalin pH 6.5 followed by formalin pH 11.0. After fixation, mouse pancreas were placed in OCT medium and cryopreserved using isopentane and liquid nitrogen. Tissue blocks were cut in 6 µm sections and stained with primary antibodies rabbit anti-mouse insulin and anti-FITC. Invitrogen Tyramide signal amplification kit was utilized for developing the biotin and FITC labeled TCR-like Fab staining. Tissues were viewed with an inverted Leica fluorescence microscope with digital cameras at a 40x magnification. TCR-like Fab staining alone was shown in A, C, E, and G. The overlay of TCR-like Fab and Dapi was shown in B, D, F, and H. No binding of control Fab fE75 or fHA in NOD mice was detected.

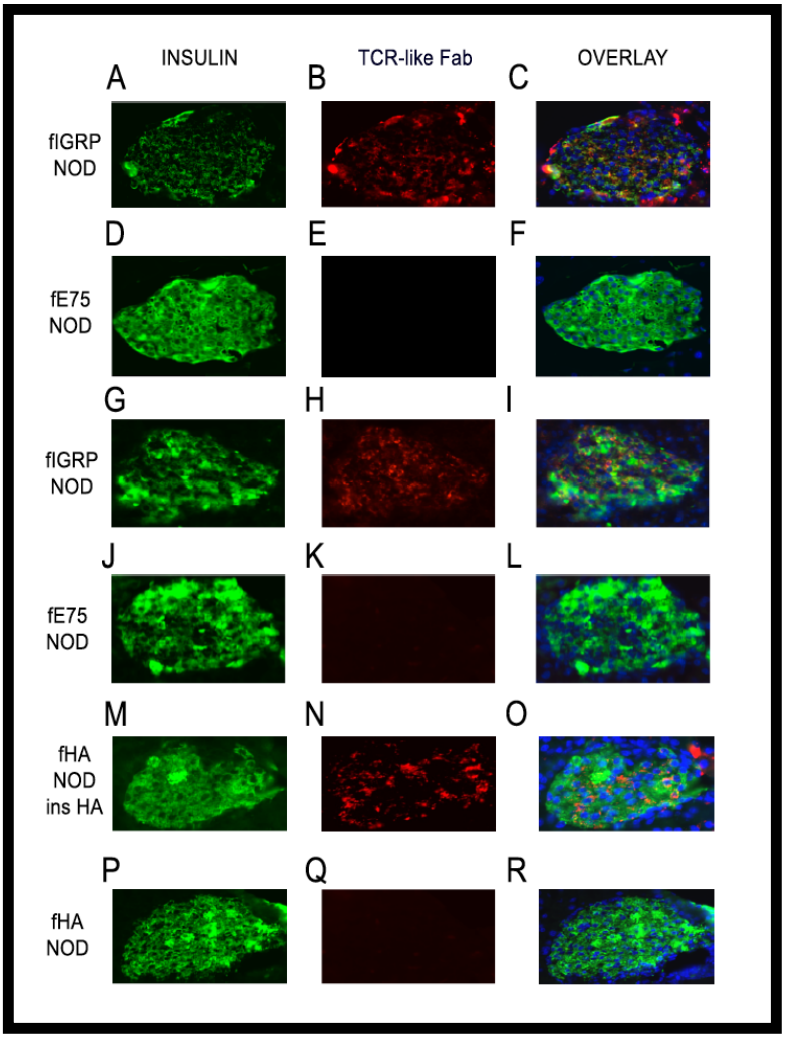

Supplemental Figure 2: TCR-like Fabs accumulate on beta cells when injected *in vivo.* Immunofluorescence staining of representative pancreatic islets in 8-10-week old male NOD mice using TCR-like Fab, fIGRP, specific for IGRP/H-2K^{d} (A, B, C, G, H, I) or control TCR-like Fab, fE75, specific for E75/HLA-A2 (D, E, F, J, K, L) and representative pancreatic islets in 12-week old male NOD insHA (M,N,O) and control NOD (P, Q, R) mice using TCR-like Fab, fHA, specific for HA/H-2Kd. Fabs were injected into mice via tail-vein. Mouse pancreas were harvested 3 hr post injection and were prepared by placing in formalin pH 6.5 followed by formalin pH 11.0. After fixation, mouse pancreas were placed in OCT medium and cryopreserved using isopentane and liquid nitrogen. Tissue blocks were cut in 6 µm sections and stained with primary antibodies rabbit anti-mouse insulin and anti-FITC. Invitrogen Tyramide signal amplification kit was utilized for developing the biotin and FITC labeled TCR-like Fab staining. Tissues were viewed with an inverted Leica fluorescence microscope with digital cameras at a 40x magnification. Insulin staining alone was shown in A, D, G, J, M, and P; TCR-like Fab staining alone was shown in B, E, H, K, N, and Q. The overlay of insulin, TCR-like Fab, and Dapi was shown in C, F, I, L, O, and R.

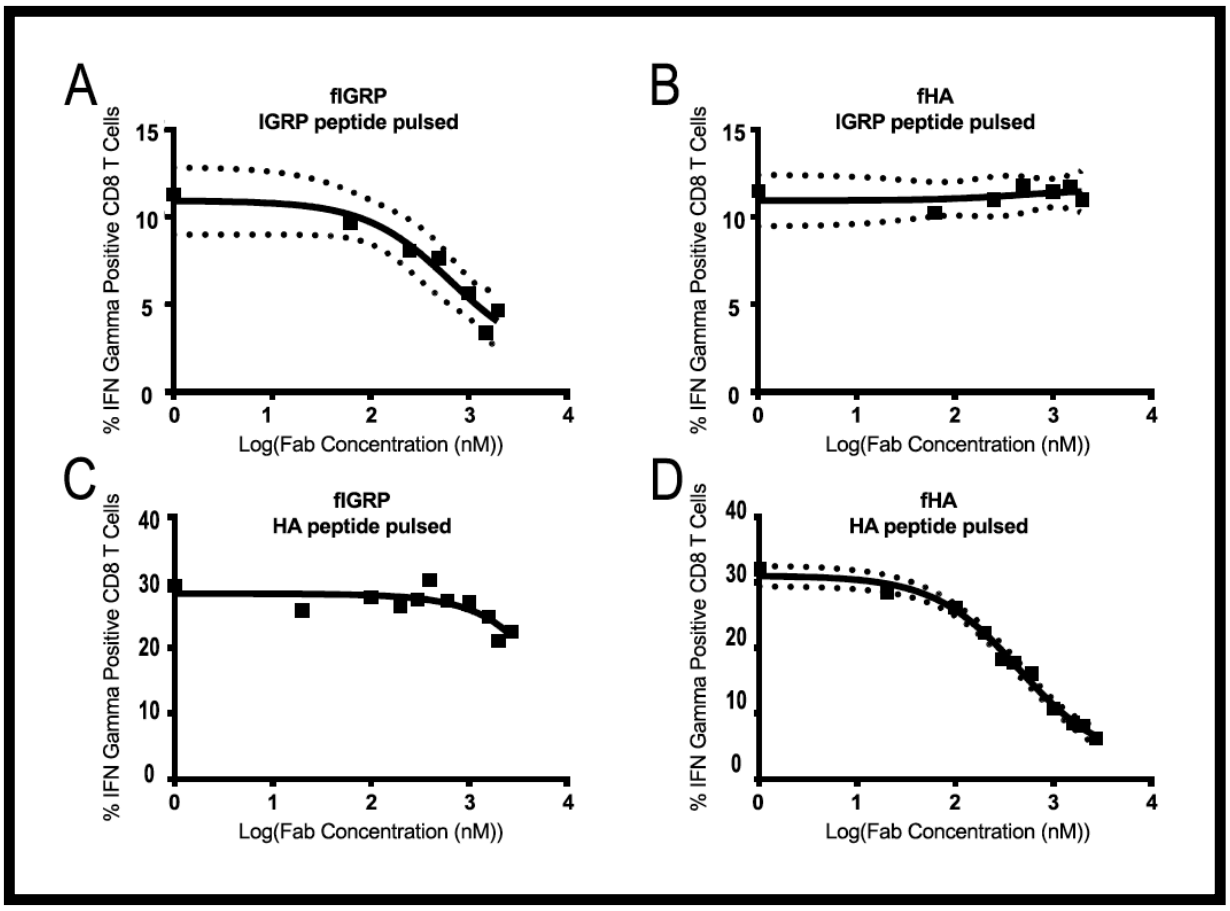

Supplemental Figure 3: TCR-like Fabs block intracellular interferon-gamma production of autoreactive T cells. Spleen cells from NOD mice were incubated with either IGRP peptide (A, B) or HA peptide (C,D) for four hours. Increasing concentrations of fIGRP or fHA were added to the peptide pulsed spleen cells for 30 minutes. Following incubation, 8.3 or CL4 TCR-transgenic CD8 T cells were added at a 1 to 1 target to effector ratio to IGRP peptide pulsed spleen cells or HA peptide pulsed spleen cells respectively. After 24 hr, the cell mixtures were stained for T cell surface expression markers (CD3 and CD8) and intracellular interferon-gamma expression and analyzed by flow cytometry. The Fab concentrations selected were based on the K_D of the given Fab. The black line is the curve fit for one-to-one competitive binding. 95% confidence intervals are shown as dotted lines. 95% confidence interval could not be determined in C because it did not converge.

3.4 Discussion

Over the past 20 years, our understanding of the critical events that lead to the initiation and progression of T1D has vastly improved. While many diabetic patients are living longer, healthier lives, there is still no cure for T1D. As a result, there is a critical need to better understand the triggering factors of the disease to assist in the development of effective therapeutics. In addition, while assessment of autoantibody production and family history has contributed to early diagnosis of the disease, there remains a glaring absence of reagents for noninvasive beta cell imaging. Such a reagent would allow for quantitative measurements and spatial visualization of individual patients' beta cell mass to evaluate either progression of disease and/or response to treatment. Currently, the only method to accurately quantitate beta cell mass is via autopsy. Although Magnetic Resonance Imaging (MRI) and Computed Tomography (CT) can identify the pancreas with a spatial resolution of approximately 100 micrometers, these techniques cannot identify the islets of Langerhans, which only represent 2-3% of the pancreatic tissue. Diagnostic equipment such as Positron Emission Tomography (PET) and CT can provide the needed high sensitivity and spatial resolution, but the equipment's detection of specific cells requires an agent that will selectively target beta cells. The sulfonylurea receptor 1 and monoamine transporter 2 (44), and glucagon-like peptide 1 (45) have been used for PET imaging, but these imaging agents bind to other cell types thereby increasing background noise. To overcome these hurdles, we are developing an approach that will be of great value to research and diagnosis/treatment to 1) identify where and when beta-cell-specific autoantigens

are presented to autoreactive T cells and 2) image beta cells specifically.

Our approach to these issues began with the understanding that islet reactive CTL recognize a complex on the plasma membrane of beta cells comprised of a beta cell-specific peptide bound to a Major Histocompatibility Complex (MHC) (46, 47). In addition, both antigenic peptides (24-28) and the particular MHC allotypes (48-51) are critical to development of T1D. Therefore, since the pMHC targeted by the immune system is specific, a reagent that mimics a given TCR found on islet-reactive CTL could be utilized to assess the expression of unique pMHC on endogenous beta cells.

As a result, we developed TCR-like antibody fragments that mimic the autoreactive TCR specific for pMHC found on NOD beta cells. Since isolation of monoclonal antibodies that target specific pMHC have proven very difficult by traditional methods, we used an antibody fragment formatted phage display library to isolate TCR-like Fabs specific to beta cell pMHC. Fabs confer numerous advantages over TCRs including higher affinities, ease of production and manipulation, and greater stability (52, 53). Additionally, Fabs are superior to traditional antibodies for imaging and therapy due to a reduced total size (~54 kDa) and the absence of a fragment crystallizable (Fc) region. The small size of Fabs allows faster and greater tissue penetration, while the lack of an Fc region dampens potential immunity against the antibody itself, a particularly important issue in the context of imaging beta cells in diabetic patients (54, 55). Monoclonal antibodies with TCR specificity have previously been generated from bacteriophage libraries and recent improvements to isolation protocols have increased binding affinities into

the nanomolar range (56). Our synthetic phage library demonstrates that nanomolar affinity antibodies (Figure 1) can be selected without the need for affinity maturation.

Using immunofluorescence, our T1D TCR-like antibody fragments were able to specifically identify beta cells within the pancreas. Importantly, both Fabs were highly selective for beta *in vivo,* despite exposure to thousands of other peptide/H-2K^d complexes while traveling from the vasculature of the tail vein to the pancreas. While specificity of these TCR-like Fabs has been established, the ability to use these reagents for noninvasive imaging *in vivo* is still an outstanding question. One potential pitfall, however, is that the monomeric Fab has a half-life of approximately one minute, precluding significant accumulation in the pancreas. Therefore, multimerization may be required for suitable imaging in future studies. If successful, accurate imaging of the beta cell mass in at-risk patients could allow for improved diagnosis, as well as for more effective development and evaluation of treatment strategies for T1D. Furthermore, the ability to specifically target the beta cell mass *in vivo* may improve the localized accumulation of therapeutics to dampen the autoreactive response and restore beta cell mass (57-60).

In addition to acting as imaging reagents, TCR-like Fabs may have potential as an immunotherapeutic. We showed that both fIGRP and fHA can block the activation of antigen specific CTL *in vitro*, as determined by targeting Fabs reduced IFN-γ secretion (Figure 5). While current immunotherapies for T1D have attempted to dampen the autoimmune response, these treatment regimens often suffer from short- and long-term toxicity with limited long-term benefit. Restoration/regeneration of the beta cell mass has been attempted by islet transplantation with some short-

term success, but this procedure is costly and requires continuous immunosuppression to prevent organ rejection (58-63). Furthermore, adding exogenous beta cells without first dampening the autoimmune response is ill-advised. Currently, promising Phase III clinical trials are underway for two anti-CD3 antibodies that target all T cells for improved T1D prognosis. While stabile insulin production has been observed, cessation of treatment results in repopulation of the patient with autoreactive T cells (64, 65). In addition, loss of all T cells is problematic and can leave the patients open to recurrent opportunistic infections. Alternatively, our approach targets only the autoreactive T cells, by preventing the interaction of beta clel specific T cells with beta cell pMHC. Surprisingly, as we show here and others have shown, Fabs with nanomolar binding affinities for pMHC can competitively block T cell interaction with the target (66), while leaving the rest of the immune system unmanipulated. As a result, future studies will seek to address the functionality of these Fabs as therapeutics when given to p re-diabetic and recent on-set diabetic NOD mice.

In summary, we have demonstrated that TCR-like Fabs specific for beta cell pMHC can be isolated from a bacteriophage library. These Fabs have high affinity for cognate pMHC and effectively traffic to, and bind endogenous beta cells *in vivo*. Furthermore, both fIGRP and fHA block the activation of CTL *in vitro* in an antigen specific manner. As a result, TCR-like antibody-based molecules could be used in a multitude of applications. First and foremost, treatment with TCR-like Fabs can allow direct visualization of antigen presentation on host cells, improving studies concerning where and when specific autoantigens are presented and by which cell

types during the progression of T1D. Moreover, as shown in our research, TCR-like Fabs could be utilized as an immunotherapy for dampening the engagement and activation of autoreactive T cells in various autoimmune diseases.

3.5 References

1. Bjorkman, P. J., M. A. Saper, B. Samraoui, W. S. Bennett, J. L. Strominger, and D. C. Wiley. 1987. The foreign antigen binding site and T cell recognition regions of class I histocompatibility antigens. *Nature* 329: 512–518.

2. Little, A. M., and P. Parham. 1999. Polymorphism and evolution of HLA class I and II genes and molecules. *Rev Immunogenet* 1: 105–123.

3. Wucherpfennig, K. W., and D. Sethi. 2011. T cell receptor recognition of self and foreign antigens in the induction of autoimmunity. *Semin. Immunol.*23: 84–91.

4. Clements, C. S., M. A. Dunstone, W. A. Macdonald, J. McCluskey, and J. Rossjohn. 2006. Specificity on a knife-edge: the alphabeta T cell receptor. *Curr. Opin. Struct. Biol.* 16: 787–795.

5. Wilson, D. B., D. H. Wilson, K. Schroder, C. Pinilla, S. Blondelle, R. A. Houghten, and K. C. Garcia. 2004. Specificity and degeneracy of T cells. *Mol. Immunol.* 40: 1047–1055.

6. Alberti, S. 1996. A high affinity T cell receptor? *Immunol. Cell Bio.* 74: 292–297.

7. Collins, E. J., and D. S. Riddle. 2008. TCR-MHC docking orientation: natural selection, or thymic selection? *Immunol. Res.* 41: 267–294.

8. Wulfing, C., and A. Plückthun. 1994. Correctly folded T-cell receptor fragments in the periplasm of Escherichia coli. Influence of folding catalysts. *J. Mol. Bio.* 242: 655–669.

9. Plaksin, D., K. Polakova, P. McPhie, and D. H. Margulies. 1997. A three-domain T cell receptor is biologically active and specifically stains cell surface MHC/peptide complexes. *J. Immunol.* 158: 2218–2227.

10. Michaeli, Y., G. Denkberg, K. Sinik, L. Lantzy, C. Chih-Sheng, C. Beauverd, T. Ziv, P. Romero, and Y. Reiter. 2009. Expression hierarchy of T cell epitopes from melanoma differentiation antigens: unexpected high level presentation of tyrosinase-HLA-A2 Complexes revealed by peptide-specific, MHC-restricted, TCR-like antibodies. *J. Immunol.* 182: 6328–6341.

11. Dolan, B. P. 2013. Quantitating MHC class I ligand production and presentation using TCR-like antibodies. *Methods Mol. Biol.* 960: 169–177.

12. Low, J. L., A. Naidoo, G. Yeo, A. J. Gehring, Z. Z. Ho, Y. H. Yau, S. G. Shochat, D. M. Kranz, A. Bertoletti, and G. M. Grotenbreg. 2012. Binding of TCR multimers and a TCR-like antibody with distinct fine-specificities is dependent on the surface density of HLA complexes. *PLoS ONE* 7: e51397.

13. Wittman, V. P., D. Woodburn, T. Nguyen, F. A. Neethling, S. Wright, and J. A. Weidanz. 2006. Antibody targeting to a class I MHC-peptide epitope promotes tumor cell death. *J. Immunol.* 177: 4187–4195.

14. Ji, C., K. S. R. Sastry, G. Tiefenthaler, J. Cano, T. Tang, Z. Z. Ho, D. Teoh, S. Bohini, A. Chen, S. Sankuratri, P. A. Macary, P. Kennedy, H. Ma, S. Ries, K. Klumpp, E. Kopetzki, and A. Bertoletti. 2012. Targeted delivery of interferon-α to hepatitis B virus-infected cells using T-cell receptor-like antibodies. *Hepatology* 56: 2027–2038.

15. Makler, O., K. Oved, N. Netzer, D. Wolf, and Y. Reiter. 2010. Direct visualization of the dynamics of antigen presentation in human cells infected with cytomegalovirus revealed by antibodies mimicking TCR specificity. *Eur. J. Immunol.* 40: 1552–1565.

16. Held, G., M. Matsuo, M. Epel, S. Gnjatic, G. Ritter, S. Y. Lee, T. Y. Tai, C. J. Cohen, L. J. Old, M. Pfreundschuh, Y. Reiter, H. R. Hoogenboom, and C. Renner. 2004. Dissecting cytotoxic T cell responses towards the NY-ESO-1 protein by peptide/MHC-specific antibody fragments. *Eur. J. Immunol.* 34: 2919–2929.

17. Chames, P., R. A. Willemsen, G. Rojas, D. Dieckmann, L. Rem, G. Schuler, R. L. Bolhuis, and H. R. Hoogenboom. 2002. TCR-like human antibodies expressed on human CTLs mediate antibody affinity-dependent cytolytic activity. *J. Immunol.* 169: 1110–1118.

18. Miller, K. R., A. Koide, B. Leung, J. Fitzsimmons, B. Yoder, H. Yuan, M. Jay, S. S. Sidhu, S. Koide, and E. J. Collins. 2012. T cell receptor-like recognition of tumor in vivo by synthetic antibody fragment. *PLoS ONE* 7: e43746.

19. Campbell, P. D., E. Estella, N. L. Dudek, G. Jhala, H. E. Thomas, T. W. H. Kay, and S. I. Mannering. 2008. Cytotoxic T-lymphocyte-mediated killing of human pancreatic islet cells in vitro. *Hum. Immunol.* 69: 543–551.

20. Durinovic-Belló, I. 1998. Autoimmune diabetes: the role of T cells, MHC molecules and autoantigens. *Autoimmunity* 27: 159–177.

21. Yoon, J. W., and H. S. Jun. 2001. Cellular and molecular pathogenic mechanisms of insulin-dependent diabetes mellitus. *Ann. N. Y. Acad. Sci.* 928: 200–211.

22. Serreze, D. V., E. H. Leiter, G. J. Christianson, D. Greiner, and D. C. Roopenian. 1994. Major histocompatibility complex class I-deficient NOD-B2mnull mice are diabetes and insulitis resistant. *Diabetes* 43: 505–509.

23. Sumida, T., M. Furukawa, A. Sakamoto, T. Namekawa, T. Maeda, M. Zijistra, I. Iwamoto, T. Kolke, S. Yoshida, and H. Tomioka. 1994. Prevention of insulitis and diabetes in B2-microglobulin-deficjent non-obese diabetic mice. *Int. Immunol.* 6: 1445–1449.

24. Dubois-LaForgue, D., J. C. Carel, P. F. Bougnères, J. G. Guillet, and C. Boitard. 1999. T-cell response to proinsulin and insulin in type 1 and pretype 1 diabetes. *J. Clin. Immunol.* 19: 127–134.

25. Hassainya, Y., F. Garcia-Pons, R. Kratzer, V. Lindo, F. Greer, F. A. Lemonnier, G. Niedermann, and P. M. van Endert. 2005. Identification of naturally processed HLA-A2--restricted proinsulin epitopes by reverse immunology. *Diabetes* 54: 2053–2059.

26. Palmer, J. P., C. M. Asplin, P. Clemons, K. Lyen, O. Tatpati, P. K. Raghu, and T. L. Paquette. 1983. Insulin antibodies in insulin-dependent diabetics before insulin treatment. *Science* 222: 1337–1339.

27. Baekkeskov, S., H. J. Aanstoot, S. Christgau, A. Reetz, M. Solimena, M. Cascalho, F. Folli, H. Richter-Olesen, P. De Camilli, and P. D. Camilli. 1990. Identification of the 64K autoantigen in insulin-dependent diabetes as the GABA-synthesizing enzyme glutamic acid decarboxylase. *Nature* 347: 151–156.

28. Ouyang, Q., N. E. Standifer, H. Qin, P. Gottlieb, C. B. Verchere, G. T. Nepom, R. Tan, and C. Panagiotopoulos. 2006. Recognition of HLA class I-restricted beta-cell epitopes in type 1 diabetes. *Diabetes* 55: 3068–3074.

29. DiLorenzo, T. P., R. T. Graser, T. Ono, G. J. Christianson, H. D. Chapman, D. C. Roopenian, S. G. Nathenson, and D. V. Serreze. 1998. Major histocompatibility complex class I-restricted T cells are required for all but the end stages of diabetes development in nonobese diabetic mice and use a prevalent T cell receptor alpha chain gene rearrangement. *Proc. Natl. Acad. Sci. U.S.A.* 95: 12538–12543.

30. Amrani, A., J. Verdaguer, P. Serra, S. Tafuro, R. Tan, and P. Santamaria. 2000. Progression of autoimmune diabetes driven by avidity maturation of a T-cell population. *Nature* 406: 739–742.

31. Trudeau, J. D., C. Kelly-Smith, C. B. Verchere, J. F. Elliott, J. P. Dutz, D. T. Finegood, P. Santamaria, and R. Tan. 2003. Prediction of spontaneous autoimmune diabetes in NOD mice by quantification of autoreactive T cells in peripheral blood. *J. Clin. Invest.* 111: 217–223.

32. Unger, W. W. J., G. G. M. Pinkse, S. Mulder-van der Kracht, A. R. van der Slik, M. G. D. Kester, F. Ossendorp, J. W. Drijfhout, D. V. Serreze, and B. O. Roep. 2007. Human clonal CD8 autoreactivity to an IGRP islet epitope shared between mice and men. *Ann. N. Y. Acad. Sci.* 1103: 192–195.

33. Degermann, S., C. Reilly, B. Scott, L. Ogata, H. von Boehmer, and D. Lo. 1994. On the various manifestations of spontaneous autoimmune diabetes in rodent models. *Eur. J. Immunol.* 24: 3155–3160.

34. Garboczi, D. N., D. T. Hung, and D. C. Wiley. 1992. HLA-A2-peptide complexes: refolding and crystallization of molecules expressed in Escherichia coli and complexed with single antigenic peptides. *Proc. Natl. Acad. Sci. U.S.A.* 89: 3429–3433.

35. Fellouse, F. A., K. Esaki, S. Birtalan, D. Raptis, V. J. Cancasci, A. Koide, P. Jhurani, M. Vasser, C. Wiesmann, A. A. Kossiakoff, S. Koide, and S. S. Sidhu. 2007. High-throughput generation of synthetic antibodies from highly functional minimalist phage-displayed libraries. *J. Mol. Biol.* 373: 924–940.

36. Sidhu, S. S., H. B. Lowman, B. C. Cunningham, and J. A. Wells. 2000. [21] Phage display for selection of novel binding peptides. *Methods Enzymol.* 328: 333–IN5.

37. Homola, J. 2006. *Surface plasmon resonance based sensors*. Springer-Verlag, Berlin Heidelberg; :3–44.

38. Verdaguer, J., D. Schmidt, A. Amrani, B. Anderson, N. Averill, and P. Santamaria. 1997. Spontaneous autoimmune diabetes in monoclonal T cell nonobese diabetic mice. *J. Exp. Med.* 186: 1663–1676.

39. Morgan, D. J., R. Liblau, B. Scott, S. Fleck, H. O. McDevitt, N. Sarvetnick, D. Lo, and L. A. Sherman. 1996. CD8(+) T cell-mediated spontaneous diabetes in neonatal mice. *J. Immunol.* 157: 978–983.

40. Yi, Z., R. Diz, A. J. Martin, Y. M. Morillon, D. E. Kline, L. Li, B. Wang, and R. Tisch. 2012. Long-term remission of diabetes in NOD mice is induced by nondepleting anti-CD4 and anti-CD8 antibodies. *Diabetes* 61: 2871–2880.

41. Roep, B. O., and M. Peakman. 2012. Antigen targets of type 1 diabetes autoimmunity. *Cold Spring Harb Perspect Med* 2: a007781.

42. Eigenbrot, C., M. Randal, L. Presta, P. Carter, and A. A. Kossiakoff. 1993. X-ray structures of the antigen-binding domains from three variants of humanized anti-p185HER2 antibody 4D5 and comparison with molecular modeling. *J. Mol. Biol.* 229: 969–995.

43. Lee, C. V., W.-C. Liang, M. S. Dennis, C. Eigenbrot, S. S. Sidhu, and G. Fuh. 2004. High-affinity human antibodies from phage-displayed synthetic Fab libraries with a single framework scaffold. *J. Mol. Biol.* 340: 1073–1093.

44. Schneider, S. 2008. Efforts to develop methods for in vivo evaluation of the native beta-cell mass. *Diabetes Obes Metab* 10 Suppl 4: 109–118.

45. Mukai, E., K. Toyoda, H. Kimura, H. Kawashima, H. Fujimoto, M. Ueda, T. Temma, K. Hirao, K. Nagakawa, H. Saji, and N. Inagaki. 2009. GLP-1 receptor antagonist as a potential probe for pancreatic beta-cell imaging. *Biochem. Biophys. Res. Commun.* 389: 523–526.

46. DiLorenzo, T. P., and D. V. Serreze. 2005. The good turned ugly: immunopathogenic basis for diabetogenic CD8+ T cells in NOD mice. *Immunol. Rev.* 204: 250–263.

47. Gojanovich, G. S., and P. R. Hess. 2012. Making the most of major histocompatibility complex molecule multimers: applications in type 1 diabetes. *Clin. Dev. Immunol.* 2012: 380289.

48. Todd, J. A., and L. S. Wicker. 2001. Genetic Protection from the Inflammatory Disease Type 1 Diabetes in Humans and Animal Models. *Immunity* 15: 387–395.

49. Wandstrat, A., and E. Wakeland. 2001. The genetics of complex autoimmune diseases: non-MHC susceptibility genes. *Nat. Immunol.* 2: 802–809.

50. Acha-Orbea, H., and H. O. McDevitt. 1987. The first external domain of the nonobese diabetic mouse class II IA beta chain is unique. *Proc. Natl. Acad. Sci. U.S.A.* 84: 2435–2439.

51. Nepom, G. T., and W. W. Kwok. 1998. Molecular basis for HLA-DQ associations with IDDM. *Diabetes* 47: 1177–1184.

52. Cohen, C. J., G. Denkberg, A. Lev, M. Epel, and Y. Reiter. 2003. Recombinant antibodies with MHC-restricted, peptide-specific, T-cell receptor-like specificity: new tools to study antigen presentation and TCR-peptide-MHC interactions. *J. Mol. Recognit.* 16: 324–332.

53. Denkberg, G., and Y. Reiter. 2006. Recombinant antibodies with T-cell receptor-like specificity: novel tools to study MHC class I presentation. *Autoimmun Rev* 5: 252–257.

54. King, D. J. 1998. *Applications And Engineering Of Monoclonal Antibodies*. CRC Press.

55. Chapman, A. P. 2002. PEGylated antibodies and antibody fragments for improved therapy: a review. *Adv. Drug Deliv. Rev.* 54: 531–545.

56. Stewart-Jones, G., A. Wadle, A. Hombach, E. Shenderov, G. Held, E. Fischer, S. Kleber, N. Nuber, F. Stenner-Liewen, S. Bauer, A. McMichael, A. Knuth, H. Abken, A. A. Hombach, V. Cerundolo, E. Y. Jones, and C. Renner. 2009. Rational development of high-affinity T-cell receptor-like antibodies. *Proc. Natl. Acad. Sci. U.S.A.*106: 5784–5788.

57. Pozzilli, P., and R. D. Leslie. 2009. New prospects for immunotherapy at diagnosis of type 1 diabetes. *Diabetes Metab. Res. Rev.* 25: 299–301.

58. Cernea, S., and K. C. Herold. 2006. Drug insight: New immunomodulatory therapies in type 1 diabetes. *Nat Clin Pract Endocrinol Metab* 2: 89–98.

59. Nichols, J., and A. Cooke. 2009. Overcoming self-destruction in the pancreas. *Curr. Opin. Biotechnol.* 20: 511–515.

60. Waldron-Lynch, F., and K. C. Herold. 2009. Advances in Type 1 diabetes therapeutics: immunomodulation and beta-cell salvage. *Endocrinol. Metab. Clin. North Am.* 38: 303–17– viii.

61. Begum, S., W. Chen, K. C. Herold, and V. E. Papaioannou. 2009. Remission of type 1 diabetes after anti-CD3 antibody treatment and transplantation of embryonic pancreatic precursors. *Endocrinology* 150: 4512–4520.

62. Harrison, L. C. 2008. Vaccination against self to prevent autoimmune disease: the type 1 diabetes model. *Immunol. Cell Biol.* 86: 139–145.

63. Sherry, N. A., W. Chen, J. A. Kushner, M. Glandt, Q. Tang, S. Tsai, P. Santamaria, J. A. Bluestone, A.-M. B. Brillantes, and K. C. Herold. 2007. Exendin-4 improves reversal of diabetes in NOD mice treated with anti-CD3 monoclonal antibody by enhancing recovery of beta-cells. *Endocrinology* 148: 5136–5144.

64. Bach, J. F., and L. Chatenoud. 2001. Tolerance to islet autoantigens in type 1 diabetes. *Annu. Rev. Immunol.*19: 131–161.

65. Steele, C., W. A. Hagopian, S. Gitelman, U. Masharani, M. Cavaghan, K. I. Rother, D. Donaldson, D. M. Harlan, J. Bluestone, and K. C. Herold. 2004. Insulin secretion in type 1 diabetes. *Diabetes* 53: 426–433.

66. Neumann, F., C. Sturm, M. Hülsmeyer, N. Dauth, P. Guillaume, I. F. Luescher, M. Pfreundschuh, and G. Held. 2009. Fab antibodies capable of blocking T cells by competitive binding have the identical specificity but a higher affinity to the MHC-peptide-complex than the T cell receptor. *Immunol. Lett.* 125: 86–92.

Chapter 4

The Future Applications of T Cell Receptor-Like Molecules

4.1 Introduction

The most promising technologies under development to deliver therapeutics involve nanoparticles. Regardless of whether those nanoparticles are lipid based or some other formulation, all would benefit from some way to target them to the correct/most optimal biological location. Peptide-associated major histocompatibility complex (pMHC) molecules are promising markers to deliver such particles for treatment of cancer, viral, and autoimmune diseases. Recent advances using phage-display technology have improved the generation of T cell receptor (TCR)-like antibody-derived molecules targeting a wide variety of pMHC molecules. These TCR-like proteins have strong binding affinities and high specificity for their cognate pMHC. Therefore, TCR-like molecules have been utilized to understand antigen presentation in tumors, virus-infected cells, and professional antigen presenting cells. Moreover, TCR-like molecules have the potential to assist immunotherapeutics by targeting drugs to sites of disease. We have shown as proof of concept that high affinity (nanomolar) and high specificity TCR-like antibody fragments can be isolated by phage display and used for imaging of human epidermal growth factor receptor (HER2/neu) positive tumors and imaging of non-obese diabetic (NOD) mouse beta cells in type 1 diabetes. The next stage of research with TCR-like protein molecules is to further the understanding of antigen

presentation in disease, improvement of immunotherapeutic targeting, and to apply these TCR-like proteins to aid other medical research fields including nanoparticle delivery.

4.2 Probing antigen-presentation

TCR-like antibody-derived proteins provide a tool to study presentation in the immune system. Development of effective vaccines and immunotherapies depends on a thorough understanding of the immune mechanisms responsible for disease prevention. The advent of recombinant pMHC molecules complexed to form tetramers has provided a means to track sets of T cells with known antigen specificity (1). These tetramers allow researchers to study the frequency of T cells upon immunization and/or disease, but a major part of the immune system picture that has been missing is a measure of the antigen presentation by antigen presenting cells (APCs). Numerous studies have demonstrated that the route of antigen administration to experimental animals is significant in eliciting an effective immune response (2-4). The effectiveness of the response is hypothesized to be due to the antigen trafficking to the nearest lymph node and dependent on the specific type of APCs utilized. Until now, there were not useful tools to monitor *in vivo* antigen presentation after antigen administration. By utilizing TCR-like proteins, vaccine formulations can be improved and an enhanced picture of antigen presentation can be established. For example, Sousa and Germain used a TCR-like antibody specific for hen egg lysozyme (HEL) bound to I-A^k to analyze adjuvant function on HEL antigen presentation and the tissue distribution of APCs in mice. The results suggest that bacterial adjuvants, such as endotoxin, promote T cell

immunity by mobilizing antigen specific and activate dendritic cells to secondary lymphoid tissue for activation of a T cell response (5). Moreover, antigen specific tolerance induction by intravenous injection of soluble proteins is shown to be due to the interaction of antigen specific pMHC bearing B cells with naïve antigen-specific T cells (6). Application of TCR-like antibody-derived molecules for effective vaccine development for cancer, human immunodeficiency virus (HIV) infection, tuberculosis (TB) infection, and severe acute respiratory syndrome (SARS) are just a few of the many diseases that would benefit from TCR-like molecules.

4.3 Improving cancer therapeutics with TCR-like molecules

We have shown that highly specific and strong affinity TCR-like antibody fragments can be used for positron emission tomography/computed tomography (PET/CT) imaging of xenotransplanted human tumors in mice (7). A major drawback of our studies is that the signal to noise could not be optimized because of the relatively short half-life of binding of the TCR-like Fab. If the half-life could be increased, the signal will accumulate and the non-specific signal (noise) will decrease. One way that we can increase the time of association is to increase the valency of binding. We are attempting to do that now. Once in hand, our future research will involve identifying/quantifying the expression hierarchy of T cell epitopes present on cancer cells as a function of disease progression or therapy. Reiter et al. have identified expression hierarchies of melanoma tumor-associated antigens, but their work relied on cell lines and histology for quantitation instead of noninvasive *in vivo* imaging (8). Upon understanding the pMHC expression levels during a cancer's life cycle, stage-specific cancer therapeutics can be developed

and targeted using the TCR-like proteins. High affinity TCR-like antibody-derived molecules, usually in the nanomolar to picomolar range, allow longer association times on cells expressing the cancer specific pMHC. This increases the likelihood for therapeutic delivery of the drug via endocytosis and/or activation of immune effector mechanisms including antibody-dependent cell-mediated cytotoxicity and complement deposition.

Improvement of the selection of therapeutically relevant T-cell epitopes on cancer cells needs to be enhanced to optimize the TCR-like antibody therapeutic approach. Research has shown that monoclonal antibodies are more effective against high density membrane antigens on cancer cells compared to membrane associated antigens of lower expression densities (9). One specific example as a potential target is in melanoma, where these cancer cells have high expression of the tyrosinase antigen (8). This may be a very attractive target for the TCR-like molecule therapeutic applications. Therefore, proteomic and mass spectrometry in combination with TCR-like molecules will enable a personalized medicine approach to cancer therapy (10). Cocktails of multiple TCR-like antibody-derived molecules specific for various pMHC molecules identified from the patient specific tumor antigen presentation hierarchy have the potential to enhance treatment effectiveness even against malignant cancers that can mutate to have a decreased or absent expression of one or more target antigens. Moreover, this approach and other therapeutic applications of TCR-like proteins need to be further tested experimentally with the ultimate goal of application and practice in a clinical setting.

One of the most significant contributions that TCR-like antibody-derived molecules and our work on cancer and T1D specific TCR-like antibody fragments can have is on targeted delivery of nanoparticles. Nanoparticles can be loosely defined as particulates with at least one dimension in the 1-100 nm range. They can be made by a variety of different chemistries including nanocrystalline synthesis, polymer synthesis, and inorganic chemistries among others (11). They are usually nonspecific and rely on other features such as the enhanced retention and permeability (EPR) effect for efficient delivery of imaging/therapeutic agents to solid tumors (12). Thus, systemic toxicity can be an issue when using nanoparticles. Due to the heterogeneity of cancers, personalized disease imaging and treatments based on the individual patients' unique cancer chemistry are needed. TCR-like protein molecules can assist in targeting these nanoparticles for imaging or therapeutic effect based on the patient's cancer proteome. The pMHC molecule that the TCR-like protein targets is a representation of the entire cancer cell's proteome. Thus, unique differences between individual patients' cancers can be identified and used to tailor specific TCR-like molecule targeted nanoparticle therapies for imaging and drug delivery.

4.4 TCR-like proteins for elucidating type 1 diabetes autoimmune mechanisms

The research presented for Type 1 Diabetes (T1D) in Chapter 3 is a proof of concept demonstrating the TCR-like molecule technology application in autoimmune disease. Our research showed that TCR-like antibody fragments can be isolated and used to image beta cells in T1D. Future research will focus on when, where, and the quantity of pMHC molecules presented during the autoimmune disease.

Professional antigen presenting cells are actively involved in T1D (13). By utilizing TCR-like antibody-derived proteins specific for T1D-associated pMHC, an improved picture of the mechanism of immune activation and development can be achieved. TCR-like molecules in principle are as revolutionary to the field of immunology as recombinant pMHC molecules were for studying TCR specific T cell populations (14).

In T1D, there are still important questions to be answered regarding antigen presentation during disease development. One major area is the pancreatic lymph node (PLN), which is believed to be essential for the initial activation of autoimmune T cells before their migration to the islets. The PLN drains the acinar component of the pancreas and segments of the intestine (15). Removal of the PLN by surgical excision from NOD mice results in loss of T cell priming and no diabetes incidence (16). Moreover, proliferation of autoreactive CD4 and CD8 T cells has been observed in the PLN (17-20). The main mechanism by which the PLN APC obtains and then presents beta cell antigens is still unknown. TCR-like proteins specific for autoimmune pMHC would allow *in vivo* monitoring of antigen presentation as T1D progresses. One hypothesis is that beta cell antigens are released from beta cells and/or by islet dendritic cells (DCs) and travel via the lymphatic vessels to the draining PLN. Calderon and collegues hypothesize that it is the migration of islet DCs that sensitize the PLN as part of a normal process of DC turnover (13). TCR-like molecules specific for autoimmune-associated pMHC can elucidate when and where DC subtypes are in the pancreas and surrounding tissue during T1D progression. A powerful approach to interpreting the autoimmune response in T1D

could be developed where TCR-like molecules are used to monitor location and quantification of APCs and recombinant pMHC molecules are used to identify and quantify specific T cell subsets during disease. This has special promise for *in vivo* imaging and real time imaging of the autoimmune process.

Another area of interest in T1D that TCR-like antibody-derived proteins can aid is the phenomenon of epitope spreading. Research suggests that initial T1D onset is due to responses against the epitope from the insulin B chain 9-23 region followed by responses against other epitopes on insulin and other antigens during overt disease in NOD mice (21). This was further supported by research involving transgenic mice hyper-expressing either proinsulin or islet specific glucose-6-phosphatase catalytic subunit related protein (IGRP). It was observed that the mice over expressing proinsulin did not develop insulitis even when injected with proinsulin or IGRP. The IGRP over-expressing mice did not develop insulitis when injected with IGRP peptide, but did when given the proinsulin. Thus, IGRP is hypothesized to be a secondary autoantigen compared to proinsulin and is due to pathogenic epitope spreading (22). Similar hypothesizes about proinsulin in human T1D have been proposed where epitope spreading following proinsulin assault leads to GAD autoantigens (23, 24). TCR-like molecules can be used to monitor these primary and secondary autoantigens to discover if there are differences in expression of their pMHC complexes on APCs or endogenous beta cells corresponding to the epitope spreading. This would assist in understanding the route that epitope spreading takes and to confirm that proinsulin is the primary autoantigen in T1D.

4.5 Improving production of TCR-like proteins

Another application of TCR-like proteins is understanding the biochemical aspects of pMHC recognition. By x-ray crystallography, crystal structures of TCR-like antibody fragments bound to the SIINFEKL peptide from ovalbumin bound to H-2K^b MHC showed unique mechanisms of binding between the TCR-like antibody fragments and the pMHC molecule. The modes of binding were either by contacting the peptide directly, similar to a TCR, or by identifying unique pMHC conformations (25, 26). The TCR-like protein generation procedure can be improved by such information. TCR-like binding of TCR-like molecules would be confirmed by mapping of residues responsible for pMHC recognition within the peptide, MHC molecule, and the TCR-like molecule's corresponding residues in the complementary determining regions (CDRs). Thus, residues required for specificity against a specific peptide could be favored when preparing the phage display library enabling more CDR loop combinations to be tested and potentially faster production of high affinity TCR-like proteins.

Information on the mechanism of recognition of TCR-like antibody-derived molecules for pMHC can improve production of alternative formats of TCR-like proteins. Most generated TCR-like molecules are antibodies or antibody fragments. Both these protein formats are multi-domain glycoproteins dependent on disulfide bonds, which cannot be made in the cytosol of microbial hosts due to the reducing environment. In the world of biological engineering, alternative protein backbone structures are being created that are without disulfide bonds or glycosylation sites, are thermostable, and are five to ten times smaller in molecular weight as a single-

domain protein (27). Potential protein scaffolds that could be screened by phage display include affibodies, cysteine knot proteins, and DARPins. Affibodies are ~6kDa three-helix bundles of 58 amino acid residues. They are cysteine-free and are a natural immunoglobulin-binding domain resulting in the potential for high-affinity complexes on the surface-exposed residues on the helices (28). Affibodies against the human epidermal growth-factor receptor 2 (HER2) have been isolated with picomolar affinity (29). Cysteine knot peptides are 30-50 amino acid proteins that are produced by solid phase polypeptide synthesis avoiding the periplasm of *E. coli*. These molecules have a high degree of thermal and proteolytic stability (30). Designed ankyrin repeat proteins (DARPins) are hypothesized to work the best as an alternative format as a TCR-like molecule because they have loops that can be altered to more closely resemble the binding of a TCR. These molecular scaffold proteins consist of a repeated units of a beta-turn and two antiparallel alpha helices with an unstructured loop leading to the repeat of this structure (31). DARPins with nanomolar binding affinity for epidermal growth-factor receptor (EGFR) have been isolated by phage display (32). Overall, the limitations of antibodies and antibody fragments have lead to alternative protein scaffolds that provide solutions to the problems of immunoglobulin domains. Research will be needed to determine if such alternative scaffolds can be used to make a TCR-like protein with high affinity and specificity at a fraction of the size of regularly generated TCR-like antibodies.

4.6 Conclusion

In summary, TCR-like molecules specific for pMHC molecules are a novel tool for targeting and studying antigen presentation during disease. There is much

potential for the future of TCR-like molecules in elucidating the mechanisms of immunity and aiding in the development of effective vaccines. Moreover, they can assist in effective delivery of imaging and therapeutic agents to the sites of disease. Before any TCR-like proteins are used in the clinic, further studies of their specificity, side effects and toxicity are required. Thus, a new age of highly personalized, tailored medicine is in the future using TCR-like molecules to understand a patient's unique cellular proteome.

4.7 References

1. Hansen, T. H., J. M. Connolly, K. G. Gould, and D. H. Fremont. 2010. Basic and translational applications of engineered MHC class I proteins. *Trends Immunol.* 31: 363–369.

2. Crowley, M., K. Inaba, and R. M. Steinman. 1990. Dendritic cells are the principal cells in mouse spleen bearing immunogenic fragments of foreign proteins. *The J. Exp. Med.* 172: 383–386.

3. Guéry, J.-C., F. Ria, F. Galbiati, S. Smiroldo, and L. Adorini. 1997. The mode of protein antigen administration determines preferential presentation of peptide-class II complexes by lymph node dendritic or B cells. *Int. Immunol.* 9: 9–15.

4. Liu, L. M., and G. G. MacPherson. 1993. Antigen acquisition by dendritic cells: intestinal dendritic cells acquire antigen administered orally and can prime naive T cells in vivo. *J. Exp. Med.* 177: 1299–1307.

5. Reis e Sousa, C., and R. N. Germain. 1999. Analysis of adjuvant function by direct visualization of antigen presentation in vivo: endotoxin promotes accumulation of antigen-bearing dendritic cells in the T cell areas of lymphoid tissue. *J. Immunol.* 162: 6552–6561.

6. Zhong, G., C. R. e Sousa, and R. N. Germain. 1997. Antigen-unspecific B cells and lymphoid dendritic cells both show extensive surface expression of processed antigen–major histocompatibility complex class II complexes after soluble protein exposure in vivo or in vitro. *J. Exp. Med.* 186: 673–682.

7. Miller, K. R., A. Koide, B. Leung, J. Fitzsimmons, B. Yoder, H. Yuan, M. Jay, S. S. Sidhu, S. Koide, and E. J. Collins. 2012. T cell receptor-like recognition of tumor in vivo by synthetic antibody fragment. *PLoS ONE* 7: e43746.

8. Michaeli, Y., G. Denkberg, K. Sinik, L. Lantzy, C. Chih-Sheng, C. Beauverd, T. Ziv, P. Romero, and Y. Reiter. 2009. Expression hierarchy of T cell epitopes from melanoma differentiation antigens: unexpected high level presentation of tyrosinase-HLA-A2 Complexes revealed by peptide-specific, MHC-restricted, TCR-like antibodies. *J. Immunol.* 182: 6328–6341.

9. Mimura, K., K. Kono, M. Hanawa, M. Kanzaki, A. Nakao, A. Ooi, and H. Fujii. 2005. Trastuzumab-mediated antibody-dependent cellular cytotoxicity against esophageal squamous cell carcinoma. *Clin. Cancer Res.* 11: 4898–4904.

10. Weidanz, J. A., P. Piazza, H. Hickman-Miller, D. Woodburn, T. Nguyen, A. Wahl, F. Neethling, M. Chiriva-Internati, C. R. Rinaldo, and W. H. Hildebrand. 2007. Development and implementation of a direct detection, quantitation and validation system for class I MHC self-peptide epitopes. *J. Immunol. Methods.* 318: 47–58.

11. Bao, G., S. Mitragotri, and S. Tong. 2013. Multifunctional Nanoparticles for Drug Delivery and Molecular Imaging. *Annu Rev Biomed Eng*.

12. Maeda, H., H. Nakamura, and J. Fang. 2013. The EPR effect for macromolecular drug delivery to solid tumors: Improvement of tumor uptake, lowering of systemic toxicity, and distinct tumor imaging in vivo. *Adv. Drug Deliv. Rev.* 65: 71–79.

13. Calderon, B., and E. R. Unanue. 2012. Antigen presentation events in autoimmune diabetes. *Curr. Opin. Immunol.* 24: 119–128.

14. Gojanovich, G. S., and P. R. Hess. 2012. Making the most of major histocompatibility complex molecule multimers: applications in type 1 diabetes. *Clin. Dev. Immunol.* 2012: 380289.

15. Turley, S. J., J.-W. Lee, N. Dutton-Swain, D. Mathis, and C. Benoist. 2005. Endocrine self and gut non-self intersect in the pancreatic lymph nodes. *Proc. Natl. Acad. Sci. U.S.A.* 102: 17729–17733.

16. Gagnerault, M.-C., J. J. Luan, C. Lotton, and F. Lepault. 2002. Pancreatic lymph nodes are required for priming of beta cell reactive T cells in NOD mice. *J. Exp. Med.* 196: 369–377.

17. Tang, Q., J. Y. Adams, A. J. Tooley, M. Bi, B. T. Fife, P. Serra, P. Santamaria, R. M. Locksley, M. F. Krummel, and J. A. Bluestone. 2006. Visualizing regulatory T cell control of autoimmune responses in nonobese diabetic mice. *Nat. Immunol.* 7: 83–92.

18. Zhang, Y., B. O'Brien, J. Trudeau, R. Tan, P. Santamaria, and J. P. Dutz. 2002. In situ beta cell death promotes priming of diabetogenic CD8 T lymphocytes. *J. Immunol.* 168: 1466–1472.

19. Kurts, C., R. M. Sutherland, G. Davey, M. Li, A. M. Lew, E. Blanas, F. R. Carbone, J. F. Miller, and W. R. Heath. 1999. CD8 T cell ignorance or tolerance to islet antigens depends on antigen dose. *Proc. Natl. Acad. Sci. U.S.A.* 96: 12703–12707.

20. Kurts, C., J. F. Miller, R. M. Subramaniam, F. R. Carbone, and W. R. Heath. 1998. Major histocompatibility complex class I-restricted cross-presentation is biased towards high dose antigens and those released during cellular destruction. *J. Exp. Med.* 188: 409–414.

21. Prasad, S., A. P. Kohm, J. S. McMahon, X. Luo, and S. D. Miller. 2012. Pathogenesis of NOD diabetes is initiated by reactivity to the insulin B chain 9-23 epitope and involves functional epitope spreading. *J. Autoimmun.* 39: 347–353.

22. Krishnamurthy, B., N. L. Dudek, M. D. McKenzie, A. W. Purcell, A. G. Brooks, S. Gellert, P. G. Colman, L. C. Harrison, A. M. Lew, and H. E. Thomas. 2006. Responses against islet antigens in NOD mice are prevented by tolerance to proinsulin but not IGRP. *J. Clin. Invest.* 116: 3258–3265.

23. Ott, P. A., M. T. Dittrich, B. A. Herzog, R. Guerkov, P. A. Gottlieb, A. L. Putnam, I. Durinovic-Bello, B. O. Boehm, M. Tary-Lehmann, and P. V. Lehmann. 2004. T cells recognize multiple GAD65 and proinsulin epitopes in human type 1 diabetes, suggesting determinant spreading. *J. Clin. Immunol.* 24: 327–339.

24. Narendran, P., S. I. Mannering, and L. C. Harrison. 2003. Proinsulin-a pathogenic autoantigen in type 1 diabetes. *Autoimmun Rev* 2: 204–210.

25. Mareeva, T., E. Martinez-Hackert, and Y. Sykulev. 2008. How a T cell receptor-like antibody recognizes major histocompatibility complex-bound peptide. *J. Biol. Chem.* 283: 29053–29059.

26. Mareeva, T., T. Lebedeva, N. Anikeeva, T. Manser, and Y. Sykulev. 2004. Antibody specific for the peptide.major histocompatibility complex. Is it T cell receptor-like? *J. Biol. Chem.* 279: 44243–44249.

27. Banta, S., K. Dooley, and O. Shur. 2013. Replacing Antibodies: Engineering New Binding Proteins. *Annu Rev Biomed Eng*.

28. Nygren, P.-A. 2008. Alternative binding proteins: affibody binding proteins developed from a small three-helix bundle scaffold. *FEBS J.* 275: 2668–2676.

29. Orlova, A., M. Magnusson, T. L. J. Eriksson, M. Nilsson, B. Larsson, I. Höidén-Guthenberg, C. Widström, J. Carlsson, V. Tolmachev, S. Ståhl, and F. Y. Nilsson. 2006. Tumor imaging using a picomolar affinity HER2 binding affibody molecule. *Cancer Res.* 66: 4339–4348.

30. Moore, S. J. and J. R. Cochran. 2012. Engineering knottins as novel binding agents. Methods Enzymol. 503: 223-251.

31. Kohl, A., H. K. Binz, P. Forrer, M. T. Stumpp, A. Plückthun, and M. G. Grütter. 2003. Designed to be stable: crystal structure of a consensus ankyrin repeat protein. *Proc. Natl. Acad. Sci. U.S.A.* 100: 1700–1705.

32. Boersma, Y. L., G. Chao, D. Steiner, K. D. Wittrup, and A. Plückthun. 2011. Bispecific designed ankyrin repeat proteins (DARPins) targeting epidermal growth factor receptor inhibit A431 cell proliferation and receptor recycling. *J. Biol. Chem.* 286: 41273–41285.